

University of Southern Queensland
Faculty of Health, Engineering and Sciences

Performance Evaluation of GFRP Reinforced Railway
Sleepers

A dissertation submitted by
Jacob Verrall

In fulfilment of the requirements of
ENG4111 and 4112 Research Project
towards the degree of
Bachelor of Engineering (Honours) (Civil)
Submitted October, 2019

Abstract

Australia's rail network is an integral part of Australia's transportation network as 1.3 billion tonnes of freight is moved by rail annually. The majority of Australia's rail infrastructure remains timber which is susceptible to rot, splitting and insect attack. Recent studies have estimated that 90% of the existing timber sleepers in Australia will deteriorate beyond repair by 2025 meaning they will need to be replaced at an estimated cost of more than \$1 billion. To reduce maintenance costs, the rail industry is seeking a more durable alternative than traditional timber sleepers. Composite sleepers have emerged as an effective solution but many are still failing before their predicted design life as they are susceptible to cracking and corrosion. This research has designed, manufactured and evaluated the performance of two new composite sleepers using Portland concrete and epoxy based polymer concrete reinforced with glass fibre reinforced polymer (GFRP) bars. These materials have purposely been selected in an attempt to manufacture a more robust and durable sleeper in comparison to timber and other composite sleepers currently available.

To design the GFRP reinforcement, two finite element simulation models based on elastic foundation theory were used to determine maximum bending moment and shear force acting on a sleeper. Once the reinforcement was designed, two test sleepers were manufactured. The polymer concrete sleeper was designed with a traditional concrete core as research highlighted that polymer concrete has a relative low stiffness. Destructive and non-destructive test methods were used to evaluate the performance of these two composite sleepers.

Non-destructive tests proved that both sleepers were able to achieve an acceptable effective modulus of elasticity. By using polymer concrete, the sleeper's modulus was reduced by 29.44% compared to Portland concrete. This justifies the use of a traditional concrete core to retain an acceptable effective modulus. Stress analysis principles have proven that GFRP bars are a suitable replacement for steel reinforcement. Non-destructive results were also used to predict that both sleepers will fail due to concrete crushing while the GFRP bars will be utilised up to 70% of their tensile strength. Destructive testing showed that both sleepers failed due to negative bending moment at the centre, indicating that this behaviour should be carefully considered in the sleeper design. However, minor modifications on the proposed 5-point bending test may be needed to achieve a reasonable ratio of positive-to-negative bending moment and to closely replicate on how the sleeper would be loaded in-track. This theory was proven in Strand 7 as simulations of the test setup indicate that flexural failure first occurred at the middle support which doesn't align with the failure mode predicted. Although the sleepers failed prematurely, some creditable results were found. One of the most significant findings was that polymer concrete helped to reduce the degree of cracking; the major cause of premature concrete sleeper deterioration. Destructive testing also highlighted that the transverse shear capacity of GFRP bars and deflection might be two limiting design factors.

University of Southern Queensland
Faculty of Health, Engineering and Sciences
ENG4111 & ENG4112 Research Project

Limitations of Use

The Council of the University of Southern Queensland, its Faculty of Health, Engineering and Sciences, and the staff of the University of Southern Queensland, do not accept any responsibility for the truth, accuracy or completeness of material contained within or associated with this dissertation.

Persons using all or any part of this material do so at their own risk, and not at the risk of the Council of the University of Southern Queensland, its Faculty of Health, Engineering and Sciences or the staff of the University of Southern Queensland.

This dissertation reports an educational exercise and has no purpose or validity beyond this exercise. The sole purpose of the course pair entitles “Research Project” is to contribute to the overall education within the student’s chosen degree program. This document, the associated hardware, software, drawings, and any other material set out in the associated appendices should not be used for any other purpose: if they are so used, it is entirely at the risk of the user.

Certification

I certify that the ideas, designs and experimental work, results, analyses and conclusions set out in this dissertation are entirely my own effort, except where otherwise indicated and acknowledged.

I further certify that the work is original and has not been previously submitted for assessment in any other course or institution, except where specifically stated.

Jacob Aaron Verrall

Student Number: XXXXXXXXXX

Acknowledgements

I would like to acknowledge and thank the efforts of my supervisor over the duration of my research project, Associate Professor Allan Manalo. Thank you for always answering my questions and encouraging me to work hard. I would also like to thank any USQ laboratory staff who helped me during the testing phase of my research project and USQ for allowing me to use their testing facilities. Finally, I would like to thank my friends and family for their continuous support throughout my studies at USQ.

Table of Contents

ABSTRACT	I
LIMITATIONS OF USE	II
CERTIFICATION	III
ACKNOWLEDGEMENTS	IV
LIST OF FIGURES	VIII
NOMENCLATURE	XI
STANDARDS AND TECHNICAL SPECIFICATIONS	XIII
CHAPTER 1 INTRODUCTION	1
1.1 Project Background	1
1.2 Railway Sleepers	2
1.3 Alternative Materials	4
1.4 Purpose of Research	5
1.5 Project Aim	6
1.6 Research Objectives	6
1.7 Scope and Limitations	7
1.8 Expected Outcomes and Benefits	8
1.9 Dissertation Overview	8
1.10 Ethics and Consequences	9
CHAPTER 2 LITERATURE REVIEW	11
2.1 Chapter Overview	11
2.2 Railway Track Components	11
2.3 Timber Sleepers	13
2.4 Precast Concrete Sleepers	14
2.5 Fibre Composite Sleepers	15
2.6 Precast Concrete Railway Sleeper Standards	16
2.7 Designing a Railway Sleeper	16
2.8 Calculating the Rail Seat Load	21

2.9	Axle Load Distribution Factor	24
2.10	Dynamic Load Coefficient Factor	24
2.11	Rail Gauge Width	25
2.12	Dimensions of a Sleeper	26
2.13	Glass Fibre Reinforced Polymer	26
2.14	GFRP Reinforcement Standards	31
2.15	Current Issues with Portland Cement Production	35
2.16	Polymer concrete; an alternative cementitious sleeper material	35
2.17	Previous Studies	38
2.18	Research Gap	40
2.19	Project Feasibility	41
CHAPTER 3 FINITE ELEMENT ANALYSIS		42
3.1	Chapter Overview	42
3.2	Benefits of Creating a Finite Element Model	42
3.3	Analysing a Sleeper	43
3.4	Preliminary Sleeper Design	44
3.5	Developing the Finite Element Model	47
3.6	Finite Element Modelling Results	51
3.7	Model Verification	53
3.8	Summary of Finite Element Modelling	54
3.9	Reinforcement Design Considerations	55
3.10	Flexural Reinforcement Design based on Finite Element Results	57
3.11	Shear reinforcement design based on Finite Element Results	60
3.12	Designing the Polymer Concrete Sleeper	64
CHAPTER 4 EXPERIMENTAL PROGRAM		66
4.1	Chapter Overview	66
4.2	Safety Considerations	66
4.3	Materials	67
4.4	Preparation of Test Sleepers	68

4.5	Concrete Pour	70
4.6	Non Destructive Testing Method	72
4.7	Destructive Testing Method	73
CHAPTER 5 NON-DESTRUCTIVE TESTING OBSERVATIONS, RESULTS		
AND DISCUSSION		74
5.1	Chapter Overview	74
5.2	Non Destructive Testing Assessment	74
5.3	Non Destructive Testing Observations	74
5.4	Non-destructive Test Results and Discussion	76
5.5	Key Findings from Non-destructive Testing	91
CHAPTER 6 DESTRUCTIVE TESTING OBSERVATIONS, RESULTS AND		
DISCUSSION		93
6.1	Chapter Overview	93
6.2	Destructive Testing Assessment	93
6.3	Destructive Testing Observations	93
6.4	Destructive Test Results and Discussion	96
CHAPTER 7 CONCLUSION		109
7.1	Project Outcomes	109
7.2	Future Work	113
REFERENCE LIST		114
APPENDIX A	ENG4111/4112 RESEARCH PROJECT	120
APPENDIX B	TRACK-CT.172 DESIGN SPECIFICATIONS	122
APPENDIX C	TABLE 4.1 FROM AUSTRALIAN STANDARD; AS1085.14	129
APPENDIX D	MATERIALS LIST	130
APPENDIX E	MECHANICAL CHARACTERISTICS OF GFRP BARS	131

List of Figures

<i>Figure 1-1: The distribution of freight movement in Australia (Hossain, 2016)</i>	1
<i>Figure 1-2: Cross-section of a railway (Note, 2018)</i>	2
<i>Figure 2-1: A typical concrete fastener (Kaewunruen and Remennikow, 2008)</i>	12
<i>Figure 2-2: Common failure methods for timber sleepers (Ferdous and Manalo, 2014)</i>	13
<i>Figure 2-3: Stress distribution pattern on a concrete sleeper (Bezgin 2017)</i>	14
<i>Figure 2-4: Common modes of failure experienced by concrete sleepers (Ferdous and Manalo, 2014)</i>	15
<i>Figure 2-5: Empirical bearing distribution when calculating MR+ (AS1085.14, 2012)</i>	18
<i>Figure 2-6: Empirical bearing distribution when calculating Mc- (AS1085.14, 2012)</i>	19
<i>Figure 2-7: A schematic diagram of the BOEF method (AS1085.14, 2012)</i>	19
<i>Figure 2-8: Empirical chart used to obtain the DF (AS1085.14, 2012)</i>	24
<i>Figure 2-9: Different gauge tracks across Australia (Merkert & Hensher, 2014)</i>	25
<i>Figure 2-10: Pultrusion method (GFRP Components for Facades, n.d)</i>	27
<i>Figure 2-31: Bend tests conducted on different concrete sections (Jabbar and Farid, 2018)</i>	28
<i>Figure 2-12: Designing shear reinforcement in accordance with AS3600 (Manalo, 2018)</i>	33
<i>Figure 2-13: More GFRP reinforcement is required than steel (Baker, 2016)</i>	39
<i>Figure 3-1: Finite Element Model 1</i>	44
<i>Figure 3-2: Finite Element Model</i>	44
<i>Figure 3-3: The dimensions of the GFRP reinforced sleeper under investigation (mm)</i>	47
<i>Figure 3-4: Nodes and elements within Model 1</i>	49
<i>Figure 3-5: Nodes and elements within Model 2</i>	49
<i>Figure 3-6: Strand 7 beam parameters</i>	50
<i>Figure 3-7: A 3D view of Model 1 developed in Strand 7</i>	50
<i>Figure 3-8: A 3D view of Model 2 developed in Strand 7</i>	51
<i>Figure 3-9: Maximum positive bending moment diagram obtained from model 1</i>	51
<i>Figure 3-10: Maximum negative bending moment diagram obtained from model 2</i>	51
<i>Figure 3-11: Maximum shear force diagram obtained from model 1</i>	52
<i>Figure 3-12: Vector diagram showing the expected magnitude and direction of deflection</i>	52
<i>Figure 3-13: Proposed flexural detailing</i>	60
<i>Figure 3-14: Design for shear diagram</i>	62
<i>Figure 3-15: Shear reinforcement detailing</i>	63
<i>Figure 3-16: Polymer concrete sleeper with a Portland concrete core</i>	65
<i>Figure 4-1: Risk assessment criteria (What is Risk?, 2018)</i>	66
<i>Figure 4-2: Cable ties used to fix flexural and shear reinforcement together</i>	68
<i>Figure 4-3: Attaching strain gauges to the GFRP bars using super glue</i>	69
<i>Figure 4-4: The assembled reinforcement cage in the precast sleeper mould</i>	69
<i>Figure 4-5: The concrete core inside the GFRP reinforcement cage before the polymer concrete was poured</i>	70

<i>Figure 4-6: Standard pouring methods were used to cast the sleepers</i>	71
<i>Figure 4-7: Screeded sleeper in its precast mould</i>	71
<i>Figure 4-8: SANS machine setup for non-destructive testing</i>	72
<i>Figure 4-9: Destructive test setup</i>	73
<i>Figure 5-1: Portland concrete sleeper under loading (left) and polymer concrete sleeper under loading (right)</i>	74
<i>Figure 5-2: Portland concrete sleeper developed flexural cracks during non-destructive testing</i>	75
<i>Figure 5-3: No cracks were developed in the polymer concrete sleeper during non-destructive testing</i>	76
<i>Figure 5-4: Non-destructive load versus deflection diagram</i>	77
<i>Figure 5-5: Recorded strain data vs load; Portland concrete sleeper</i>	81
<i>Figure 5-6: Strain distribution over the Portland concrete sleeper</i>	81
<i>Figure 5-7: Recorded strain data vs load; Polymer concrete sleeper</i>	82
<i>Figure 5-8: Strain distribution over the polymer concrete sleeper</i>	82
<i>Figure 5-9: Optimal strain distribution for Portland concrete sleeper</i>	83
<i>Figure 5-10: Optimal strain distribution for polymer concrete sleeper</i>	84
<i>Figure 5-11: Predicted failure distribution for the Portland concrete sleeper</i>	87
<i>Figure 5-12: Predicted failure distribution for the polymer concrete sleeper</i>	88
<i>Figure 6-1: The destructive test setup and the DIC device in front of load cell</i>	93
<i>Figure 6-2: Observed deflection at maximum applied load for the polymer concrete sleeper</i>	94
<i>Figure 6-3: Observed deflection at maximum applied load for the Portland concrete sleeper</i>	94
<i>Figure 6-4: Cracking observed in the Portland concrete sleeper at the middle support and the rail seat</i>	95
<i>Figure 6-5: Cracking observed in the polymer concrete sleeper at the middle support and the rail seats</i>	96
<i>Figure 6-6: Spalled concrete was removed to reveal a ruptured longitudinal GFRP bar</i>	97
<i>Figure 6-7: Load verses strain plot for the Portland concrete sleeper</i>	98
<i>Figure 6-8: Load verses strain plot for the Polymer concrete sleeper</i>	99
<i>Figure 6-9: Load verses strain plot for the timber sleeper</i>	100
<i>Figure 6-10: The node and element configuration of the 5-point bend test in Strand 7</i>	101
<i>Figure 6-11: Bending moment diagram at failure for the Portland concrete 5-point bend test</i>	101
<i>Figure 6-12: Shear force diagram at failure for the Portland concrete 5-point bend test</i>	102
<i>Figure 6-13: Bending moment diagram at failure for the polymer concrete 5-point bend test</i>	102
<i>Figure 6-14: Shear force diagram at failure for the polymer concrete 5-point bend test</i>	102
<i>Figure 6-15: Experimental Shear force at 150 kN</i>	104
<i>Figure 6-16: Destructive Load vs deflection diagram for the Portland concrete sleeper</i>	106
<i>Figure 6-17: Destructive Load vs deflection diagram for the polymer concrete sleeper</i>	107
<i>Figure 6-18: Destructive Load vs deflection diagram for the timber sleeper</i>	107
<i>Figure 7-1: Future research could be done on a sleeper reinforced with a rectangular GFRP hollow section</i>	113

List of Tables

<i>Table 2-1: Possible bearing distribution patterns underneath a sleeper (Abbasi & Ali Zakeri, 2013).....</i>	17
<i>Table 2-2: Rail seat load calculation methods (Barkan et. al, 2014).....</i>	22
<i>Table 2-3: Common track gauges in Australia (Merkert & Hensher, 2014).....</i>	26
<i>Table 2-4: Basic dimensions and characteristics of a sleeper (TRACK-CT.172).....</i>	26
<i>Table 2-5: Allowable deflections in GFRP reinforced sections (Newhook and Svecova, 2007).....</i>	34
<i>Table 2-6: Common fillers added to polymer concrete and their intended benefits (Ferdous et. al., 2016)</i>	36
<i>Table 2-7: Durability of polymer concrete Vs Portland concrete (Kirlikovali, 1981).....</i>	38
<i>Table 3-8: Sleeper model properties.....</i>	46
<i>Table 3-9: Strand 7 node positions for Model 1.....</i>	49
<i>Table 3-3: Strand 7 node positions for Model 2.....</i>	49
<i>Table 3-10: A summary of significant Strand 7 results.....</i>	52
<i>Table 3-11: Finite model validation by comparing results calculated using the analytical method.....</i>	53
<i>Table 3-12: Finite model validation by comparing results calculated using the Empirical method.....</i>	54
<i>Table 3-13: Fu of GFRP bars supplied by Inconmat Australia (V-ROD Fiberglass Rebar Canada, 2012)</i>	56
<i>Table 4-14: Risk assessment scores and precautionary actions.....</i>	66
<i>Table 5-1: Comparative sleeper modulus.....</i>	80
<i>Table 5-2: Predicted behaviour and performance of the sleepers based on non-destructive test results....</i>	91
<i>Table 6-1: Comparison between theoretical and experimental results.....</i>	103
<i>Table 6-2: Deflection at failure.....</i>	108

Nomenclature

A	=Length of ballast supporting the sleeper beneath each rail seat
a	=Shear span
A_{GFRP}	=Area of GFRP reinforcement
A_{sv}	=Area of shear reinforcement
b	=Width of beam
C	=Distance from rail seat load to centre of sleeper
c	=Neutral axis depth
Cz	=Compressive force times lever arm
D	=Full depth of the sleeper
d	=Effective depth of section
d_b	=Diameter of flexural reinforcement
DF	=Axle Load distribution factor
d_s	=Diameter of shear reinforcement
e	=Eccentricity
E_{eff}	=Effective bending modulus
E_s	=Young's modulus of sleeper
f_{cv}	=Concrete shear strength
f'_c	=Compressive strength of concrete
f'_t	=Characteristic tensile strength of concrete
g	=Distance between rail centres
I_{eff}	=Effective moment of inertia
I_s	=Sleeper moment of inertia about horizontal neutral axis
k_s	=Dynamic load coefficient factor
L	=The length of the sleeper
l	=Span length
M^*	=Maximum moment
M^{CR}	=Moment at rail centre
n	=Distance from sleeper end to rail seat load
P	=Force in tendons
P_{dv}	=Factored vertical wheel load
P_2	=Load criterion where no structural cracking should be present
Q	=Static wheel load
R_v	=Design rail seat load

s	=Spacing of shear reinforcement
Tz	=Tensile force times lever arm
U	=Sleeper support modulus
V^*	=Design shear force
$V_{u.max}$	=Ultimate shear strength limited by web crushing
$V_{u.min}$	=Ultimate shear strength of a beam with minimum shear reinforcement
V_{uc}	Ultimate shear strength excluding shear reinforcement
X	=Distance from the end of the sleeper
Z	=Section modulus
α_1	=Coefficient, CSA S806-12
β_1	=Coefficient from CSA S806-12 =Compressive strength factor; AS3600
β_2	=Compressive strength factor
β_3	=Compressive strength factor
θ_v	=Angle of shear cracking
σ_u	=Ultimate stress in GFRP fibres
ϕ	=Capacity reduction factor
λ	=Sleeper stiffness parameter
ε_{GFRP}	=Strain value of GFRP bars

Standards and Technical Specifications

AS1085.14 Australian Standard: Railway track material – Prestressed Concrete Sleepers

AS3600 Australian Standard: Concrete Structures

CSA S806-12 Design and Construction of Building Components with Fibre Reinforced Polymers

Chapter 1 Introduction

1.1 Project Background

Australia's economy is reliant on a functioning rail network as it's extensively used to transport bulk materials and mining resources over large distances (Hossain, 2016). Australia's rail network is the sixth largest in the world with over 33 300 kilometres of heavy rail and 300 kilometres of light rail (Hossain, 2016). In recent years, the popularity of transporting materials using rail has even surpassed trucks as seen in figure 1-1.

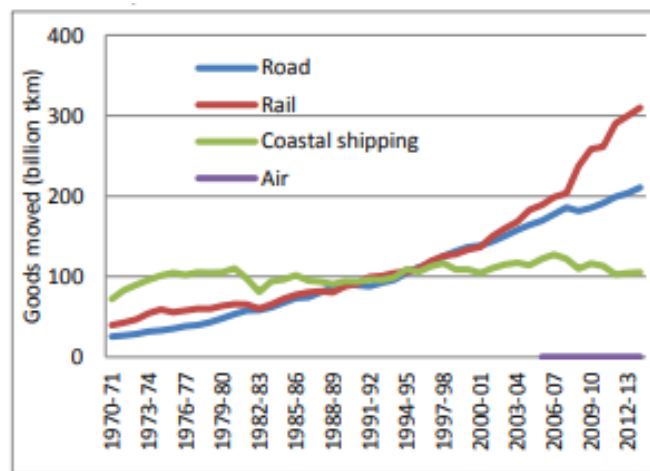


Figure 4-1: The distribution of freight movement in Australia (Hossain, 2016)

This shift in popularity has created great strain on Australia's ageing rail network as many railway sleepers and structures remain timber. According to Hollingworth & Brown (2017), this is problematic as timber sleepers only have a design life of approximately 5 to 15 years. This means that track maintenance costs are currently enormous. Other studies have also found that many timber sleepers are performing at the low end of this spectrum as they are susceptible to weathering, chemical attack and splitting in Australia's harsh climate while being prone to insect infestation (Railway Sleepers, 2018).

Queensland Rail's regional network alone has in excess of 2.4 million timber sleepers in service which must be replaced in the near future by alternative products (Queensland Rail; QRP-15-150A Tender Information Report, 2016). From 2018 to 2023, Queensland Rail aims to replace 130 000

timber sleepers per annum with 115mm alternative composite sleepers. The performance of these alternative sleepers will then be evaluated over a twelve month period to determine their adequacy (Queensland Rail; QRP-15-150A Tender Information Report, 2016). Therefore, Queensland rail are seeking expressions of interest from industry suppliers to design and manufacture alternative railway sleepers in accordance with a number of technical and performance specifications set by Queensland Rail. Technical and performance specifications set by Queensland Rail for alternative sleepers can be found in a document titled ‘Material Supply Specification (TRACK-CT.172)’ (Queensland Rail; QRP-15-150A Tender Information Report, 2016).

1.2 Railway Sleepers

Railway sleepers are an integral part of a railway system as they are laid perpendicular underneath the railroad tracks and are primarily used to transfer the loads of the passing train to the ballast and subgrade underneath (Railway Sleepers, 2018). Railroads are traditionally fixed to the underlying sleepers using fasteners and rail joints. This ensures that the railroads are permanently fixed at the correct track gauge and to prevent longitudinal rail movement (Railway Sleepers, 2018). A typical cross-section of a railway track is shown in figure 1-2.

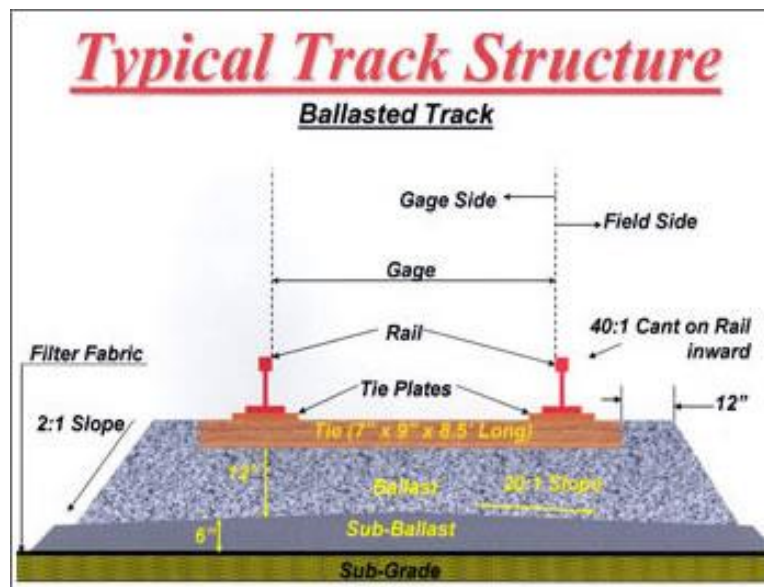


Figure 1-5: Cross-section of a railway (Note, 2018)

Although traditionally made from timber, composite sleepers have been manufactured in the past with great success as they enable trains to increase their travel speed, are more fire resistant, reduce carbon emissions associated with timber production and require less generic maintenance (Carey, 2012). The most significant advantage of concrete railway sleepers is their durability as they have the ability to last up to 60 years or 4 times longer than timber (Carey, 2012). This capability easily offsets greater capital costs thus making composite railway sleepers a good investment.

However, one of the major problems with concrete sleepers is their high stiffness compared to timber. Having a high stiffness limits the products ability to be easily integrated with existing timber sleepers and infrastructure as older and more flexible timber will experience accelerated degradation. This means that the entirety of a track segment much be replaced at a single time (Andersson et al., 2013). Concrete's high stiffness also means that the sleeper is susceptible to cracking under short and intense loadings (Andersson et al., 2013). Cracking is very undesirable as it enables moisture to reach the sleeper's reinforcement.

To withstand high loads generated by passing trains, concrete sleepers must be adequately designed with steel reinforcement. However, steel reinforcement is vulnerable to chemical attack meaning it can weaken and cause premature structural failure (Corrosion of Embedded Metals, 2018). To prevent this problem, companies are currently required to implement a range of expensive maintenance techniques to help restore or prevent further deterioration of steel reinforcement (Corrosion of Embedded Metals, 2018).

To overcome durability issues, engineers in recent years have been trying to find alternative materials which can outperform steel while still being cost effective. Fibre composite materials have emerged as a potential replacement for steel and timber as researchers have found ways to reduce costs by optimising production processes while the materials mechanical properties can easily be manipulated to suit many applications (McMillan, 2017). One of the main reasons why fibre composite materials have become favourable over steel and timber is its ability to resist chemical attack (McMillan, 2017). Glass fibre reinforced polymer (GFRP) composite materials have also proven to be strong, durable and lightweight which are all favourable characteristics in the construction industry (McMillan, 2017). Consequently, designing a new railway sleeper reinforced with GFRP bars could potentially help composite sleepers reach their expected 60 year design life without the need for ongoing maintenance and sleeper replacement. If successful, this newly designed sleeper could save Queensland Rail and rail companies around the world millions of dollars.

In order to correctly develop a concrete sleeper reinforced with GFRP bars, many parameters and standards must be considered. The development of concrete railway sleepers in Australia is governed

by the Australian Standard, AS1085.14; Prestressed concrete Sleepers (2012). This standard states that the design of a railway sleeper should be governed by flexural strength. For this investigation, consideration should also be given to the technical and performance specifications in TRACK-CT.172 set by Queensland Rail.

Although the popularity of GFRP bars continues to rise around the world, no codes or standards currently exist in Australia to govern the use of fibre composite reinforcement. Use of GFRP in Australia currently relies on the adoption of Canadian Standards called 'Design and Construction of Building Components with Fibre-Reinforced Polymers' (CSA S806-12) (Designing with composite Rebar, n.d). This problem is severely affecting the acceptance of GFRP materials in the Australian construction and civil industry. Consequently, more Australian based research is required to help develop new design standards and outline the limits of safe design using GFRP bars.

1.3 Alternative Materials

According to The Concrete Conundrum (2008), concrete is the most widely used material in the world as approximately 2 billion tonnes is produced per annum. This figure is set to double by 2050 as concrete is extensively used in many civil applications because it has many desirable characteristics such as high compressive strength, high temperature resistance, easy workability and highly durability. Its properties can also be easily manipulated to suit any strength or serviceability requirements. The most generic type of cement used to create concrete around the world is currently Portland cement. Cement is an essential ingredient in concrete mix design as it acts as a binding agent and gives concrete its strength when hydrated with water. However, a major downfall of the concrete industry is the magnitude of carbon dioxide created during the production of Portland cement.

Research outlined in The Concrete Conundrum (2008) estimates that one tonne of carbon dioxide emissions is produced per tonne of traditional Portland cement produced. This means that concrete production is responsible for 5% of all carbon dioxide pollution annually. Many companies have now realised that these pollution levels are unacceptable and not sustainable. This problem has prompted many companies around the globe to begin researching innovative solutions which could potentially reduce carbon emissions created from cement production. Companies are particularly researching the potential use of newly developed plasticisers, special admixtures and industrial waste products. In recent years, polymer concrete has emerged as a practical and more sustainable concrete product compared to traditional Portland concrete. According to research conducted by Aldred (2013), some polymer concrete products can surpasses some of the structural benefits of general concrete and can reduce carbon emissions by 80-90%. A study conducted by Ferdous et. al. (2016) also suggests

polymer concrete offers some rail specific benefits such as better durability in harsh climates, more resistant to cracking and its low modulus of elasticity makes it easier to attach tracks fasteners.

In relation to these claims, the adequacy of using polymer concrete to manufacture narrow gauge track railway sleepers should be investigated. Manufacturing a sleeper made from polymer concrete also meets the design brief set by Queensland Rail as they specifically want to design, manufacture and test alternative railway sleeper materials (Queensland Rail; QRP-15-150A Tender Information Report, 2016).

1.4 Purpose of Research

In a recent study, Baker (2018) has used AS1085.14 to determine the most critical loading conditions and hence the highest maximum theoretical bending moment and shear forces acting on a sleeper. Baker then proceeded to use these values to theoretically design and test a simple GFRP reinforced where the concepts feasibility was accessed. Baker concludes that it is plausible to design a functional GFRP reinforced sleeper but no physical experimental data exists to prove these claims.

Evidentially, a significant research gap exists here as there is a lack of physical testing which focuses on critically evaluating the performance of a GFRP reinforced railway sleeper. Physically evaluating the performance of a GFRP sleeper must be done in order to determine the sleepers true failure mode, evaluate the adequacy of shear and flexural reinforcement designed in accordance with finite element models and evaluating the severity of serviceability problems such as deflection and cracking. Physical testing could also be used to collect stress and strain data. Such data could be analysed to further understand the behaviour and performance of GFRP bars in lieu to steel reinforcement.

Performing physical testing also provides an opportunity to study and evaluate whether polymer concrete, an emerging product, is comparable or even better than traditional Portland concrete railway sleepers. As expressed by Aldred (2013), this product has evolved quiet rapidly in recent years and now has many benefits over traditional concrete. This recent spike in popularity justifies the need to conduct more research on polymer concrete and prove whether it does have significant benefits which benefits the performance of railway sleepers.

This research project has the potential to design and develop a much more sustainable sleeper which also has a longer design life compared to other sleepers currently available.

1.5 Project Aim

The aim of this research project is to successfully develop and evaluate the flexural performance of a GFRP reinforced railway sleeper in accordance with TRACK-CT.172 released by Queensland Rail and determine whether these sleepers are suitable for narrow gauge track applications. To determine the optimal amount of GFRP reinforcement required, a finite element model will be developed and used to determine maximum theoretical bending moments and shear forces acting on the sleeper. Loads acting on the sleeper will be determined in alignment with specifications set by Queensland Rail. In conjunction, two unique railway sleepers will be manufactured for comparison purposes; one from Polymer concrete and the other from ordinary Portland concrete. Although made from different concrete, these two sleepers will have the same reinforcement design. The aim is to evaluate the flexural performance of polymer concrete in contrast to Portland concrete. Results from this investigation will be used to conclude whether polymer concrete has any significant advantages in narrow gauge track applications.

1.6 Research Objectives

The objectives of this dissertation are summarised below.

1. Research the properties of polymer concrete and the behaviour of GFRP material as reinforcement
2. Review existing standards relating to railway sleepers and GFRP materials
3. Develop a finite element model of a railway sleeper in Strand7 to theoretically determine maximum bending moments and shear forces acting on the sleeper and predict the sleepers general behaviour under loading
4. Manufacture two railway sleepers based on the results of finite element analysis. The two sleepers shall be manufactured using Portland concrete and polymer concrete respectively. Experimental testing shall then be carried out at USQ's to individually evaluate the flexural performance and serviceability of both sleepers.
5. Critically analyse the data obtained from testing and compare the data to a developed theoretical model

6. Conclude whether polymer concrete has any noticeable advantages over traditional Portland concrete and whether the newly designed sleeper met the design criterion outlined in TRACK-CT.172
7. Provide comments on the overall performance of the sleeper and give recommendations if necessary

1.7 Scope and Limitations

Chapter 4 within TRACK-CT.172 outlines an extensive number of parameters which must be accessed to determine the overall performance of a railway sleeper. Some of these parameters such as fire resistance, thermal properties and ultraviolet radiation exposure are outside the scope of this research project while some would be hard test in the time frame permitted. Consequently, testing will focus on the following parameters as specified in TRACK-CT.172:

- The flexure of the sleeper in service
- Failure under ultimate loading
- Material strain failure based on characteristic or appropriately tested values
- Deflection under serviceability loading
- Local failure if any

A major limitation to consider during this study is time as this research project has a strict timeline of 35 weeks. Consequently, no testing will be done on the GFRP bars directly. This project will only evaluate and comment on how the material behaves when bonded with the concrete. Testing the sleepers durability will also be outside the scope of this study as testing will purely focus on the sleeper's flexural performance and whether the new design can meet serviceability requirements. Practical things such as manufacturing processes and the cost of an individual sleeper will also be disregarded.

The cost of materials for this project will not limit the scope of this research project as the university has a developed a strong partnership with Austrack Australia; a world leader in sleeper design and production. This company has recently renewed their partnership with USQ's Centre of Future Materials as they aim to stay ahead of their competitors by continuing to research new sleeper designs with a focus on utilising new materials. Consequently, any resources required for this investigation will be readily available.

1.8 Expected Outcomes and Benefits

As railway tracks are extensively used all around the world, findings from this report have the potential to benefit many companies. It is expected that this project can clearly determine whether GFRP reinforcement and polymer concrete can successfully be used together in narrow gauge track applications. If successful, this innovative sleeper could potentially save the rail industry millions per annum by reducing track maintenance costs.

This project is particularly interested in polymer concrete as it's a much more sustainable product compared to traditional Portland concrete. Although polymer concrete has a much lower modulus than other concretes, it is expected that a polymer concrete sleeper can successfully be manufactured and perform much the same or better than traditional concrete. However, as its modulus is much lower, more reinforcement or a special design might be required to reduce the degree of deflection.

As no codes or standards currently exist in Australia to govern the use of fibre composite reinforcement, further testing related to GFRP reinforcement in Australia is required. This research project provides a great opportunity to test GFRP bars and understand how they differ from traditional steel reinforcement. If this project is successful, it is expected that GFRP bars will become more popular in rail applications as they have the potential to increase a sleeper's design life. During testing, it is expected that the sleeper will deflect more than if the section was reinforced with steel as GFRP bars have a lower modulus than steel.

Although testing and design producers will be done in accordance with Queensland Rail and Australian Standards, it is expected that any technical advancements made during this project can easily be adapted to suit other regions of Australia and countries.

1.9 Dissertation Overview

To ensure all research objectives are met, the dissertation is structured into the following chapters:

Chapter 2 Literature Review

This chapter critically evaluates past research and literature available online. The literature review will particularly study text related to railway sleepers and how they are designed, the physical properties of GFRP bars and the advantages/disadvantages of polymer concrete.

- Chapter 3 Finite Element Analysis
This chapter will explain how the rail seat loads acting on the sleeper were calculated in accordance with TRACK-CT.172 and AS1085.14. This chapter will also explain how finite element models based on beam on elastic foundation theory were used to design the GFRP reinforcement.
- Chapter 4 Experimental Program
This chapter outlines any safety concerns, the equipment required and testing procedures. This chapter also explains the manufacturing process of each sleeper.
- Chapter 5 Non-destructive Test Observations, Results and Discussion
All observations and results from the non-destructive tests will be explained in this chapter. Any key findings related to the aim of this research project will be highlighted and discussed.
- Chapter 6 Destructive Test Observations, Results and Discussion
All observations and results from the destructive tests will be explained in this chapter. Any key findings related to the aim of this research project will be highlighted and discussed.
- Chapter 7 Conclusion
This chapter links all significant findings throughout this report to the research objectives. Future research areas and recommendations will also be provided.

1.10 Ethics and Consequences

All research within this report must be covered by a number of ethical publication standards to ensure that all findings are consistent and true. As this is an undergraduate research project, official publication of this report is restricted by the USQ; refer to the 'Limitations of Use' statement for further details. This statement clearly details that the author is solely responsible for the quality and integrity of the work completed. To help ensure that all findings are creditable and reliable, it is paramount that accurate referencing is used throughout the report as this adds a level of authenticity and gives others credit for their work/ideas which is also a legal requirement. Throughout this report, APA 6th referencing style will be used.

Some ethics must be implemented to ensure the safety of all participants during manufacturing and testing of railway sleepers. Before using the lab facilities and equipment at USQ, a safety induction must be completed. This induction clearly explains safety procedures, required personal protective equipment (PPE) and how to safely operate machinery. When manufacturing the sleeper, participants must be cautious of the risks associated with different materials. Fibre composite materials are particularly toxic when burnt and can also cause respiratory problems similar to asbestos if its fibres are released into the atmosphere (Doroudiani, 2012). Cement mixtures can also cause ill health by skin contact, eye contact, or inhalation (Cement Hazards and Controls, 2019). These health hazards have a low likelihood and can easily be managed using the correct PPE.

As sleepers are an integral structural component of rail infrastructure, the risk of failure must be minimised to ensure public safety. This means that both serviceability and strength requirements must equally be considered during the design process. If designed correctly, these sleepers should be safer than traditional timber and concrete sleepers as they are less likely to weather and corrode. However, as only a small sample size of sleepers will be tested during this project, it is recommended that more testing should be done to determine their average performance before implementing them in real-life track applications. Additional testing will help guarantee the public's safety.

Chapter 2 Literature Review

2.1 Chapter Overview

This chapter will critically analyse many sources of literature in order to determine how a railway sleeper is analysed and designed, the physical properties and advantages of GFRP reinforcement and the advantages of polymer concrete. This chapter will also be used to identify a suitable research gap and explain the feasibility of this particular research project. All Information compiled in this chapter must be in alignment with relevant Australian standards and design guidelines.

2.2 Railway Track Components

According to Kaewunruen and Remennikow (2008), Australia's railway system has experienced great deterioration in recent years due to population growth while more freight is being moved from rural areas of Australia due to increased mining activity. An increase in traffic has accelerated track deterioration while a lack of new infrastructure has created a high dependency on certain rail lines. As a result, some tracks cannot be maintained properly as they are being used so frequently. Ferdous and Manalo (2014) suggest that some track closures in Australia due to maintenance can cost companies up to \$10 to \$20 million per day in lost revenue.

Kaewunruen and Remennikow (2008) suggest that ballasted railway tracks are widely implemented around the world due to their simplistic design. Its components can be broken down into two categories: superstructure and substructure. The superstructure includes the structural elements of the track such as the rail, sleepers, fastening systems and rail pads while the substructure considers the geotechnical elements of the track which include the ballast, sub ballast and subgrade (refer to figure 1-2). The ballast layer is generally made from the interlocking of coarse, irregular shaped aggregates which provides good drainage and acts as a tensionless elastic support for the resting sleepers. This layer can act as a spring which can easily absorb shock and impacts while even helping to dampen noise and protect the track from unwanted vegetation growth.

Any loads generated by a passing train are initially absorbed by the fasteners and then transferred to the sleepers. Fasteners are therefore an essential component of the superstructure as they have to withstand significant vertical and horizontal loads. The loading distribution pattern acting on the sleeper is dependent on what type of fastener is used and its application. Fasteners also stop

overturning moments while importantly stopping the gauge of the rail roads from changing. A typical concrete fastening system is shown below in figure 2-1.

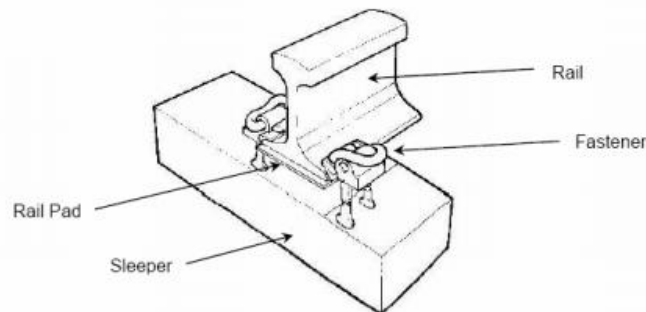


Figure 2-1: A typical concrete fastener (Kaewunruen and Remennikow, 2008)

Kaewunruen and Remennikow (2008) continues to explain that sleepers are responsible for uniformly distributing loads carried from the fasteners to the ballast bed and subgrade below. Sleepers traditionally lie semi-embedded in the ballast and sit perpendicular to the rails so they can resist longitudinal, lateral and vertical movements caused by large bending moments. Although typically made from timber, many different materials and designs are currently available. Designing a concrete railway sleeper is a complex process as many variables must be considered. TRACK-CT.172 outlines the many variables which can affect the design and overall performance of concrete railway sleepers (refer to Appendix B). It is important to note that the design of railway sleepers can vary depending on location and track gauge. The parameters discussed in TRACK-CT.172 are relevant to Queensland, Australia.

Kaewunruen and Remennikow (2008) explain that rail pads are another essential component of the superstructure as they are used to reduce the impact of dynamic loads caused by the train's moving wheels before being transferred to the sleeper below. Pads are generally made from polymeric compounds, rubber or composite materials as these materials have the capacity deform and adsorb such dynamic forces. Great care should be taken when installing and using rail pads as misuse increases the likelihood of the sleepers cracking.

2.3 Timber Sleepers

Timber sleepers were originally implemented due to their ease of use, availability and low cost. According to Ferdous and Manalo (2014), traditional timber sleepers are susceptible to rot, splitting and insect attack. However, timber sleepers also have many desirable characteristics such as excellent dynamic, electrical and sound-insulating properties. Timber sleepers are traditionally made from beech and oak wood but can be made from pine wood if hardwood timbers are not readily available (History and development of the wooden sleeper, n.d).

To improve the durability and expected design life of timber sleepers, a number of design principles are usually followed. The first design principle generally requires the timber to be stored for a significant period of time before being processed. Storing the timber helps to optimise the moisture content in the sleeper which ultimately helps to prevent cracking. Cracking can be further mitigated by attaching a crack prevention plate to the sleeper's ends after storing period (History and development of the wooden sleeper, n.d). The sleeper is then coated with creosote or a modern derivative called pigment emulsified creosote which is less toxic to humans. This treatment is used to deter insect infestation and helps to prevent wood rot and weathering (History and development of the wooden sleeper, n.d). As timber is a natural product, the exact behaviour of individual sleepers may slightly differ meaning it's impossible to control all failure mechanisms. Figure 2-2 shows the most common failure modes for timber sleepers.

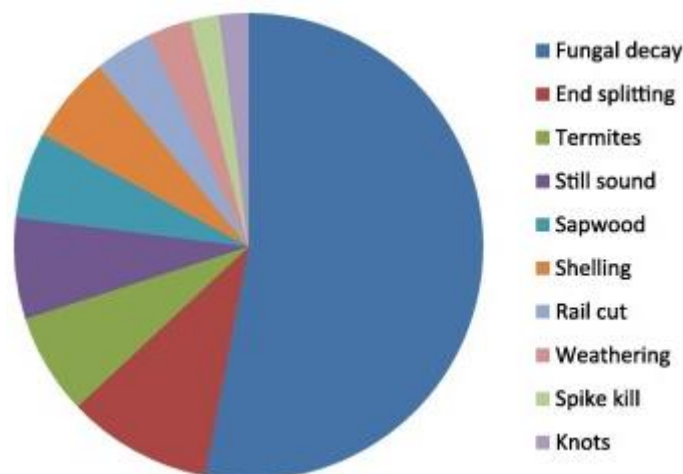


Figure 2-2: Common failure methods for timber sleepers (Ferdous and Manalo, 2014)

2.4 Precast Concrete Sleepers

According to Kaewunruen and Remennikow (2008), two types of concrete sleepers are currently available with both designs having strengths and weaknesses. A monoblock concrete sleeper spans underneath both rails while a twin-block concrete sleeper design has two smaller concrete blocks which independently sit under each rail. Ferdous and Manalo (2014) suggest that the current trend of the rail industry is to adopt concrete railway sleepers as they have many more favourable characteristics compared to traditional timber sleepers. Concrete sleepers have excellent strength and durability characteristics while being immune to bug infestation, easy to manufacture and are resistant to fire. Being fire resistant is a major advantage especially in Australia as large bushfires are common in rural areas where the majority of tracks exist. Around the world, high performance concrete sleepers are commonly being implemented in high-speed rail lines and heavy haul routes as they provide greater stability. Under loading, a concrete railway sleeper is usually subjected to the following stress distribution pattern as shown in figure 2-3.

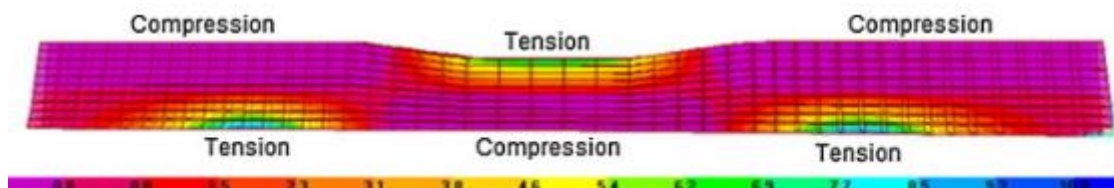


Figure 2-3: Stress distribution pattern on a concrete sleeper (Bezgin 2017)

Ferdous and Manalo (2014) have identified that concrete sleepers are not a perfect solution as they can be expensive, heavy, have a low impact resistance and require specific fasteners. A significant problem with concrete sleepers is their relatively high stiffness. Due to their high stiffness, concrete sleepers are particularly susceptible to cracking under high live loads at the rail seat. According to Gribniak, Rimkus, Torres and Hui (2018), cracking is the leading cause of deterioration in regards to reinforced concrete as cracking exposes the sections internal reinforcement which is susceptible to corrosion once exposed to moisture. Other common modes of failure experienced by concrete sleepers are shown in figure 2-4.

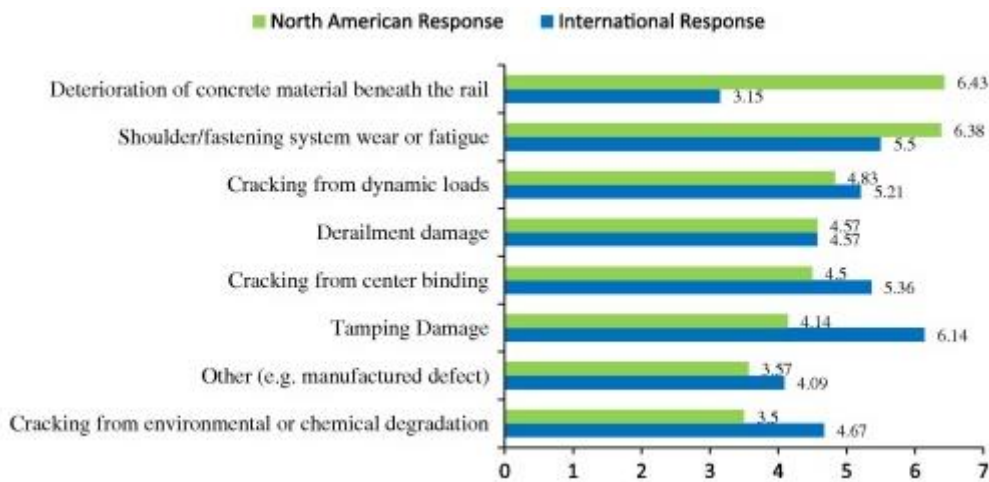


Figure 2-4: Common modes of failure experienced by concrete sleepers (Ferdous and Manalo, 2014)

2.5 Fibre Composite Sleepers

According to Ferdous and Manalo (2014), many companies around the world are investigating and trying to develop new sleepers from a range of different recycled plastics, fibre composites, rubber or even a combination of these materials. These sleepers could potential to be a sustainable alternative to traditional concrete and timber sleepers as some incorporate recyclable materials. This broad domain can be separated into 3 main categories; Sleepers with short or no fibre reinforcements, sleepers with long fibre reinforcement in the longitudinal direction and sleepers with fibre reinforcement in longitudinal and transverse directions.

The first classification, sleepers with short or no fibre reinforcements, refers to sleepers which consist of recycled plastics or bitumen and fillers only. The performance of these sleepers is dependent on the strength of individual polymer bonds as these sleepers do not have any internal reinforcement. Without reinforcement, these sleepers are currently restricted to light rail applications only as current materials and production techniques cannot manufacture a sleeper that can endure the demands of other rail applications. Besides their lack of strength, these sleepers have many desirable characteristics such as easy workability, low cost while being durable.

The second classification, sleepers with long fibre reinforcement, refers to sleepers which are reinforced with fibre composite materials such as GFRP bars. These sleepers can easy be integrated into existing ballast tracks and can be used in heavy rail applications. Some advantages of these sleepers include: easy to drill and cut, excellent durability and superior flexural strength. As these sleepers have many favourable characteristics, their popularity has increased dramatically in recent

years. This trend has triggered an increase in research into sleepers with long fibre reinforcement. However, the use of these sleepers is currently restricted due to high manufacturing costs and concerns about meeting serviceability requirements.

The third classification refers to sleepers made from polymer or composite materials which are configured into different lattice structures. This type of design provides the sleeper with longitudinal and transverse reinforcement which ensures the sleeper has superior mechanical performance. This design also enables the amount of flexibility to be controlled. However, current production processes and costs make these sleepers impractical.

2.6 Precast Concrete Railway Sleeper Standards

Australian Standard AS1085.14 (Railway track material part 14: Prestressed concrete sleepers), is used as a guide to develop and test concrete railway sleepers in Australia. These standards outline how to determine the axial load acting on the sleeper, structurally analyse the sleeper and how to perform a number of standardised tests to determine some the sleeper's characteristics.

According to clause C2.1 in AS1085.14, the overall performance of a sleeper is controlled by the condition of the rail, joints and the rail fastening system. However, when performing tests on concrete sleepers, each rail component should independently be examined. This statement means that a concrete sleeper can be individually tested and it's the performance evaluated without considering the use of different fastening systems.

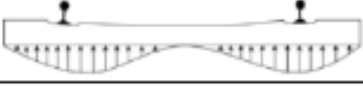
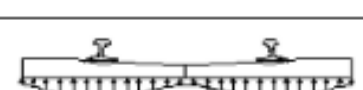
2.7 Designing a Railway Sleeper

Accurately predicting a sleeper's flexural performance is very important as it helps ensure the safety of the public. In today's society, trains are typically loaded to their maximum capacity to handle higher freight demands while technological advancements have enabled trains to travel at higher speeds. Consequently, sleepers must be able to withstand higher axle loads than in the past. According to Sadeghi and Youldashkhan (2005), some analysis methods have become outdated and cannot accurately determine some critical design parameters such as maximum bending moment, shear force and deflection. This means a sleeper could unexpectedly fail under increased loading if no amendments are made to the design and analysis processes. The study concludes that analysis methods must evolve and be more carefully when considering the effects of the following parameters: stress distribution under the sleeper, the type of rail-seat load (distributed or point load) and the

dynamic coefficient factor. Some consideration should also be given to parameters such as track lifecycle costs and passenger riding comfort.

Sadeghi and Youldashkhan (2005) states that the flexural performance of a sleeper is primarily governed by the condition of the ballast underneath the sleeper as it determines the bearing distribution pattern. This parameter directly affects the sleeper's ability to effectively transfer vertical loads to the ground. The condition of the ballast is normally based on the degree of voiding which is affected by the amount of traffic, aggregation quality of the ballast, amount of tamping, erosion and the geotechnical properties of the subgrade. Some of the sleeper's mechanical properties such as its rigidity can also affect the bearing distribution pattern. Determining the bearing distribution pattern is typically the first phase in the design process as it can servilely affect the sleeper's maximum bending moment. According to Manalo et. al. (2012) variations in support modulus between 10MPa to 40MPa can increase the maximum bending moment by approximately 15%. It is important to mention that the design bearing pressure exerted by a sleeper on the supporting ballast shall not exceed 75 MPa under any circumstances (TRACK-CT.172, 2015). According to Abbasi & Ali Zakeri (2013), various hypothetical bearing distribution patterns have been developed in an attempt to accurately predict the exact bearing distribution in real life track applications. These are summarised in Table 2-1.

Table 2-1: Possible bearing distribution patterns underneath a sleeper (Abbasi & Ali Zakeri, 2013)

Distribution of contact pressure underneath the concrete sleeper	Description	Developer
	Uniform distribution	AREA [8], Talbot [15], Raymond [16]
	According to laboratory test	ORE [9], Talbot [17]
	Maximum pressure under the rails	ORE, Talbot [15]
	Concentration of pressure in sleeper center	Talbot [17]
	Tamping effects and ballast compaction in the vicinity of rails	ORE [9], Talbot [15], Bartlett [18], Clark [19]
	According to field test	Zakeri and Sadeghi [2]

Although many bearing distribution theories exist, only two methods are accepted in Australia. These two methods are clearly outlined in AS1085.14. One of the theories is known as the empirical method and the other is known as the analytical method which assumes the sleeper is sitting on an elastic foundation. Both of these models will be explained further in section 2.7.1 and 2.7.2.

2.7.1 Empirical Method

According to AS1085.14, this method is conservative and simulates the track just after being tamped. This means there is little to no contact between the ballast at the centre the sleeper. The maximum positive design bending moment along the entire length of the sleeper occurs directly underneath the rail seat (M_{R+}) causing compression stress at the top of the sleeper and tensile stress at the bottom. The bearing pressure distribution pattern shown in figure 2-5 should be used to calculate M_{R+} .

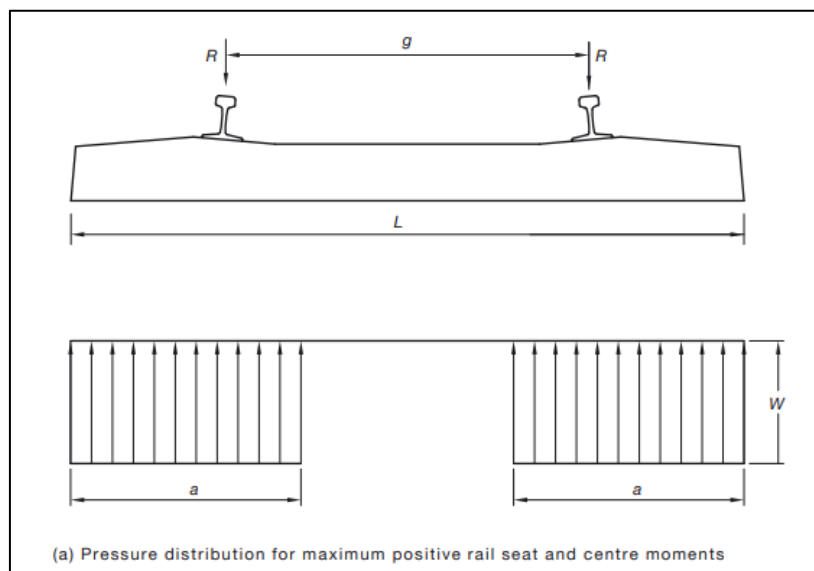


Figure 2-5: Empirical bearing distribution when calculating M_{R+} (AS1085.14, 2012)

Meanwhile, a negative design bending moment at the rail seat (M_{R-}) shall be taken no less than 67% of M_{R+} . Along with M_{R+} and M_{R-} , design positive and negative bending moments at the centre of the sleeper, M_{C+} and M_{C-} respectively, can be determined using the equations in derived in Table 4.1 from AS1085.14; refer to Appendix C.

When calculating M_{C-} , the bearing distribution pattern should be altered so the sleeper remains in contact with the ballast along its entire length; refer to figure 2-6. This causes tensile stress at the top of the sleeper and compressive stress at the bottom.

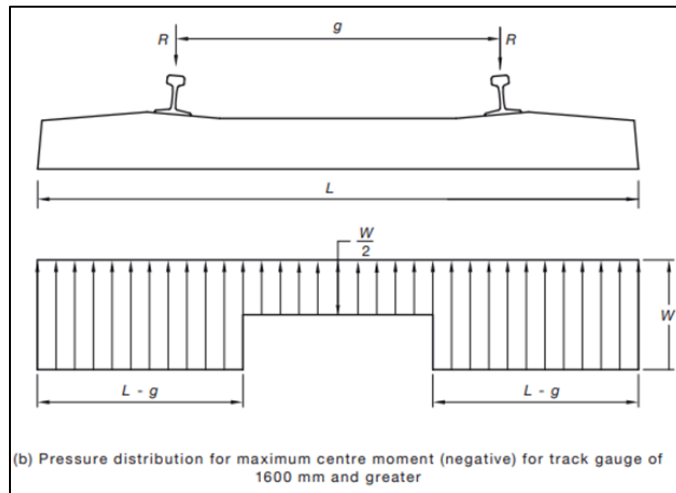


Figure 2-6: Empirical bearing distribution when calculating M_c - (AS1085.14, 2012)

2.7.2 Analytical Method

According to Australia Standard; AS1085.14 (2012), this method of analysis was originally derived by Hetenyi in 1967 and is used to represent a finite beam loaded by two equal concentrated forces placed symmetrically. One of the major assumptions associated with this method is that the sleeper sits on an elastic foundation (BOEF). A schematic diagram of the BOEF method is shown in figure 2-7. The BOEF method is used to accurately determine bending moments and deflections depending on the sleepers bearing pressure. The BOEF method is generally favoured over the empirical method as calculations yield results very similar to finite element models which are developed using computers. This means that the BOEF method can be used to verify and assess the accuracy of user defined finite element models.

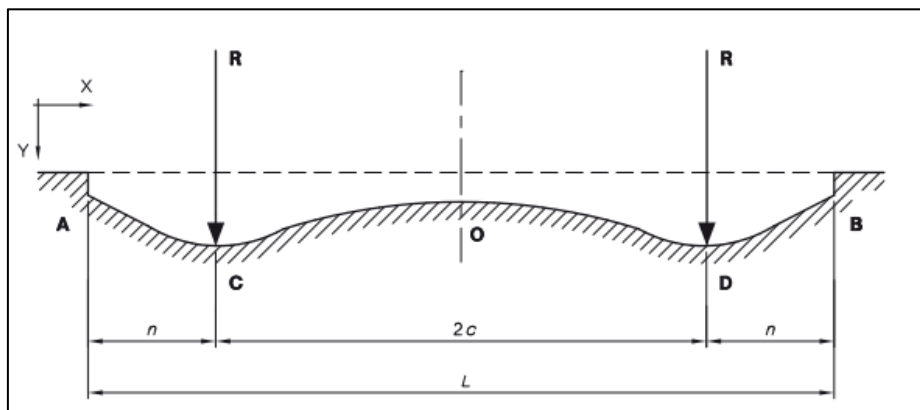


Figure 2-7: A schematic diagram of the BOEF method (AS1085.14, 2012)

In accordance with figure 9, a moment coefficient factor can be calculated at any point between A and C and at the mid span of the beam. The following equations can be used to find the moment coefficient factors:

Bending moment along portion A to C (x varies from 0 to n)—

$$C_{BM(x)} = \frac{1}{2\lambda} \frac{1}{\sinh \lambda L + \sin \lambda L} \{2 \sinh \lambda x \sin \lambda x [\cosh \lambda n \cos \lambda(L-n) + \cosh \lambda(L-n) \cos \lambda n] + (\cosh \lambda x \sin \lambda x - \sinh \lambda x \cos \lambda x) [\cosh \lambda n \sin \lambda(L-n) - \sinh \lambda n \cos \lambda(L-n) + \cosh \lambda(L-n) \sinh \lambda(L-n) \cos \lambda n]\} \quad (1.1)$$

Bending moment at sleeper centre ($x = L/2$)—

$$C_{BM(o)} = \frac{1}{2\lambda} \frac{1}{\sinh \lambda L + \sin \lambda L} \{ \sinh \lambda c [\sin \lambda c + \sin \lambda(L-c)] + \sin \lambda c [\sinh \lambda c + \sinh \lambda(L-c)] + \cosh \lambda c \cos \lambda(L-c) - \cos \lambda c \cosh \lambda(L-c) \} \quad (1.2)$$

Where: x = distance from the end of the sleeper (m)
 n = distance from sleeper end to rail seat load (m)
 U = sleeper support modulus (Pa)
 I_s = sleeper moment of inertia about horizontal neutral axis (mm^4)
 c = distance from rail seat load to centre of sleeper (m)
 λ = sleeper stiffness parameter
 E_s = Young's modulus of sleeper (MPa)

After calculating the moment coefficient factor, the design bending moment can be calculated using the following equation:

$$M_d = RC_{BM(Max)} \quad (1.3)$$

Where: R = Design rail seat load

$RC_{BM(Max)}$ = The greater moment coefficient factor out of $C_{BM(x)}$ and $C_{BM(o)}$.

The largest bending moment generally occurs immediately beneath the rail seat. This means the greatest moment coefficient factor is usually equal to $C_{BM(x=n)}$.

The BOEF method can also be used to estimate the sleeper's maximum deflection. Maximum deflection can be calculated using the following equation:

$$y_{\max} = \frac{R\lambda}{2U} \frac{1}{\sinh \lambda l + \sin \lambda l} \left[2 \cosh^2 \lambda n (\cos 2\lambda c + \cosh \lambda l) \right. \\ \left. + 2 \cos^2 \lambda n (\cosh 2\lambda c + \cos \lambda l) + \sinh 2\lambda n (\sin 2\lambda c - \sinh \lambda l) \right. \\ \left. - \sin 2\lambda n (\sinh 2\lambda c - \sin \lambda l) \right] \quad (1.4)$$

2.8 Calculating the Rail Seat Load

According to Barkan et. al (2014), the type and magnitude of loading acting on a concrete railway sleepers governs its performance. Many formulas have been developed over time in an attempt to accurately predict wheel loads acting on an individual sleeper. Some common parameters which must be considered when calculating a wheel load are: the spacing between sleepers, the track modulus, weight of the passing train, the sleeper's stiffness, rail pad stiffness and speed of the passing train.

In reality, a sleeper can experience up to four different types of loads; static, quasi-static, dynamic and impact loads. Static loading occurs when the train is at rest hence only the dead load of the train acts on a sleeper. The term Quasi-static loading can be summarised as a combination between the static load and the effects of the static load at speed, independent of time. Dynamic loads are much harder to quantify as they consider loads associated with high-frequency effects of the wheel/rail interaction and the performance of individual track components. Lastly, impact loads are often intense over a short time period and generally occur due to track or wheel irregularities. A number of rail seat load calculation methodologies have been modified over time in an attempt to incorporate and accurately account for more of these loading types.

According to Barkan et. al (2014), the American Railway Engineering and Maintenance Association (AREMA) have widely accepted the use of three rail seat load approximation methodologies. These three methods are: AMEMA, Talbot and Kerr. Table 2-2 provides a basic overview of the three methods and what parameters each method takes into account.

Table 2-2: Rail seat load calculation methods (Barkan et. al, 2014)

Dynamic factor	Expression for rail seat load (metric)	Parameters Included						
		Train speed	Wheel diameter	Static wheel load	Sleeper spacing	Modulus of elasticity	Moment of inertia	Track modulus
AREMA ⁸	$(61.52x + 12.811)P/100$			•	•			
Talbot ¹²	$\frac{(P + 0.01P(0.62V - 5)) \times S \times \sqrt[4]{\frac{10.41u}{EJ}}}{.051}$	•		•	•	•	•	•
Kerr ¹⁴	$\frac{(1 + 0.52\frac{v}{D}) \times P \times \alpha \times \sqrt[4]{\frac{10.41k}{EJ}}}{.051}$	•	•	•	•	•	•	•

Variable	Definition	Standard value (metric)
V, v	Train speed	96.56 km/h
D	Wheel diameter	91.44 cm
u, k	Track modulus	41.37 N/mm ²
x, a, S	Sleeper spacing	0.61 m
P	Static wheel load	14,912 kg
I	Moment of inertia	3900 cm ⁴
E	Modulus of elasticity of rail	206,843 N/mm ²

After reviewing Table 2-2, it is apparent that each approximation method has been developed to incorporate more parameters over time. Consequently, the accuracy of each load approximation method has also improved. It is therefore critical that more modern rail seat approximation are used as older methods may either overestimate the rail seat load, increasing the cost of reinforcement materials or underestimate the rail seat load, which might lead to premature sleeper failure.

According to Barkan et. al (2014), all load approximation methods generally begin with static load analysis. The AREMA method requires the least number of inputs as this method is a static only analysis. Meanwhile, Talbot and Kerr methods both have additional inputs to account for dynamic loading and changing track conditions. Accurately estimating the rail seat load is very important as these loads directly affect the magnitude of moment, shear force and deflection; the three parameters which govern the design of concrete railway sleeper.

When incorporating the trains speed into the rail seat load calculations, Barkan et. al (2014) found that the Kerr method yields the highest rail seat load compared to the Talbot method as it assumes a

greater track modulus. The tracks modulus is greater in the Kerr method to account for tracks situated in colder climates. This also justifies why different parameters are used for track modulus in Table 2-2 (u and k). For comparison, the theoretical rail seat load calculated using the Kerr method is 32% greater than the Talbot method when a train is travelling at 100km/hr. When comparing results, Barkan et. al (2014) found conflicting trends when comparing the accuracy of rail seat load approximations with laboratory testing and field testing. Evidently, Barkan et. al (2014) concludes that the tracks support condition such as its modulus and the degree of tamping has the greatest impact on the actual rail seat load. This means the accuracy of rail seat load approximations can be improved by using real life track modulus measurements instead of approximate values given by standards.

The rail seat load equations proposed in AS1085.14 are also widely accepted and can be used to accurately estimate a rail seat load. In section 3 of AS1085.14, Clause 3.1 states that the standards shall be used to calculate static wheel load (Q) which is then factored to take into account a number of track and vehicle variables. This factored vertical wheel load (P_{dv}) can be approximated as two point loads acting on the sleeper at a distance equal to the tracks gauge width. These loads are then distributed through the rail seat to find the rail seat load (R_v). Once the rail seat load has been calculated, sleeper stresses and deflections can be determined.

Equations given in Australian Standard; AS1085.14 (2012) are:

$$P_{dv} = k_s \times Q \quad (1.5)$$

Where: $k_s = \text{Dynamic coefficient factor}$
 $Q = \text{Static wheel load}$

Both of these parameters can be determined in accordance with TRACK-CT.172; Appendix B.

Now:

$$R_v = \frac{P_{dv} \times DF}{100} \quad (1.6)$$

Where: $DF = \text{Axle Load distribution factor}$

2.9 Axle Load Distribution Factor

Barkan et. al (2014) states that a wheel load being applied to the rail is distributed over several sleepers, even when the wheel is located directly above a single sleeper. Therefore, the spacing of individual sleepers is a critical parameter to consider when calculating the design rail seat load. According to TRACK-CT.172, spacing of a sleeper in Queensland cannot exceed 685mm.

When calculating the design rail seat load, an axle Distribution Factor (DF) is usually applied to approximate the distribution of load from an individual axle over multiple sleepers. According to Manalo (2012), a DF of 48% simulates the worst case scenario. The distribution factor for 47kg/m rails can also be determined in accordance with figure 2-8 provided in AS1085.81.

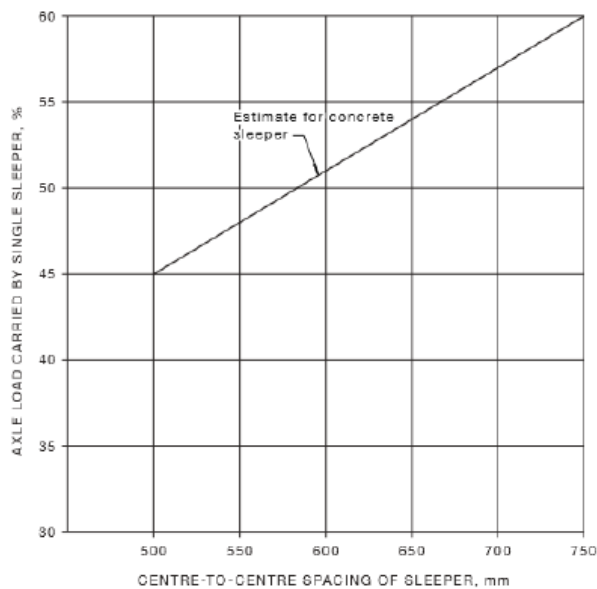


Figure 2-8: Empirical chart used to obtain the DF (AS1085.14, 2012)

2.10 Dynamic Load Coefficient Factor

It is very complex to calculate the exact vertical force acting on a sleeper as real loads are considered dynamic. According to Bezgin (2017), many studies have investigated different methods to determine an appropriate static axle load. It was concluded that the static load is mainly dependent on the trains speed, axle suspension system, wheel diameter, sleeper spacing, train/freight weight and overall track conditions. To accurately account for the load being dynamic, a factor is generally applied to the static rail road. According to Australian Standard AS1085.14-2003, the life cycle of a precast concrete sleeper is based on 50 years meaning a load factor of 2.5 should be used to increase the static axle load to incorporate dynamic effects (Kaewunruen, Martin and Remennikov, 2008). This value is also agreed upon by standards set out in TRACK-CT.172.

2.11 Rail Gauge Width

As shown in figure 2-9, considerable gauge differences still exist across Australia. According to Merkert & Hensher (2014), a lack of consistency has particularly hampered the movement of passengers between capital cities within Australia. Having multiple gauge widths also introduces many engineering implications. The magnitude of the bearing pressure provided by the ballast underneath is also affected as sleepers used in wide gauge track applications are generally longer in length. This is significant as Manalo et. al. (2012) has found that variations in support modulus can increase the maximum bending moment.

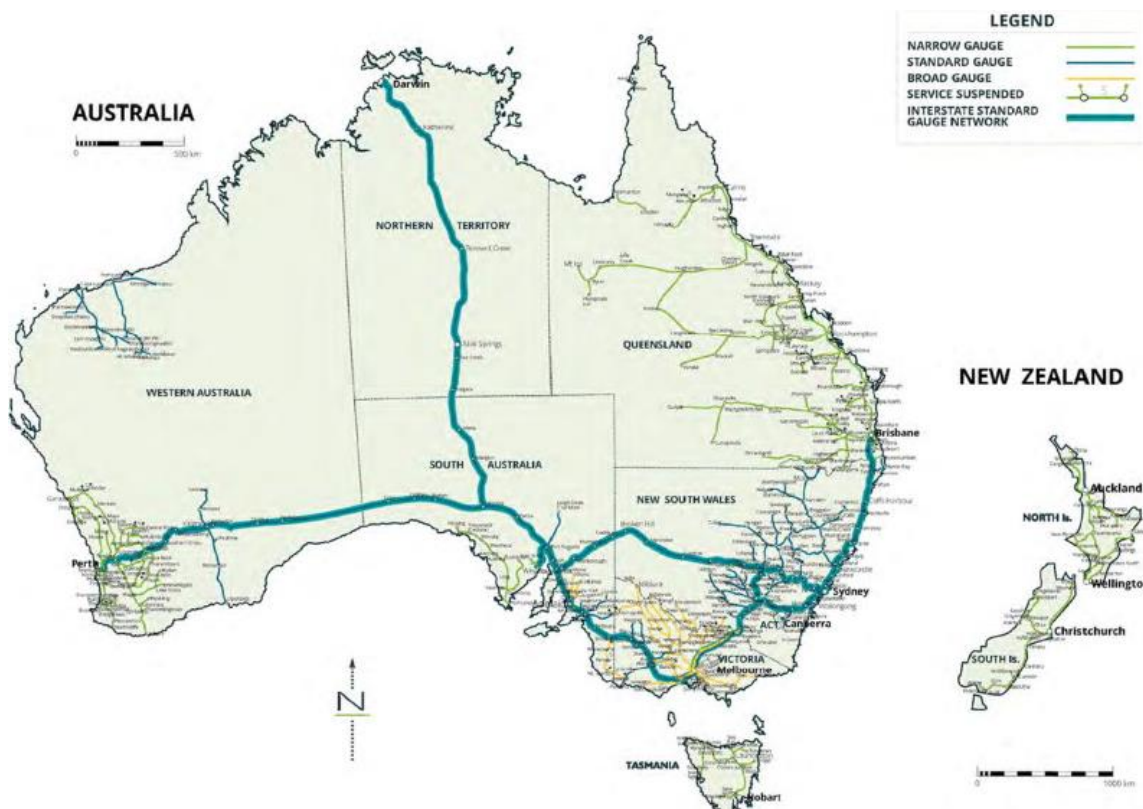


Figure 2-9: Different gauge tracks across Australia (Merkert & Hensher, 2014)

Three common gauge widths are used throughout Australia. The three common gauge widths are shown in table 2-3. As seen in figure 2-9, narrow gauge track is predominately used throughout Queensland hence this track type will be analysed throughout this entirety of the research project.

Table 2-3: Common track gauges in Australia (Merkert & Hensher, 2014)

Gauge Type	Width (mm)
Narrow track	1067
Standard track	1435
Broad track	1600

2.12 Dimensions of a Sleeper

Clause 2.3.2 from AS1085.14 suggests that the dimensions of a sleeper may vary slightly and its cross-section may not be uniform. The length of a sleeper is dependent on the tracks gauge while the width is usually determined by the allowable bearing pressure. As specified in TRACK-CT.172 in appendix B, a standard size, main sleeper in Queensland should have the following dimensions as shown in table 2-4.

Table 2-4: Basic dimensions and characteristics of a sleeper (TRACK-CT.172, 2015)

Sleeper Type	Dimension	Design Dimensional Envelope	
		Minimum (mm)	Maximum (mm)
Main line sleepers – Standard narrow track	Length	2125	2175
	Width at base	225	255
	Depth at rail seat	110	125

2.13 Glass Fibre Reinforced Polymer

According to Sheikh and Kharal (2018) GFRP is an alternative high performance product which can replace traditional rebar. The composite material is comprised of many strong individual glass fibres which are bonded together by a durable bonding resin which may either be epoxy or polyester. The resin doubly acts as a protection barrier which prevents the fibres from experiencing weathering and chemical attack while helping to be evenly transfer stresses between all fibres. When these fibres are compressed together and bonded by the resin, a strong and stiff material is formulated. A study done by Sheikh and Kharal (2018) has found that fibre composite materials have the ability to have a higher stress capacity than steel and acts linear elastic until failure. Hu and Liu (2010) explains that the glass fibres are made predominately from silica sand and other minor ingredients which are heated to high temperatures until molten glass is formed. The molten glass is then forced through a mould with small holes ranging from 5 to 24 μm to form fine strands. Once these strands are then cooled, they are

gathered and wound together to form fibre creel. Pultrusion technology is then commonly used to impregnate the fibres with resin to form the GFRP bars; refer to figure 2-10.

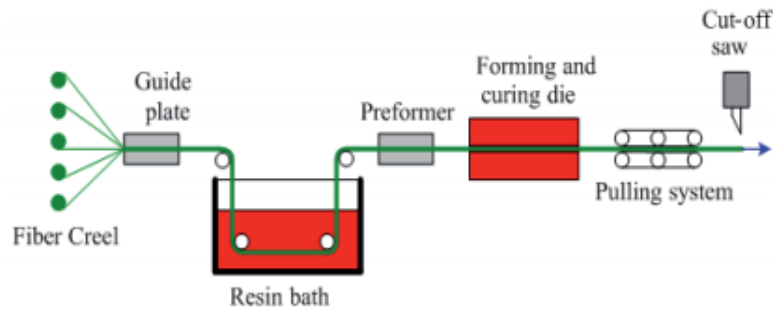


Figure 2-10: Pultrusion method (GFRP Components for Facades, n.d)

2.13.1 Tensile and Compressive Strength

An experimental study carried out by Jabbar and Farid (2018), highlights that GFRP cannot directly be substituted with steel in reinforced concrete design as some key mechanical properties differ between the two materials. Experimentation involved testing and comparing the tensile strength, bending strength and compressive strength of unreinforced concrete, smooth GFRP reinforced concrete, sand coated GFRP reinforced concrete and steel reinforced concrete. Results confirmed that GFRP bars have very good strength in tension as they are capable of having a higher yield strength compared to traditional steel rebar. However, to avoid creep rupture, codes released by American Concrete Institution recommends that a strength reduction factor should be applied to the ultimate tensile strength (GFRP Characteristics and Behaviours, 2018).

Results from a study conducted by Sheikh and Kharal (2018) found that GFRP bars used in compressive applications can resist stress levels up to about 60% of the bars tensile strength. However, when GFRP bars were used as longitudinal reinforcement in columns, the column demonstrated a lower strength and stiffness compared to similar columns with steel reinforcement. This demonstrates that GFRP bars are not always better than steel reinforcement in every application.

2.13.2 Modulus of Elasticity

When testing the bending strength, Jabbar and Farid (2018) found that the strain percentage at initial failure was greater compared to steel. Consequently, GFRP rebars experience much greater deflections before failure. This is significant as the design and application of GFRP reinforcement can be governed by serviceability requirements whereas steel designs are generally controlled by

ultimate limit states. Research done by El-Nemr et. al. (2018) confirms that GFRP bars can experience greater deflections than steel as its modulus of elasticity is approximately 25% less than mild steel.

Experimental data collected by Jabbar and Farid (2018) found that specimens reinforced with GFRP bars were not capable of achieving the same strength characteristics as sections reinforced with steel. Their results are shown in the stress vs strain diagram in figure 2-11. To achieve the same flexural performance as steel, Jabbar and Farid (2018) suggests that the percentage of GFRP reinforcement should be increased. However, this modification isn't that desirable as the section may become over-reinforced thus making the section inefficient. This means that the full strength of each GFRP bar won't be utilised before the concrete starts to crush. Interesting, figure 2-11 also indicates that the sand coated GFRP reinforced section experienced a brittle failure whereas the steel reinforced section experienced a ductile failure.

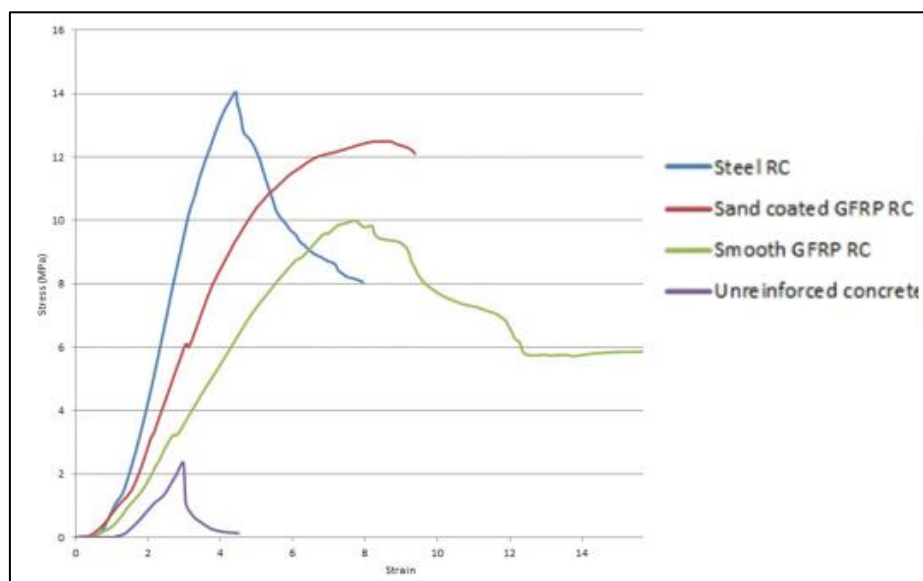


Figure 2-61: Bend tests conducted on different concrete sections (Jabbar and Farid, 2018)

A reduction in the bars modulus of elasticity can also lead to more significant and wider cracking. This was proven by Gribniak, Rimkus, Torres and Hui (2018) as this research compared the cracking patterns of beams with varying types of GFRP bars with changing stiffness. Results suggest that a decrease in stiffness leads to increased beam deformation and hence greater cracking. This is undesirable as cracking is the main cause of deterioration in reinforced concrete as it allows moisture to easily penetrate the concrete. In severe cases this can lead to spalling which can directly expose the reinforcement to the environment.

2.13.3 Bond Strength

Figure 13 also highlights how the bond strength between the reinforcement and the concrete can greatly impact the specimen's performance. The graph clearly shows that the GFRP bar which was coated with coarse sand was able to sustain a greater stress than the smooth GFRP bar. Testing conducted by El-Nemr, Ahmed, El-Safty and Benmokrane (2018) confirms that an outer sand-coating on the GFRP bar enhances the bond performance in concrete compared to bars with a helically-grooved surface or a smooth surface. The bond strength of each GFRP bar was individually determined using a standardised pull-out test. According to Arias, Vazquez and Escobar (2012) the rough granular surface is able to significantly increase friction and interlocking forces between the bars and the concrete. This enables sand coated GFRP specimens to endure larger loadings before failure as stresses are more readily transferred from the concrete to the GFRP bars which have a much higher tensile strength.

2.13.4 Non-corrosive Behaviour

Fibre composite materials are widely known for their non-corrosive properties. This characteristic is desirable as traditional steel reinforcement is susceptible to chemical attack which can weaken and cause premature structural failure. However, as fibre composite technologies are still relevantly new, many industry professionals fear that the performance and lifespan of fibre composite materials are being overestimated. These fears have been developed as many structures which utilises fibre composites have not yet reached the later years of its expected serviceability life. Therefore, the durability and lifespan of fibre composite materials have only really been determined by accelerated degradation testing. Laboratory testing has found that GFRP bars are not totally resistant to chemical attack and weathering. Yan, Lin, Zhang, Gao and Li (2017) has determined that GFRP bars are sensitive to alkaline environments, moisture, extreme temperatures and freeze thaw cycles. Results show that these climatic conditions have negative impacts on the fibres tensile strength, ultimate strain and modulus of elasticity. A cover 3 times the thickness of the reinforcement bar was deemed to be too small to sufficiently protect the GFRP bars from freeze thaw cycles as failure occurred after 75 cycles while the bars modulus of elasticity was greatly reduced by 26%.

Other testing by Fergani et. al. (2018) proved that the mechanical properties of GFRP bars are significantly affected by moisture penetration. Results gathered from experimentation found that moisture was able to diffuse through micro-cracks in the protective resin when the specimen was submerged in an alkaline solution. This process then initiated the breakdown of some chemical matrices in the glass fibres which resulted in a reduction of strength. The breakdown rate was

controlled by temperature and the concentration of alkali. Alachek, Reboul and Jurkiewicz (2018) found that specimens which were submerged in water for 10 months showed the greatest bond degradation with a 71% reduction in shear strength.

2.13.5 Using GFRP as Reinforcement

When designing traditional reinforced concrete sections, an under-reinforced section is considered desirable as the full strength of the steel will be utilised before failure. Special consideration is given to the neutral axis parameter (k_u) to ensure that the steel bars yield before undergoing a ductile failure. This type of failure is more favourable than brittle failure as the bars will deflect greatly before failure meaning engineers can potentially notice and repair structures before catastrophic failure occurs. To ensure yielding, engineers must design the concrete section so k_u which is a ratio of the ultimate strength under any combination of bending and compression between the neutral axis depth and the most extreme compressive fibre is less than 0.545. If this value is exceeded, the section is then considered to be over reinforced. This is undesirable as the section could failure without warning due to concrete crushing. A reinforced section can be further optimised if k_u is less than 0.36. If this condition is met, a balanced condition is achieved meaning the design will instantaneously fail due to the concrete crushing and the steel bars yielding. This type of design is desirable as it ensures that the section has the highest possible capacity.

Unfortunately due to some key parameter differences, these exact principles cannot be applied to sections reinforced with GFRP bars. As GFRP bars do not yield like steel, it is impossible to achieve the same balanced failure criterion as GFRP bars only act linear elastic until immediate failure. GFRP reinforced segments are also commonly over reinforced as its modulus of elasticity compared to steel. This means many GFRP designs fail via concrete crushing. Testing conducted by Khorrarnian and Sadeghian (2017) on short concrete columns reinforced with GFRP bars found that each test failed due to concrete crushing while all GFRP bars showed no sign of failing at peak load. This was determined as the strain gauges which were attached to individual GFRP bars indicated that the bars only reached 50% of their predicted strain capacity. Further testing conducted on GFRP reinforced beams by Gu, Yu and Wu (2016) determined a number of factors which clearly influenced the performance of GFRP reinforcement. A number of their key findings are listed below:

- Small bar diameters are desirable as the peak bond strength decreases when the bars diameter increases
- The shear strength of GFRP bars is generally 20% of its tensile strength

- GFRP reinforced specimens achieve about 60% of the bond strength compared with the steel reinforced
- At the same reinforcement ratio and geometric size, GFRP and steel reinforced beams roughly have the same bearing capacities. However, GFRP reinforced beams have much poorer crack control.

2.14 GFRP Reinforcement Standards

The most widely accepted and recognised standard relating to the use of fibre composite material in the construction industry has been developed in Canada; CSA S806-12 Design and Construction of Building Components with Fibre Reinforced Polymers (2012). Australia currently has no codes to guide engineers on how to safely design GFRP reinforced structures. This is a major constraint which is currently affecting the acceptance of fibre composite reinforcement materials in Australia.

2.14.1 Flexural Reinforcement

When considering the flexural capacity of a section reinforced with GFRP bars, consideration should be given to Clause 7.1.2.2 from CSA S806-12. This clause states that when GFRP bars are used for structural purposes, the tensile stress in the bars fibres under sustained loads shall not exceed 25% of its tensile failure stress. According to Gardoni et. al (2009), there is two reasons why a reduction factor must be applied to the ultimate tensile strength of GFRP bars. Firstly, research shows that the tensile capacity of GFRP bars is a function of time as they tend to deteriorate in harsh environments while the materials low modulus of elasticity must be taken into consideration. Essentially, applying a reduction also helps to avoid creep-rupture and fatigue related failures (Prince Engineering, n.d). Even though a reduction factor shall be applied to GFRP bars during the design processes, their design tensile strength can still be significantly higher than steel bars (Prince Engineering, n.d).

The design processes for flexural reinforcement outlined in CSA S806-12 and Australian Standard: Concrete Structures (AS3600) is very similar. Both standards have the same key design principle while the majority of assumptions are also the same:

Main Design Principle

- **Equilibrium:** All external forces and moments acting on the section should equal all internal forces and moments

Assumptions

- A perfect bond exists between the concrete and the bars
- Strain distribution over the depth of the section remains linear
- The tensile strength of the concrete can be ignored
- The actual curvilinear stress block of concrete in compression can be represented by an equivalent rectangular stress block
- AS3600 states that the max shear strain cannot exceed 0.003

Significant flexural design equations outline in CSA S806-12 are listed below:

$$M^* = T_z = C_z \quad (1.7)$$

Where:

$$T_z = \phi \left(A_{GFRP} * \sigma_u * \left(d - \frac{\beta_1 c}{2} \right) \right) \quad (1.8)$$

As T = C, the following equation can be derived:

$$\beta_1 c = \frac{A_{GFRP} * \sigma_u}{\alpha_1 * f'c * b} \quad (1.9)$$

The area of GFRP reinforcement required (A_{GFRP}) can be found by combining equations 1.8 and 1.9 together and solving for A_{GFRP}

$$M^* = \phi \left(A_{GFRP} * \sigma_u * \left(d - \frac{A_{GFRP} * \sigma_u}{2 * \alpha_1 * f'c * b} \right) \right) \quad (1.10)$$

Where:

- | | |
|---|---|
| • M^* = Maximum moment | • b = width of beam |
| • T_z = Tensile force times lever arm | • c = neutral axis depth |
| • C_z = Compressive force times lever arm | • A_{GFRP} = Area of GFRP reinforcement |
| • d = effective depth of section | • σ_u = Ultimate stress in GFRP fibres |
| • $f'c$ = characteristic compressive strength of concrete after 28 days | • ϕ = 0.65 for flexural calculations (CSA S806-12) |
| • $\beta_1 = 0.97 - 0.0025f'c > 0.67$ (coefficient, CSA S806-12) | • $\alpha_1 = 0.85 - 0.0015f'c > 0.67$ (coefficient, CSA S806-12) |

2.14.2 Shear Reinforcement

Unlike flexural reinforcement design, the design process specified in CSA S806-12 for shear reinforcement is considerably different to the process discussed in AS3600. The design process for shear reinforcement outlined in CSA S806-12 is quiet complex and requires many inputs. Some of these variables aren't easy to calculate.

For simplicity, AS3600 is more of an acceptable method to calculate the required amount of shear reinforcement. In AS3600, the design process for shear reinforcement is outlined in section 8.2.7. The amount of shear reinforcement required in a specific beam section can be calculated after determining where the design shear force (V^*) is positioned on the 'design for shear diagram' as depicted in figure 2-12.

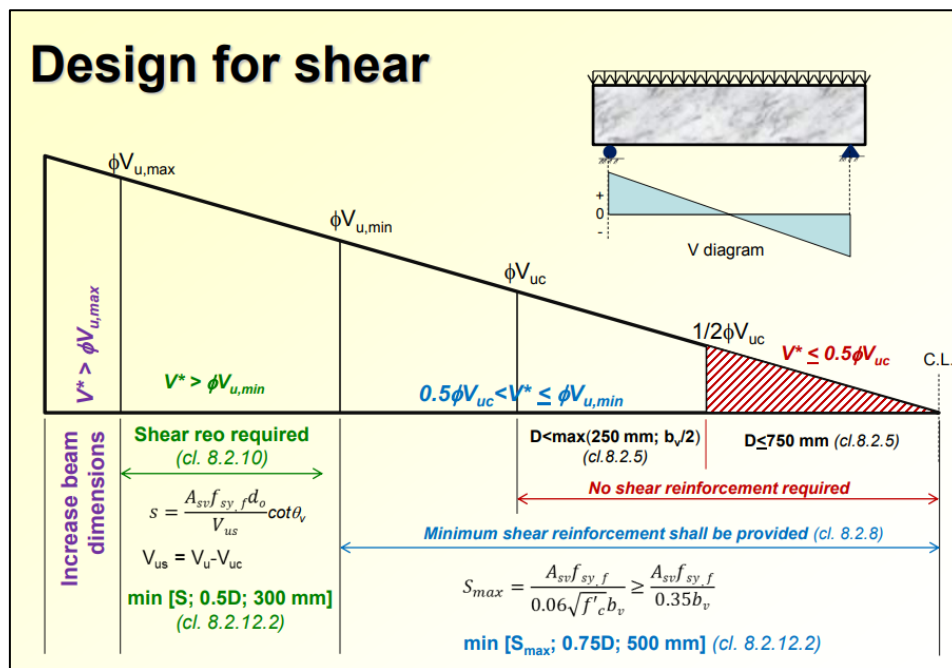


Figure 2-12: Designing shear reinforcement in accordance with AS3600 (Manalo, 2018)

Calculating ϕVu_{max} is generally the first step of the design process as this equation is used to determine whether the physical dimensions of the beam are adequate to withstand the design shear force. Where ϕVu_{max} is derived from AS3600:

$$\phi Vu_{max} = 0.2 * f'c * b * d \quad (1.11)$$

After proving that the sections dimensions are adequate, ϕVuc is then calculated:

$$\phi Vuc = \beta_1 * \beta_2 * \beta_3 * b * d * fcv * \left(\frac{Ast}{b*d}\right)^{\frac{1}{3}} \quad (1.12)$$

AS3600 states that if $V^* > 0.5\phi Vuc$, stirrups or shear reinforcement is required throughout the beam section. The spacing of these stirrups are then determined based on magnitude of V^* and $\phi Vu.min$. Where:

$$\phi Vu.min = Vuc + 0.1 * \sqrt{f'c} * b * d > Vuc + 0.6 * b * d \quad (1.13)$$

A relationship between these two parameters is depicted in figure 14. Figure 2-12 indicates that only minimum shear reinforcement is required if $V^* < \phi Vu.min$ but more than minimum shear reinforcement is required if $V^* > \phi Vu.min$. Appropriate stirrup spacing's can then be calculated using the equations shown in figure 14.

2.14.3 Serviceability

A Canadian design manual released in 2007 by Newhook and Svecova has outlined some guidelines which can be used to determine what is considered an acceptable amount of cracking and deflection. This manual highlights the importance of considering these parameters as these can be the controlling design factor when using fibre composite materials. Newhook and Svecova recommended that cracks should be limited to a width of 0.5mm to help protect GFRP bars from any aggressive environment and meet most visibility requirements. This is important as sleepers must be able to adequately perform in numerous environments across Australia and around the world. This design manual also recommends maximum deflections limits. These limits are specified in table 2-5.

Table 2-5: Allowable deflections in GFRP reinforced sections (Newhook and Svecova, 2007)

DEFLECTION TO BE CONSIDERED	DEFLECTION LIMITATION
Immediate deflection due to specified live load	$\epsilon_r/180^*$
Immediate deflection due to specified live load	$\epsilon_r/360$
That part of the total deflection occurring after detachment of non-structural elements (sum of the long-time deflection due to all sustained loads and the immediate deflection due to any additional live load)†	$\epsilon_r/480^\ddagger$
	$\epsilon_r/240^\S$

2.15 Current Issues with Portland Cement Production

The magnitude of pollution related to Portland cement production has particularly become a focal point in recent years as the amount of scientific data supporting global warming continues to rise. To produce Portland cement, huge amounts of energy are required to power large kilns which heats calcium carbonate (limestone) and other chemical compounds predominately found in raw materials up to 1500°C (Understanding Cement, 2005). This process is indirectly responsible for large amounts of pollution as great amounts of fossil fuels must be burnt to sustain the power consumption of these kilns. Research has found that 40 – 45kWh of electrical energy is consumed per ton of cement produced (Low CO₂ Concrete, 2016). The Concrete Conundrum (2008) estimates that one tonne of carbon dioxide emissions is produced per tonne of traditional Portland cement produced.

2.16 Polymer concrete; an alternative cementitious sleeper material

Sustainability concerns have particularly provoked research into new and evolving cementitious materials such as polymer concrete as it eliminates the need to produce clinker. According to Ferdous et. al. (2016) the strength of polymer concrete isn't reliant on traditional hydration processes as its strength is dependent on monomers that have been polymerized to form long polymer chains which arrange to form a strong matrix. Polymer chains are formed by an exothermic chemical reaction once a resin is activated by a hardening product. The three main components of polymer concrete are; resin, hardener and fillers.

Research conducted by Bennett-Huntley (2014) has determined that the choice of resin can greatly affect the mechanical performance of polymer concrete. Currently there are three resins are commercially available; epoxy, polyester and vinyl-ester. Bennett-Huntley's research concludes that epoxy based resins, although more expensive, has superior mechanical properties over other resin types. Experimental testing suggests that epoxy resins are better suited to withstand vibrational loads, more durable and water resistant in harsh climates whilst having superior tensile strength. Epoxy resin is also more sustainable as its more environmental friendly and safer to manufacture than other resins as it doesn't require styrene. Therefore, this report will particularly focus on epoxy based polymer concrete as it has many favourable characteristics which would best suit railway sleeper applications.

Fillers can be added to polymer concrete to help reduce its capital cost by decreasing the volume of epoxy required. Some fillers are also added to improve certain mechanical properties. Physical testing conducted by Bărbuță, Harja and Baran (2010) concludes that adding fly ash, a waste product from coal fire power generation, can improve the mechanical performance of epoxy based polymer

concrete. Further research conducted by Ferdous et. al. (2016) specifically suggests that the following fillers outlined in table 2-6 should be used if polymer concrete was used to manufacture railway sleepers.

Table 2-6: Common fillers added to polymer concrete and their intended benefits (Ferdous et. al., 2016)

Filler	Potential Benefits
Fly Ash	<ul style="list-style-type: none"> • Improve resistivity to UV degradation • Reduce the permeability of water • Reduce weathering caused by aggressive climates
Hollow microsphere	<ul style="list-style-type: none"> • Reduce the sleepers weight • Control shrinkage • Increase thermal insulation
Fire retardant	<ul style="list-style-type: none"> • Protect the sleeper from bushfires

Ferdous et. al. (2016) highlights the significance of finding the correct ratio of filler to resin as this significantly affects the mechanical properties of the polymer concrete. For example, his study found that increasing the ratio of filler from 0 to 60% reduced the concretes flexural strength by 70% while the concretes compressive strength started to decrease once the ratio of filler reached 40%. To determine the optimum ratio, Ferdous et. al. (2016) used a multi-criteria, decision-making method known as the Analytic Hierarchy Process. It was determined that a filler ratio of 30 – 50 % is acceptable if polymer concrete was to be used to manufacture railway sleepers.

2.16.1 Tensile and Compressive Strength

Lokuge & Aravinthan (2013) performed numerous tensile and compressive tests on numerous polymer concrete mixtures. Their aim was to determine how the ratio of fly ash filler and the type of resin used can affect the behaviour of polymer concrete. Results gathered from split tensile testing found that the tensile strength of polymer concrete was maximised if the amount of filler was minimised and epoxy resin was used. Their results found that increasing the ratio of filler affected the maximum tensile strength of 14.8MPa by 29%.

By comparing results gathered from tensile and compression testing, it appears as though the tensile strength of polymer concrete is significantly less than its compressive strength; a trend consistent with traditional concrete. Also similar to traditional concrete, most mixtures were able to reach their maximum compressive strength by 28 days. Unlike tensile strength tests, increasing the amount of fly ash filler improved the compressive strength of polymer concrete. This trend was attributed to the fly

ash reducing the number of air voids within the mixture. Ultimately, the compressive strength of polymer concrete is controlled by the strength of the polymer chains. This variable is dependent on the resin used. Lokuge & Aravinthan (2013) concluded that an epoxy based mixture with increasing fly ash content is most desirable as it can achieve the highest compressive strength for minimal cost.

2.16.2 Modulus of Elasticity

During testing, Lokuge & Aravinthan (2013) used strain gauges to record the stress vs strain relationship in order to determine the modulus of elasticity. Results indicate that polymer concrete has a modulus of elasticity ten times lower than traditional concrete. As modulus of elasticity is a measure of stiffness, polymer concrete is more susceptible to deflect under loading compared to traditional concrete. Although railway sleepers made from polymer concrete may experience excessive deflection, a reduction in may be beneficial as holes must be drilled into the sleeper to attach the rail seat. Drilling through traditional reinforced concrete, especially on site, is difficult due to its high stiffness.

2.16.3 Cracking

Ferdous et. al. (2016) performed flexural testing on polymer concrete samples and found that all specimens failed suddenly at their mid-spans without developing any flexural cracks prior to failure. It is noted that specimens with a small ratio of filler almost deformed like a rubber-like material while specimens with a high ratio of filler acted more rigid. Similarly, when testing the compressive strength of specimens containing less than 30% filler, these samples did not show any visible cracks even after reaching their ultimate strengths. A lack of cracking is attributed to the strong polymer bonds while the porosity of polymer concrete is extremely low.

2.16.4 Durability

One of the significant advantages of polymer concrete is its durability in comparison to traditional concrete. This means polymer concrete is better suited for use in environments which experience freeze thaw cycles and are highly corrosive. Therefore, polymer concrete has the potential to improve the design life of railway sleepers as they are often implemented in various harsh environments. Kirlikovali (1981) conducted durability testing on polymer and Portland concrete and conclusively found that polymer concrete was more durable. Kirlikovali's results are summarised in table 2-7 below.

Table 2-7: Durability of polymer concrete Vs Portland concrete (Kirlikovali, 1981)

Property	PC	Concrete
Water permeability, 10^{-4} ft/yr	0	5.3
Water absorption, %w	0.3	5.3
Freeze/thaw resistance, # of cycles	3,300	590
% weight lost	0	25
Hardness, impact hammer	55	32
Acid resistance		
% weight lost after 3 months of immersion:		
5% HCl	0.3	24
15% HCl	3	27
10% H ₂ SO ₄	1.2	39
Sulphate attack		
% expansion after 2 years of exposure	0.003	0.5
Corrosion by distilled water	None	Severe

Ferdous et. al. (2016) wanted to further understand how durable polymer concrete is by measuring the effects of UV radiation. Tests showed that polymer concrete is susceptible to surface degradation if directly exposed to UV radiation as photons can start a photo-oxidative reaction. This reaction is significant as it can change the chemical structure of epoxy molecules and cause decolourisation. Flexural testing found that the flexural strength of polymer concrete can decrease up to 48% if exposed to UV light for 2000 hours. Specimens also experienced a percentage weight loss of around 0.3% after being exposed for 2000 hours.

2.17 Previous Studies

Research has begun to find new suitable materials to replace traditional timber railway sleepers as they're susceptible to weathering. A review paper written by Ferdous et. al. (2015) was aimed at identifying a number of key constraints which are hindering the acceptance of newly design sleepers in industry. This paper highlighted that finding a material that has favourable characteristics such as high strength, low stiffness and being compatible with existing timber structures has been a significant engineering challenge. It was concluded that existing designs could be improved by adding fibre reinforcement and optimising fabrication techniques to help reduce costs.

Meanwhile, a number of research projects have been conducted by Kaewunruen and Remennikov in recent years at the University of Wollongong. Their main objective has been to optimise the design of precast concrete railway sleepers. Their studies have primarily focused on testing, developing models

and evaluating the performance of precast concrete sleepers. Information gathered from their research projects have predominately been used to improve the design of current sleeper designs and provide recommendations for future work. However, it is apparent that none of their projects have specifically tested the suitability of GFRP reinforcement. Without proper physical laboratory testing in accordance with Australian Standards and in-track trials in Australian conditions, it is still unknown whether GFRP bars are a suitable reinforcement material that can benefit the design of concrete railway sleepers.

A recent study conducted by T.Baker (2016) aimed to develop a suitable design for a GFRP reinforced sleeper. This study was able to successfully determine the most critical loading pattern and propose a suitable reinforcement design which could withstand these critical design forces. A finite element analysis model was then created to test the proposed GFRP reinforced narrow gauge concrete sleeper. Another model with steel reinforcement was created so comparisons could be made between the two designs. Results obtained from numerous models suggest that it is plausible to use GFRP bars in lieu to steel. The most significant challenge highlighted by Baker is that approximately 50% more reinforcement is required compared to steel to stop excessive deflection due the modulus of elasticity of GFRP is significantly less than steel. A comparison between the proposed steel and GFRP reinforcement designs are given in figure 2-13. The results and recommendations provided by this report may potentially be false as they have not been verified by physical testing.

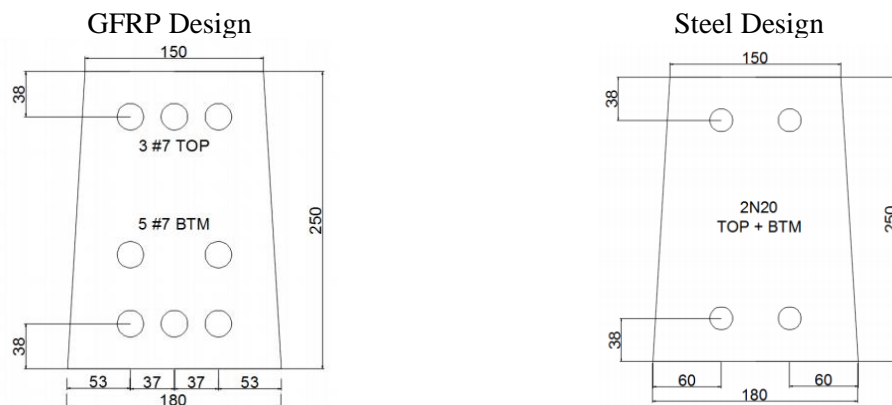


Figure 2-13: More GFRP reinforcement is required than steel (Baker, 2016)

Further research completed by A.Baker (2018) focused on determining what load and bearing pressure combinations yielded the most critical design parameters. This research project was done in alignment with the analytical method outlined in AS1085.14. All results in this report were based off results obtained from finite and fibre modelling only. Baker's results can be summarised as follows:

Calculating the maximum positive bending moment

- Point loads acting on the sleeper compared to distributed loading increased M^*
- Increasing the bearing pressure from 10MPa to 40 MPa decreased M^*

Calculating the maximum negative bending moment

- Point loads acting on the sleeper compared to distributed loading increased M^*
- Increasing the bearing pressure from 10MPa to 40 MPa increases M^*

Calculating maximum shear force

- Point loads acting on the sleeper compared to distributed loading increased V^*
- Increasing the bearing pressure from 10MPa to 40 MPa decreases V^*

Calculating maximum deflection

- Point loads acting on the sleeper compared to distributed loading increases y_{max}
- Increasing the bearing pressure from 10MPa to 40 MPa decreases y_{max}

2.18 Research Gap

After reviewing relevant literature, most rail related research projects are currently focused on theoretical modelling. Theoretical modelling is often done before expensive physical testing in order to determine whether a new concept is indeed plausible. As discussed, some theoretical testing done by Baker (2016) suggests that GFRP reinforced sleepers are theoretically possible. Current research is also utilising theoretical modelling to improve the accuracy of calculating certain parameters which governs the design of reinforced railway sleepers.

A lack of physical testing to accurately assess the mechanical behaviour of GFRP reinforced concrete sleepers is clear research gap. Baker specifically recommends that future research projects would require physical testing of sleepers to validate his proposed reinforcement design. A lack of practical and accurate data about GFRP reinforced sleepers such as their flexural performance, serviceability, cost, durability and expected lifespan is stopping the product being widely accepted by the rail industry. This proves that further research is required to verify whether GFRP reinforced sleepers are an innovative solution which can help reduce current railway maintenance costs.

There is also the potential to study whether polymer concrete can be used to manufacture railway sleepers as there is a lack of research and testing related to this emerging product. The popularity of polymer concrete is set to rise as it has many desirable characteristics as discussed previously.

Physical testing is required to determine whether polymer concrete significantly affects the sleeper's failure mode, crack distribution pattern and magnitude of deflection compared to traditional concrete.

2.19 Project Feasibility

Research conducted by Ferdous and Manalo (2014) has predicted that Australia's railway industry currently spends \$80 million per annum on track rehabilitation or complete replacement of degraded timber sleepers. This figure is set to increase as the popularity of rail in Australia continues to rise. This justifies the need to develop a highly durable sleeper which can significantly reduce current maintenance costs. Sleepers reinforced with GFRP also have the potential to surpass the design life of steel reinforced concrete sleepers as GFRP bars are non-corrosive and strong. Therefore, if a practical GFRP reinforced sleepers was designed, it would have a competitive edge on the current market.

This project will particularly continue the work of Baker (2016) who developed a finite element model of a concrete railway sleeper reinforced with GFRP bars. Physical testing is feasible as all materials and equipment is readily available within the laboratories at USQ.

Chapter 3 Finite Element Analysis

3.1 Chapter Overview

This chapter will particularly focus on explaining the theoretical design procedures implemented throughout this project and any calculations used to determine the suitable amount of GFRP reinforcement to satisfy flexural and serviceability requirements. The first phase in any design process is to determine any variables and outline any assumptions used to simplify the design process. This phase of the design process will be done in alignment with the information gathered in Chapter 2.

It is important to justify the choice of certain design parameters as the second phase of the design process, the development of a finite element model, is solely dependent on the accuracy of these inputs. This particular research project chose to implement a well-known finite element modelling software package called Strand 7 to simulate the flexural performance of an in-track railway sleeper. As the accuracy of the model is dependent on the user's inputs and judgment, it is important to document exactly how the model was created. Therefore, this chapter will clearly explain how all the models that were created in strand 7.

Once the accuracy of the models has been verified, the results gathered will be analysed in order to determine the sleeper's design moment (M^*), shear force (V^*) and deflection (y_{max}). These critical parameters will then be used in the final phase of the design process; determining the amount of reinforcement required.

3.2 Benefits of Creating a Finite Element Model

According to PreTechnologies (2014), many industrial products have complex geometry components while their performance can easily be affected by heat and material faults. Consequently, simple calculations often become obsolete as they cannot yield accurate results. This often forces people to use more complex analysis methods and equations which are more time consuming and mistake prone. Another alternative but expensive solution to this problem is to build and physically test a number of prototypes. This conundrum has led to the development of finite element analysis programs which uses advanced computational tools to quickly calculate and capture complex results compared to hand calculations and physical testing.

PreTechnologies (2014) suggest that finite element analysis relies on subdividing a component into small, individual elements separated by nodes. These individual elements are then stitched back together to form an ‘assembly of elements’ which simulates the original component as a whole. Breaking the component into many small elements enables the computer to accurately solve a system of equations which yields unique and accurate results. The degree of element subdivision is often referred to as a mesh where a fine mesh resolution produces the most accurate results. According to PreTechnologies (2014), the following reasons are why finite element modelling is beneficial:

- Safe simulation of potentially dangerous, destructive or impractical load combinations and failure modes
- Testing of several failure modes or physical events using a single common model
- Calculations are given a visual aspect which can enhance a designers ability to assess performance and help identify areas that needs improvement
- Low investment and rapid calculation time
- Simultaneous calculations of different physical parameters such as temperature change

As technology continues to progress, finite element analysis software programs have increasingly become more user friendly. Therefore, this type of analysis has become widely accepted by the civil engineering industry as it’s a very practical method to analyse the performance of new designs. Consequently, this type of analysis was chosen to determine the flexural requirements of a railway sleeper over traditional hand calculations. The flexibility of a finite element analysis model will be particularly useful when analysing a number of different load and bearing combinations acting on the sleeper.

3.3 Analysing a Sleeper

As mentioned in Chapter 2, the magnitude of bearing pressure and the type of rail load acting on the sleeper can significantly affect the magnitude of moment acting on the sleeper. Fortunately, A.Baker (2018) has already conducted significant testing on different load and bearing pressure combinations in order to determine which scenarios causes the most critical results. Based on Baker’s findings, the following models shall be created in Strand 7 to determine the most critical M^* , V^* and y_{max} . These parameters are required to design the sleepers flexural and shear reinforcement while ensuring serviceability requirements are met.

Model 1

This model shall be used to determine maximum positive bending moment, shear force and deflection. The rail seat load will be applied as a point load while the bearing pressure is minimised (10MPa) as seen in figure 3-1. The length of the bearing distribution pattern underneath the sleeper will be determined in accordance with the empirical method from AS1085.14 as outlined in Appendix C.

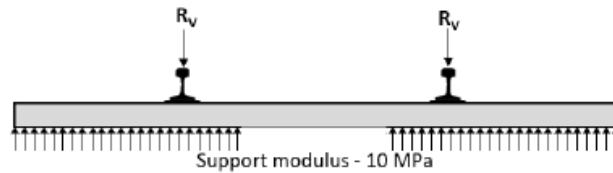


Figure 3-1: Finite Element Model 1

Model 2

This model shall be used to determine the maximum negative bending moment. The rail seat load will be applied as a point load while the bearing pressure is maximised (40MPa). As seen in figure 3-2, the sleeper will be subjected to bearing pressure along its entire length as explained in Chapter 2.

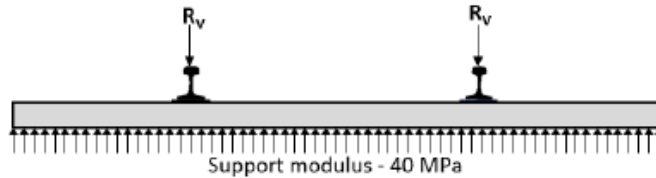


Figure 3-2: Finite Element Model 2

3.4 Preliminary Sleeper Design

Before a finite element model can be created, the sleeper's dimensions must be finalised and the rail seat load must be calculated. Such preliminary design details have been clarified in sections 3.4.1 and 3.4.2.

3.4.1 Calculating the Rail Seat Load

As mentioned in Chapter 2, many theoretical methods have been developed over time and can be used to approximate the rail seat load acting on an individual sleeper. As this project is specifically focused on developing a narrow gauge track sleeper suitable for use in Queensland, it was decided that the rail seat load should be calculated in accordance with the method outlined in Section 3 of AS1085.14. Therefore, the following calculations were used to calculate the rail seat load:

Using equation (1.5):

$$PdV = k_s Q$$

Where:

$$Q = \frac{\text{weight of passing train}}{\text{number of wheels}} \times \text{gravity}$$

The dead load of the passing train shall be taken as 20 tonnes as specified in Section 2.2 of TRACK-CT.172; Appendix B.

$$k_s = \text{dynamic load factor}$$

The dynamic load factor shall be taken as 2.5 when there is a lack of field measurements. Refer to appendix B.

Therefore:

$$Q = \frac{20 \text{ tonnes}}{2 \text{ wheels}} \times 9.81 = 98.1 \text{ kN}$$

$$k_s = 2.5$$

Hence:

$$PdV = 2.5 \times 98.1$$

$$PdV = 245.25 \text{ kN}$$

Now using equation (1.6):

$$R_v = \frac{P_{dv} DF}{100}$$

Where:

$$DF = 48\%$$

Substituting values into equation (1.6):

$$R_v = \frac{245.25 \times 48}{100}$$

$$R_v = 117.12 \text{ kN}$$

When creating the Strand 7 model, two point loads of the same magnitude (117.12 kN) should be applied to the sleeper about its centroid at a distance equal to the track's gauge width.

3.4.2 Sleeper Dimensions and Parameters

It is critical that the finite element model has exactly the same dimensions, parameters and material properties as the sleeper would in real life otherwise all theoretical results would be unrealistic. If the model is inaccurate, the sleeper may become over reinforced, increasing production costs or under reinforced, which could lead to premature failure. Both scenarios are not desirable meaning great care must be taken to ensure the finite model is developed correctly. Table 3-1 below lists the parameters which were used to create the finite element models in Strand 7.

Table 3-1: Sleeper model properties

Parameter	Measurement
Track gauge (narrow gauge)	1067mm
Width of rail at wheel (based on AS41 rail type)	63.5mm
Distance between rail centres	$1067 + 63.5 = 1130.5\text{mm}$
Concrete strength (f'c)	32 MPa
Concrete density	2400 kg/m^3
Young's modulus	30960.0 MPa
Poisson's Ratio	0.2

Finalising the sleeper's dimensions should be done in alignment with Table 2-4 in Chapter 2 as the sleepers overall dimensions must be within a standardised range to suit the design brief, TRACK-CT.172. Ease of construction is another factor which must be considered.

After discussions with university staff, it was decided that an existing precast sleeper mould should be reused for simplicity purposes. This mould is suitable for this assessment as its dimensions are within the tolerances specified in Table 2-4. Therefore, the adopted sleeper dimensions for this analysis are shown in figure 3-3.

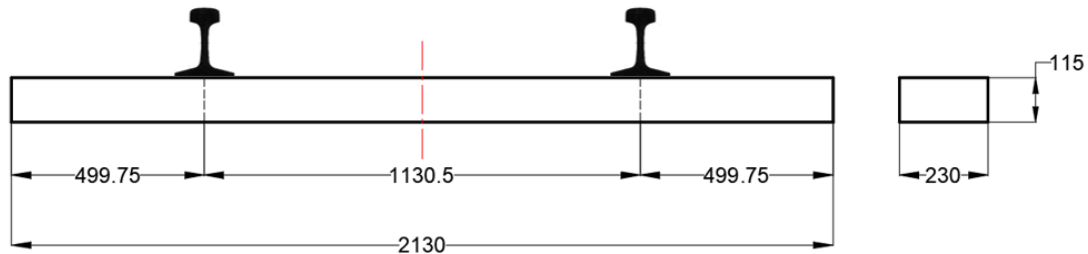


Figure 3-3: The dimensions of the GFRP reinforced sleeper under investigation (mm)

3.5 Developing the Finite Element Model

For this particular analysis, Strand 7 version 2.4.6 with an educational license only was used to simulate the performance of a sleeper on an elastic foundation. Two individual models were created using the program to determine M^* , V^* and y_{max} . The development of these models will be discussed further in sections 3.5.1 to 3.5.3.

3.5.1 Bearing Pressure Distribution

As shown in figures 3-1 and 3-2, two different bearing pressure patterns will be used to determine maximum positive and negative bending moments respectively. These two bearing patterns have been adopted from AS1085.1. In accordance with clause 4.2.1 in AS1085.14, the bearing pressure distribution beneath each rail seat and the entire length of the sleeper should be uniform. In Strand 7, the bearing pressure can be applied to the beam using a function called ‘support’. This in-built function and is specifically designed to simulate a beam sitting on an elastic foundation.

Model 1 Distribution Pattern

In accordance with Appendix C, the length of ballast supporting the sleeper beneath each rail seat can be calculated as follows:

$$A = 0.8(L - g) \quad (2.1)$$

Where: L – The length of the sleeper
 g – Distance between rail centres

Therefore, using the dimensions specified in table 3-1,

$$A = 0.8(2130 - 1130.5)$$

$$A \approx 800\text{mm}$$

The maximum positive bending moment occurs directly after the track has been freshly tamped as this causes the centre portion of sleeper to become separated with the ballast underneath. This support type maximises the positive bending moment in the bottom portion of the sleeper as the sleeper acts as though it's simply supported when loaded. Consequently, the middle portion of the sleeper (535mm) will have no bearing support when modelled in Strand 7.

Model 2 Distribution Pattern

Over time, the ballast gradually compacts and begins to support the centre portion of the sleeper. As the bearing distribution area underneath the sleeper increases, a negative bending moment can develop in the top portion of the railway sleeper when loaded. When modelling this case in Strand 7, the bearing pressure should be made uniform along the entire length of the sleeper to model the worst case scenario.

3.5.2 Point Load Application

As proven by A.Baker (2018), bending moment is maximised when the rail seat load is applied using two vertical point loads compare to two equivalent uniform distributed loads acting across the width of the rail road which sits on top of the sleeper. Therefore, it is only necessary to apply point loads to the sleeper models in Strand 7.

3.5.3 Finite Element Modelling in Strand 7

Before elements which characterize the sleeper can be added to the model, several nodes must be created at suitable positions along the length of the sleeper. Nodes are used to connect individual elements so all elements act as a continuous uniform section when analysed. The positions of these nodes are shown in table 3-2 and 3-3.

Table 3-2: Strand 7 node positions for Model 1

Node	X co-ordinate (mm)	Y co-ordinate (mm)
1	0	0
2	499.75	0
3	800	0
4	1065	0
5	1330	0
6	1630.25	0
7	2130	0

Table 3-3: Strand 7 node positions for Model 2

Node	X co-ordinate (mm)	Y co-ordinate (mm)
1	0	0
2	499.75	0
3	1065	0
4	1630.25	0
5	2130	0

For the software to fully analyse the sleeper without error messages, some of these nodes must be restrained. Therefore, the nodes at the end of the sleeper have been restrained to replicate simple roller supports. Such restraints ensure that the sleeper cannot move in x plane and cannot carry moment. However, the sleeper is free to rotate at each end. Nodes have also been purposely positioned directly underneath each rail road. Including these nodes will simplify the process of applying the rail seat loads as it enables a function within the program called ‘Node force’. This function enables a point load of any magnitude to be applied directly to the node selected.

After creating the nodes, individual sleeper elements which span between the nodes were created. Figure 3-4 and 3-5 show the interaction between the nodes and elements used to model the sleeper.

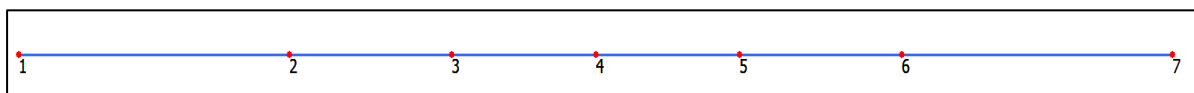


Figure 3-4: Nodes and elements within Model 1

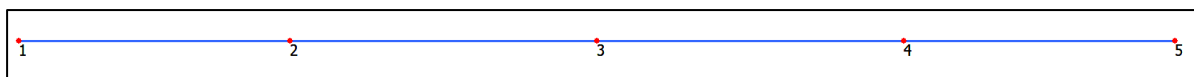


Figure 3-5: Nodes and elements within Model 2

Using dimensions and parameters listed in figure 3-3 and table 3-1 respectively, elements in Strand 7 were created. Figure 3-6 shows the exact element properties adopted in Strand 7.

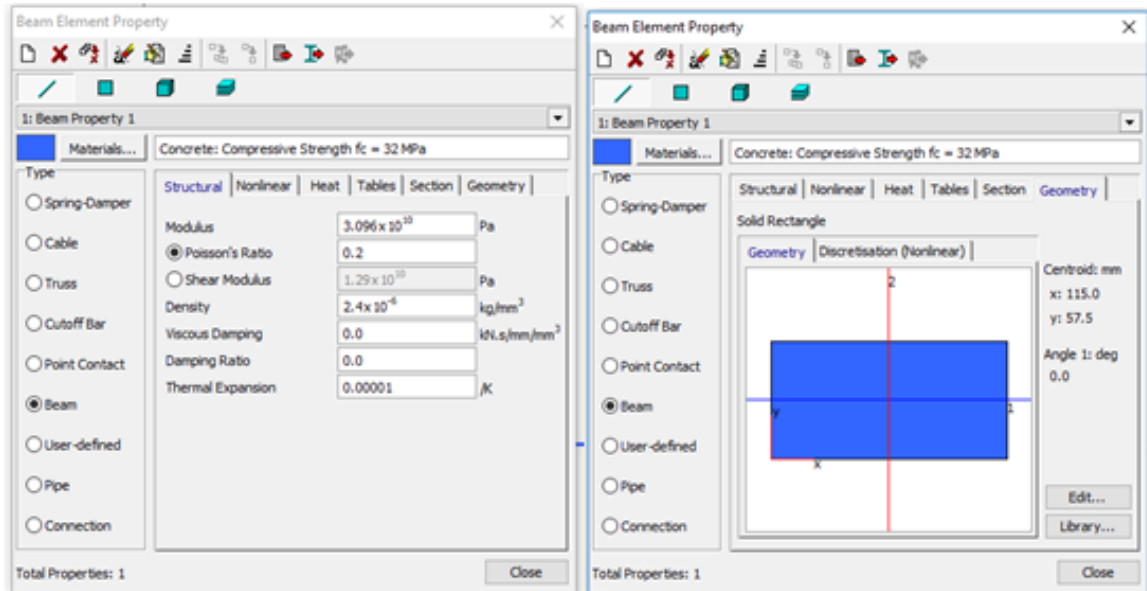


Figure 3-6: Strand 7 beam parameters

The rail seat load and the two different bearing distribution patterns were then be applied to the sleeper to complete the two models. Figure 3-7 and 3-8 shows the two models developed in Strand 7 respectively.

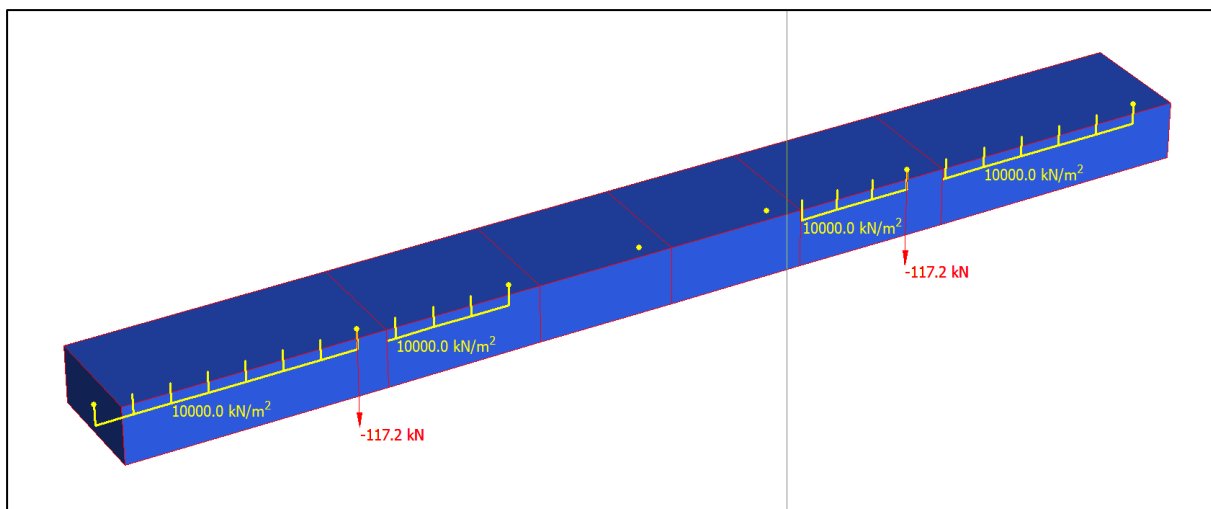


Figure 3-7: A 3D view of Model 1 developed in Strand 7

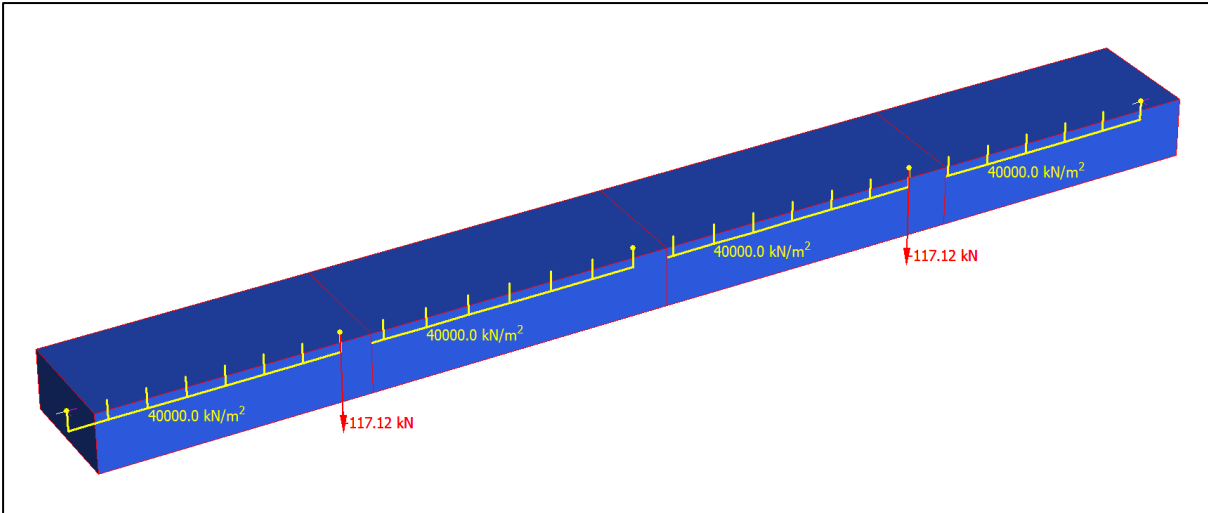


Figure 3-8: A 3D view of Model 2 developed in Strand 7

3.6 Finite Element Modelling Results

The main purpose of conducting a finite element analysis was to accurately determine the magnitude of important design parameters such as M^* , V^* and y_{max} so adequate calculations can be performed to calculate the minimum amount of GFRP reinforcement required. The following diagrams and values have been obtained from Strand 7 after solving respective models. It should be noted that only the critical diagrams and results are shown below.

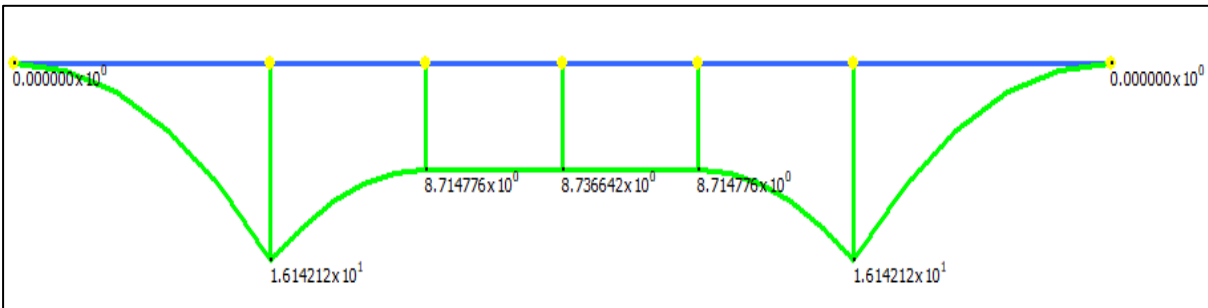


Figure 3-9: Maximum positive bending moment diagram obtained from model 1

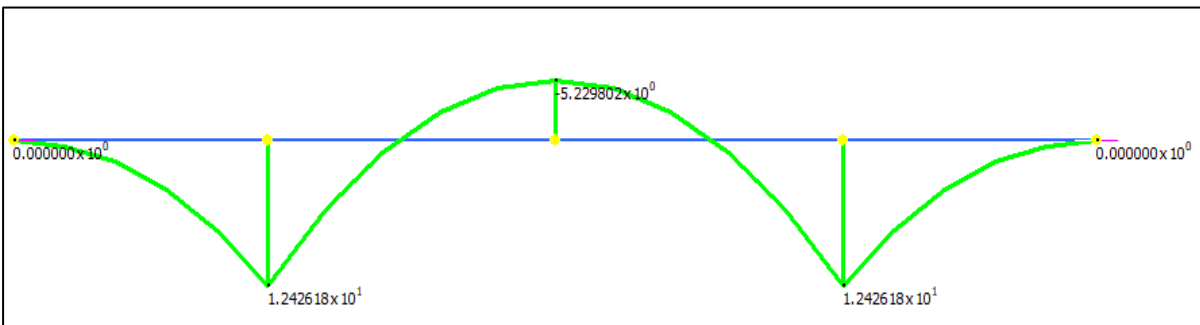


Figure 3-10: Maximum negative bending moment diagram obtained from model 2

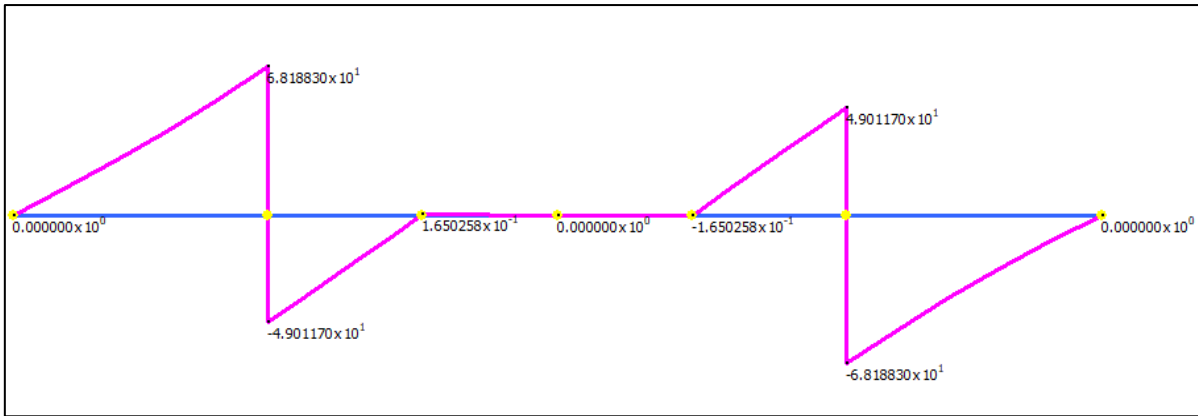


Figure 3-11: Maximum shear force diagram obtained from model 1

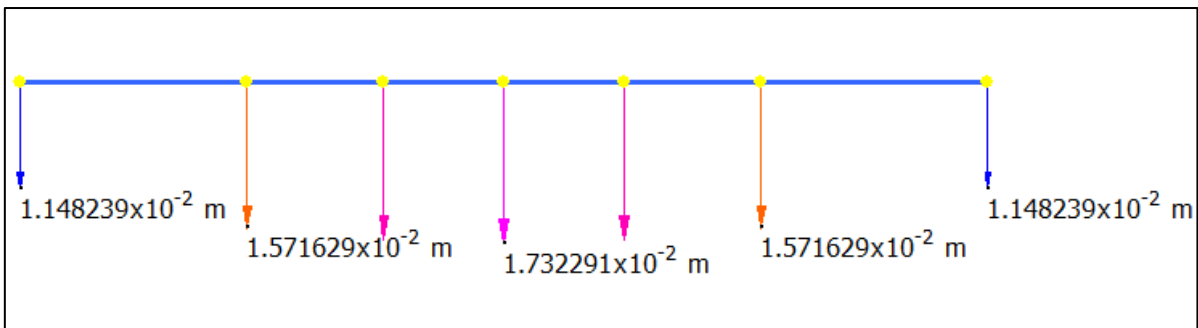


Figure 3-12: Vector diagram showing the expected magnitude and direction of deflection

Table 3-4: A summary of significant Strand 7 results

Parameter	Model Number	Figure Reference	Magnitude
M* (positive)	1	3-9	16.142 kNm
M* (negative)	2	3-10	5.229 kNm
V*	1	3-11	68.188 kN
Ymax	1	3-12	5.84 mm

3.7 Model Verification

According to Hillston (2003), model validation is the task of demonstrating that the model is a reasonable representation of the actual system and whether the model is accurate enough to satisfy research objectives. The definition of ‘reasonable’ generally changes as it is dependent on funding and time constraints. Hillston (2003) also states that there are three common aspects which should be considered during model validation:

- Assumptions
- Input parameters
- Output values

As many of the parameters and assumptions required to create these models have already been justified, this section of the report will predominately focus on validating the output obtained. As mentioned in Chapter 2, the analytical method outlined in AS1085.14 can be used to analyse the sleeper’s behaviour on an elastic foundation. Consequently, the analytical method shall be used to verify the results obtained by the finite element models. Below, table 3-5 compares the results obtained from Strand 7 and the Analytical method. It is important to note that the analytical method assumes a uniform bearing pressure along the entire length of the sleeper. This means that a fair comparison only exists between the results gathered from Model 2.

Table 3-5: Finite model validation by comparing results calculated using the analytical method

Model 2: Uniform bearing distribution pattern 40 MPa			
	Strand 7	Analytical	Difference
Mac (kNm): Based off Equation (1.1) and (1.3)	12.426	12.402	0.024
Mo (kNm): Based off Equation (1.2) and (1.3)	5.229	5.289	0.060
Ymax (mm): Based off Equation (1.4)	5.84	2.218	3.622

Overall, it appears as though the model and the analytical method yield similar moments at the centre of the sleeper and at the rail seat. Based on the consistency of moments calculated, it appears as though the model has been developed properly and is performing as expected. After reviewing table 3-5, it is evident that there is some variance in deflection between the two methods. In reference to clause 3.4.3 within AS1085.14, the magnitude of deflection is generally controlled by the condition of the ballast which varies. Therefore, it is somewhat expected to see some indifferences in deflection approximations.

It's best to compare results obtained from Model 1 with results obtained using the other structural analysis method mentioned in AS1085.14; the empirical method. The empirical method is more appropriate to validate Model 1 because the bearing pressure beneath the sleeper doesn't need to be uniform along its entire length. Using the equations depicted in Appendix C where: $a = 0.8(L-g)$, both the negative and positive bending moment can be calculated at the rail seat and the centre of the sleeper. Table 3-6 compares the results obtained from Model 1 in Strand 7, and the Empirical method outlined in Appendix C.

Table 3-6: Finite model validation by comparing results calculated using the Empirical method

Model 1: Bearing distribution pattern 10 MPa under each rail seat			
	Strand 7	Empirical	Difference
Positive bending moment at rail seat (kNm)	16.142	18.38455	-2.24255
Positive bending moment at rail centre (kNm)	8.736	11.76611	-3.03011

It was expected that the empirical method would be more conservative than the finite element model as Strand 7 simulates the sleeper sitting on an elastic foundation. As the variance in both moment calculations is less than 20%, it can be concluded that Model 1 is performing as expected.

3.8 Summary of Finite Element Modelling

It is apparent that both finite element models are a reasonable representation of an actual sleeper and are their results are accurate enough to satisfy research objectives. Research conducted by Baker (2018) was very useful during this process as it significantly reduced the number of models required to calculate the absolute maximum of the design parameters; M^* , V^* and y_{max} .

The results summarised in table 3-4 will be used to determine the amount of GFRP reinforcement required in the test sleepers. The following sections in the report will thoroughly explain the design process undertaken and any calculations used to determine the amount of flexural and shear reinforcement required.

3.9 Reinforcement Design Considerations

In order to sufficiently design reinforcement, some essential design parameters must be established. These parameters directly affect the overall flexural performance of the sleeper. Any assumptions or decisions in regards to these design parameters are discussed in the following sections.

3.9.1 Concrete Cover

The size of aggregates in a cement mixture greatly affects its workability (Concrete technology, 2014). Poor workability can lead to segregation of particles in the mix causing honeycomb patches, non-uniform sections, porous concrete and poor bonds between the reinforcement bars and the concrete itself (Concrete technology, 2014). All of these characteristics ultimately reduce the expected design life of the concrete structure (Concrete technology, 2014). As a result, concrete cover and spacing's between reinforcement bars have been governed by aggregate size. This requirement is elaborated in clause 4.10.2 within AS3600. This clause specifies that a designer should specify a cover that ensures concrete can be satisfactorily be placed and compacted around the reinforcement; hence the cover should always be greater than the maximum nominal aggregate size.

As mentioned in Chapter 2, polymer concrete does not contain large aggregates as seen in traditional Portland concrete which can reach sizes up to 20mm. Therefore, the amount of cover required when using polymer concrete can be reduced compared to Portland concrete. Reducing the cover is desirable as it helps to maximise the sections effective depth. Increasing the effective depth of a section ultimately reduces the amount of reinforcement required as it lengthens the lever arm in equation (1.7). As specified in the projects objectives, the adequacy of polymer concrete needs to be determined. Consequently, both test sleepers made from Portland and polymer concrete respectively will use the same 'reduced' cover to ideally suit polymer concrete. Standardising the cover will also ensure a fairer comparison between the two different concretes as the effective depth will remain the same.

Another major factor which determines the amount of cover required is its exposure classification. As specified in section 4.10.3 within AS3600, the strength of the concrete and its exposure classification should be used in conjunction to determine a suitable amount of cover which can adequately protect internal reinforcement from corrosion. If adequate cover isn't provided, the structure may be prone to premature failure as corrosion can cause significant weakening of flexural reinforcement. However, as highlighted in the literature review, one of the great advantages of using GFRP bars is their ability to resist chemical attack. Consequently, GFRP bars can be placed closer to the surface of a structure

without risk of corrosion. The literature review also discussed how Polymer concrete has superior weathering and chemical resistance compared to Portland concrete.

Due to these reasons, a significantly small cover has been adopted. Both test sleepers will only have a cover of 10mm. In comparison with AS3600, 10mm of cover is at least half the recommended amount of cover required when using 32MPa concrete.

3.9.2 Size of Flexural Reinforcement

The GFRP bars used for this investigation will be sourced from Inconmat Australia; an industry based company who actively collaborates with the University of Southern Queensland. This company imports ‘V-Rod’ bars from Canada which are manufactured by Pultrall Incorporated. Their product is made from high strength glass fibres which are hardened by a strong vinyl-ester resin (V-ROD Fiberglass Rebar Canada, 2012). Extensive testing has already been done on all V-Rod bars meaning their properties can be assessed using tables provided by Pultrall (V-ROD Fiberglass Rebar Canada, 2012). The ultimate strength (F_u) of bars with varying diameter is given in table 3-7 below.

Table 3-7: F_u of GFRP bars supplied by Inconmat Australia (V-ROD Fiberglass Rebar Canada, 2012)

Bar Size	Bar diameter (mm)	Minimum Guaranteed f_u (MPa)
#2	6.35	Not specified
#3	9.53	1372
#4	12.70	1312
#5	15.88	1184

In industry, small diameter bars are preferred as they are easier to handle and work with onsite, reduce the chance of high tensile stress cracks developing if the concrete shrinks and the sections effective depth is maximised (The concrete countertop institute, 2019). As mentioned in chapter 2, Gu, Yu and Wu (2016) also recommends minimising the diameter of GFRP bars as their trials found that smaller diameter bars were able to achieve a higher peak bond strength.

Ultimately, the diameter of flexural reinforcement (d_b) must suit the beams physical dimensions. Based off previous research conducted by T.Baker (2016), the required amount of flexural GFRP reinforcement is fairly small meaning it could be plausible to use the smallest bar size available; bar size #2. Although its exact f_u value is unknown, it can be assumed that its value is similar to bar size #3.

3.9.3 Size of Shear Reinforcement

The shear reinforcement used for this investigation is also sourced from Inconmat Australia. The diameter of the stirrups (d_s) is approximately 5mm. Unlike steel stirrups which are individually spaced, GFRP stirrups are manufactured as one continuous coil which wraps around the entirety of the flexural bars. The minimum f_u of the GFRP stirrups can be assumed to be the same as the bar size #3.

3.9.4 Effective Depth

The effective depth of the flexural reinforcement in the test sleepers can now be calculated as follows:

$$d = D - cover - d_s - d_b/2 \quad (2.2)$$

$$d = 115 - 10 - 5 - 6.35/2$$

$$d = 96.825 \text{ mm}$$

3.10 Flexural Reinforcement Design based on Finite Element Results

Now that the sleepers cover, size of bars and effective depth have been determined, the required amount of flexural reinforcement can be determined based on the equations discussed in Chapter 2 from CSA S806-12.

Maximum Positive moment calculated from Strand 7:

$$M^* = 16.142 \text{ kNm}$$

Equation (1.7) states:

$$M^* = T_z$$

Determining T_z using equation (1.8):

$$T_z = \phi \left(A_{GFRP} * \sigma_u * \left(d - \frac{\beta_1 c}{2} \right) \right)$$

Where:

$$\phi = 0.65$$

$$\sigma_u = 0.25 * 1372 = 343$$

$$d = 96.825$$

Equation (1.9) states:

$$\beta_1 c = \frac{A_{GFRP} * \sigma_u}{\alpha_1 * f'_c * b} = \frac{A_{GFRP} * 343}{0.802 * 32 * 230} = \frac{343 * A_{GFRP}}{5902.72}$$

Now substituting values back into equation (1.7) and Rearranging to solve for A_{GFRP} :

$$16.142 * 10^6 = 0.65 \left(A_{GFRP} * 343 * \left(96.825 - \frac{343 * A_{GFRP}}{2 * 5902.72} \right) \right)$$

$$A_{GFRP} = 1133 \text{ mm}^2$$

By using the exact standards outlined in CSA S806-12, 36 x Ø6 GFRP bars would be required to sufficiently counteract the moment cause by the two vertical rail seat loads being applied to the sleeper. Evidently, this solution isn't logical as it would be physically impossible to fit 36 bars into a section that is 230mm wide. Consequently, some modifications must be made to these calculations in order to obtain a practical result.

As discussed in literature review, GFRP bars are capable of having a much higher yield strength compared to traditional steel rebar. This fact is further highlighted in table 3-7 as size #2 bars have a minimum guaranteed f_u of 1372 MPa. This is significantly higher than steel which typically has a minimum guaranteed f_u of 500MPa. This indicates that the GFRP bars manufactured by Pultrall Incorporated are approximately 274% stronger than their steel counterparts. Although being much stronger, this additional strength isn't being utilised as current design standards applies a significantly large reduction factor to the total f_u value; 0.25. Therefore, this reduction factor will be eliminated to minimise the amount of reinforcement required. Designing the sleeper based on this modification will also help to better evaluate the flexural performance of individual GFRP bars as they will now be subjected to greater strains; an objective of this research project.

Another parameter which can be manipulated is the factor of safety or the ϕ value. As stated in CSA S806-12, ϕ is currently 0.65 which is significantly high. In comparison, the recommended ϕ value in AS3600 for flexural members is 0.8. Therefore, to help minimise the amount of reinforcement required, the ϕ value in this investigation shall be taken as the average of these two values; 0.725. The amount of flexural reinforcement was recalculated based off these two modifications.

Maximum positive moment from Strand 7:

$$M^* = 16.142 \text{ kNm}$$

Using equation (1.8) and substituting in known values:

$$16.142 * 10^6 = 0.725 \left(A_{GFRP} * 1372 * \left(96.825 - \frac{1372 * A_{GFRP}}{2 * 5902.72} \right) \right)$$

Rearranging and solving for A_{GFRP} :

$$A_{GFRP} = 224 \text{ mm}^2$$

Therefore, 8 x Ø6 GFRP bars would be required to sufficiently counteract the positive moment cause by the two vertical rail seat loads being applied to the sleeper. It is obvious that this solution is more logical.

Maximum negative moment from Strand 7:

$$M^* = 5.289 \text{ kNm}$$

Using equation (1.7) and substituting in known values:

$$5.289 * 10^6 = 0.725 \left(A_{GFRP} * 1372 * \left(96.825 - \frac{1372 * A_{GFRP}}{2 * 5902.72} \right) \right)$$

Rearranging and solving for A_{GFRP} :

$$A_{GFRP} = 58 \text{ mm}^2$$

Therefore, 2 x Ø6 GFRP bars would be required to sufficiently counteract the negative moment cause by the two vertical rail seat loads being applied to the sleeper. Figure 3-13 shows the proposed flexural reinforcement as calculated above.

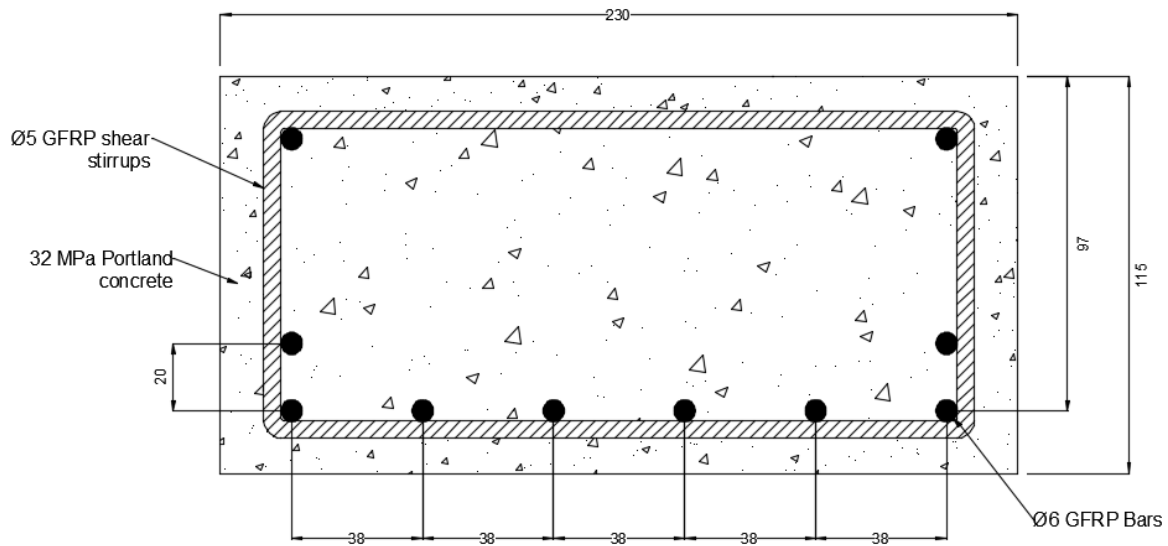


Figure 3-13: Proposed flexural detailing

3.11 Shear reinforcement design based on Finite Element Results

As discussed in Chapter 2, AS3600 will be used to determine a suitable amount of shear reinforcement throughout the sleeper. It is important to note that these calculations will also assume that the full strength of the GFRP stirrups will be utilised.

As seen in figure 3-11, shear force varies along the length of the sleeper meaning the spacings between shear stirrups does not need to be uniform. Therefore, the overall amount of reinforcement may be reduced. It is important consider such design aspects as reducing the spacings of stirrups could help reduce manufacturing costs.

As stated in table 3-4, the max shear acting on the sleeper is:

$$V^* = 68.2 \text{ kNm}$$

Using equation (1.11):

$$\phi V_u \text{ max} = 0.2 * f'c * b * d$$

Where:

$$f'c = 32 \text{ Mpa}$$

$$b = 230 \text{ mm}$$

$$d = 115 - 10 - 2.5 = 102.5 \text{ mm}$$

Therefore,

$$\phi V_{u, \max} = 0.7 * 0.2 * 32 * 230 * 102.5$$

$$\phi V_{u, \max} = 105.6 \text{ kN}$$

Using equation (1.12):

$$\phi V_{uc} = \beta_1 * \beta_2 * \beta_3 * b * d * f_{cv} * \left(\frac{A_{st}}{b * d} \right)^{\frac{1}{3}}$$

Where:

$$\beta_1 = 1.648$$

$$\beta_2 = \beta_3 = 1$$

$$b = 230 \text{ mm}$$

$$d = 102.5 \text{ mm}$$

$$f_{cv} = 3.175 \text{ MPa}$$

$$A_{st} = 8 * 3^2 * \pi = 226 \text{ mm}^2$$

Therefore,

$$\phi V_{uc} = 0.7 * 1.648 * 1 * 1 * 230 * 102.5 * 3.175 * \left(\frac{226}{230 * 102.5} \right)^{\frac{1}{3}}$$

$$\phi V_{uc} = 18.4 \text{ kN}$$

Hence:

$$0.5\phi V_{uc} = 0.5 * 18.4$$

$$0.5\phi V_{uc} = 9.2 \text{ kN}$$

Using equation (1.13):

$$\phi V_{u, \min} = V_{uc} + 0.1 * \sqrt{f'c} * b * d > V_{uc} + 0.6 * b * d$$

Where:

$$V_{uc} = \frac{18.4}{0.7} = 26.2 \text{ kN}$$

$$f'c = 32 \text{ MPa}$$

$$b = 230 \text{ mm}$$

$$d = 102.5 \text{ mm}$$

Therefore,

$$\begin{aligned}\phi V_{u,\min} &= 26.2 + (0.1 * \sqrt{32} * 230 * 102.5)/10^3 > 26.2 + (0.6 * 230 * 102.5)/10^3 \\ \phi V_{u,\min} &= 39.54 \text{ kN} > 40.34 \text{ kN} \quad (\text{false})\end{aligned}$$

Hence,

$$\begin{aligned}\phi V_{u,\min} &= 0.7 * 40.34 \text{ kN} \\ \phi V_{u,\min} &= 28.2 \text{ kN}\end{aligned}$$

Figure 3-14 shows the magnitude of V^* in comparison to the values just calculated. Figure 3-14 demonstrates that ‘more than minimum’ reinforcement will be required around the rail seats where maximum shear forces acts. As no shear force acts on the mid-section of the sleeper (refer to figure 3-11), no shear reinforcement is required through the mid-section of the sleeper. However, for ease of construction, minimum shear reinforcement shall be adopted through the mid-section as GFRP shear reinforcement is usually purchased as a singular coil which wraps around the entirety of the flexural bars.

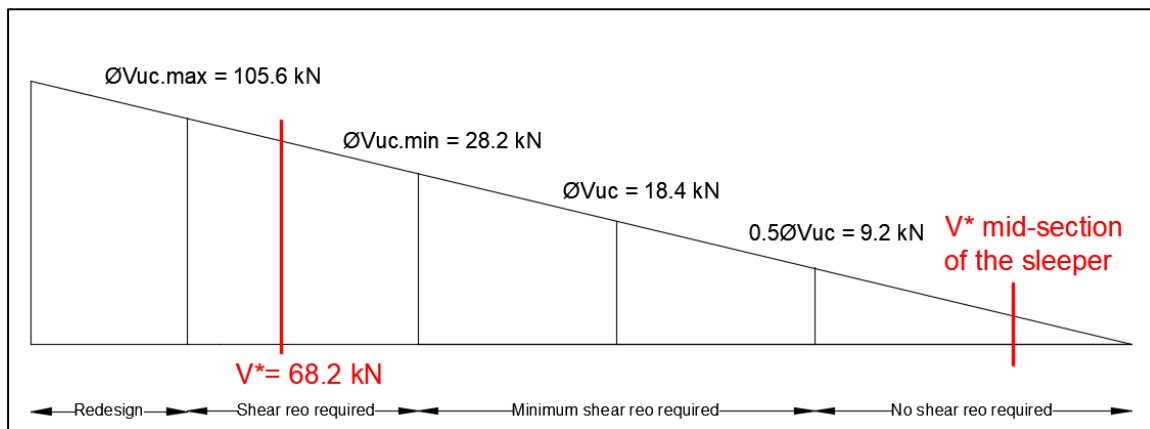


Figure 3-14: Design for shear diagram

Calculating the spacing for more than minimum shear reinforcement as required; refer to figure 2-12.

$$s = \frac{A_{sv} * f_u * d}{V_{us}} \cot(\theta_v)$$

Where:

$$A_{sv} = 2 * 2.5^2 * \pi = 39.3 \text{ mm}^2 \text{ (2 legs of } \phi 5 \text{ GFRP bars)}$$

$$f_u = 1372 \text{ MPa}$$

$$d = 102.5 \text{ mm}$$

$$V_{us} = \frac{68.2 - 18.4}{0.7} = 71.2 \text{ kN}$$

$$\theta_v = 30 + 15 \left(\frac{68.2 - 28.2}{105.6 - 28.2} \right) = 37.75^\circ = 0.658 \text{ rad}$$

Therefore,

$$s = \frac{39.3 * 1372 * 102.5}{71.2} \cot(0.658)$$

$$s = 100.2 \text{ mm}$$

The spacing of shear reinforcement shall be taken as the minimum of s, 0.5*D and 300mm

$$\text{Spacing required} = \min[100.2, 0.5 * 115, 300]$$

$$\text{Spacing required} = 57.5 \text{ mm}$$

Adopt a spacing of 50mm when more than minimum reinforcement is required and adopt a spacing of 100mm throughout the middle section of the beam where no shear reinforcement is required. Refer to shear reinforcement detailing in figure 3-15.

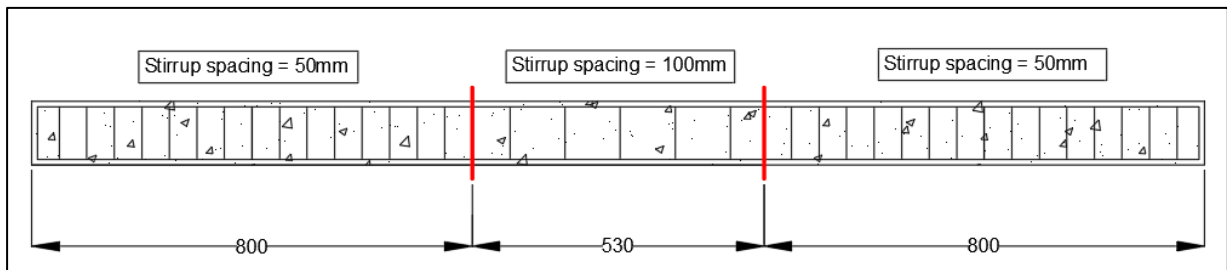


Figure 3-15: Shear reinforcement detailing

3.12 Designing the Polymer Concrete Sleeper

Initial design concepts envisioned manufacturing the entire railway sleeper using polymer concrete in lieu to Portland concrete. However, after the literature review, this concept was deemed unfeasible. A sleeper entirely made from polymer concrete was rejected because:

- Polymer concrete has a very low stiffness compared to traditional concrete hence the sleeper may deflect dramatically, affecting the trains ride quality and speed
- Polymer concrete is expensive compared to traditional concrete meaning the cost of an individual sleeper wouldn't be competitive with other designs currently on the market

At this point in the design process, more research was conducted on polymer concrete to find alternative ways to incorporate this emerging product. The concept of using polymer concrete wasn't completely rejected as initial research suggests that epoxy based polymer concrete has many favourable characteristics.

According El-Hawary et al. (2000), polymer concrete is becoming one of the most common methods to repair and rehabilitate existing concrete structures because it has great workability and superior durability characteristics. Polymer concrete it is typically grouted over deteriorating structures or directly injected into existing surface cracks. Tests done by El-Hawary et al. (2000) indicate that polymer concrete is able to bond well with traditional concrete and prevent great deterioration. Momtazi et al. (2015) also states that polymer concrete has successfully been used in the past to protect bridge decks, industrial floors and waste tanks from accelerated corrosion. Based on these findings, polymer concrete could specifically be used to protect a traditional concrete sleeper and its internal reinforcement hence extending its design life.

After conducting numerous tests on polymer concrete, Ferdous (2016) concludes that polymer concrete could sufficiently protect a composite railway sleeper. However this statement remains theoretical as no testing was actually performed on full scale polymer railway sleepers. Therefore, this research project should aim to manufacture a railway sleepers made from polymer concrete with a traditional concrete core. For this investigation, the sleeper detailed in figure 3-16 will be adopted. Note that the second row of GFRP bars in the tensile region should be cast with the concrete core but retain the same effective depth as the other sleeper. The aim of this particular design is to:

- Use polymer concrete to create a protective coating as research suggests that it more resistant to weathering, chemical attack and cracking compared to Portland concrete
- Maintain a traditional concrete core to improve stiffness and reduce production costs
- Reduce the sleepers overall carbon footprint by reducing the quantity of Portland cement used

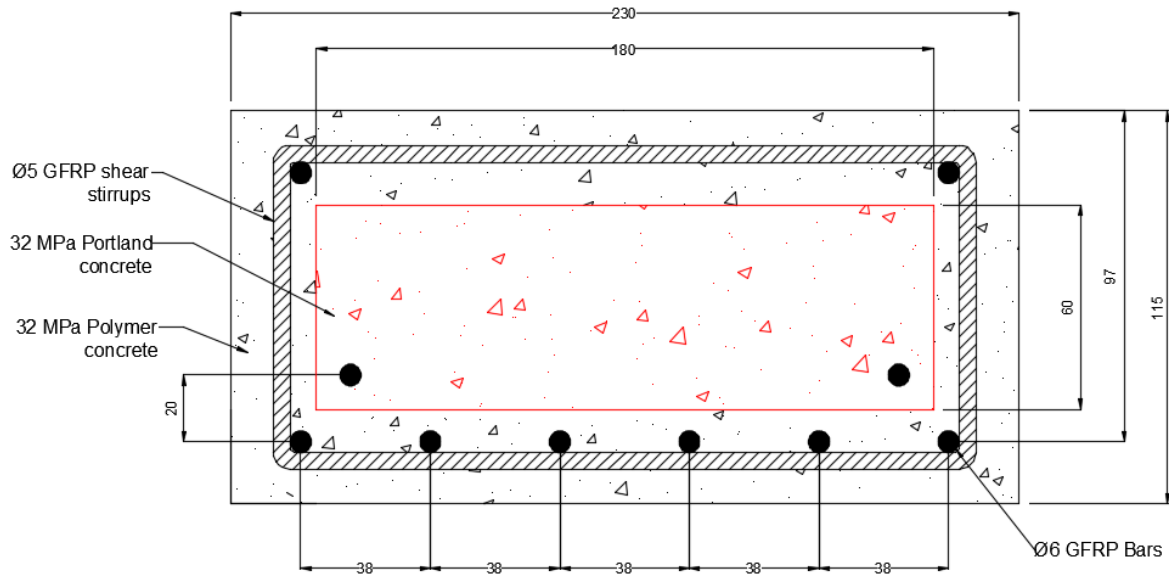


Figure 3-16: Polymer concrete sleeper with a Portland concrete core

Chapter 4 Experimental Program

4.1 Chapter Overview

This chapter will predominately focus on the materials and methods used to manufacture the test sleepers. A risk assessment was also undertaken to help identify potential hazards. Some recommendations were then provided to make sure appropriate safety precautions were followed. Both sleepers endured destructive and non-destructive testing. Due to the limited number of test specimens, the sleeper was always orientated to withstand maximum positive moment. During destructive testing, the sleeper’s deflection was also measured.

4.2 Safety Considerations

All organisations in Queensland must comply with the Work Health and Safety Act 2011 as anyone has the right to go home at the end of the day in the same condition as they arrived. Therefore, students at the University of Southern Queensland must complete an extensive risk assessment for each experimental activity before use of facilities and equipment is permitted. Any participants were also formally required to complete a lab site safety induction with a certified laboratory assistant before testing could commence.

A risk can be defined as a function of likelihood and severity (What is Risk?, 2018). In accordance with figure 4-1, each activity related to the manufacturing process was given a risk score in table 4-1. Some recommendations have been included to help minimise the degree of risk involved.



Figure 4-1: Risk assessment criteria (What is Risk?, 2018)

Table 4-1: Risk assessment scores and precautionary actions

Task	Risk Score	How can this risk be reduced
Cutting GFRP bars to size	8	Use common sense when using the hacksaw and keep hands well away from the cutting surface. Always use eye protecting while cutting and wear a mask to prevent inhaling loose glass fibres.
Attaching the strain gauges	4	Super glue will be used to attach the strain gauges to the GFRP bars. The glue could come in contact with the students hands and should be immediately washed.
Concrete products	3	These items will be heavy and precaution should be used when lifting them.
Compacting and placing the concrete	3	This task will require the use of some tools such as vibrators and trowels. Use common sense.
Setting up the experiment	3	This will involve manoeuvring the sleepers into position under the hydraulic press and connecting the leads from the strain gauges to the computer.
Testing the Sleepers	8	Testing will require the use of a large hydraulic jack which has the potential to crush limbs and cause severe injury. To minimise risk, students must stand back from the test in progress. Specimen failure may cause the concrete to spall and splinter. Therefore, a safety cage should be used around the sleeper to protect the operators from potential projectiles.

Beyond the completion of testing, no major risks have been identified. Participants should ensure that any waste concrete is placed into appropriate rubbish bins so it can be disposed of properly by USQ.

4.3 Materials

A detailed equipment list can be found in Appendix D All materials were sourced through the university. As discussed in Chapter 1, all material costs were covered by industry partners. The quality of some materials may vary depending on where they were sourced and their initial cost. Therefore, sections 4.3.1 and 4.3.2 will specifically discuss what products were used throughout this investigation.

4.3.1 GFRP bars

As mentioned previously in section 3.9.2, USQ sources GFRP bars from Inconmat Australia who directly import 'V-Rod' bars from Canada which are manufactured by Pultrall Incorporated. Their GFRP bars are made from high strength glass fibres which are hardened by a strong vinyl ester resin (V-ROD Fiberglass Rebar Canada, 2012). Their mechanical properties can be seen in Appendix E.

4.3.2 Strain Gauges

Strain gauges are small electrical devices used to measure deformation caused by an external force or moment. Strain gauges are commonly used when evaluating mechanical performance as strain data is often used to predict ultimate material failure. Therefore, strain gauges shall be attached directly to each row of flexural reinforcement at the sleeper's midpoint where the maximum strain will occur. For this investigation, 3mm long uniaxial strain gauges will be attached to the reinforcement to measure the strain developed in the flexural bars under loading while an additional two 10mm long uniaxial strain gauges will be attached to the sleeper's top and bottom surface to measure strain developed within the concrete.

4.4 Preparation of Test Sleepers

The reinforcement cage was constructed at USQ in accordance with the detailing drawings developed in Chapter 3; refer to figures 3-13, 3-15 and 3-16. In order to construct the cage, all flexural bars were initially cut to size (2110 mm) to allow 10mm of cover at each end of the sleeper. The shear reinforcement coil was then wrapped around the flexural bars while cable ties were used to fix the stirrups at appropriate spacing's; refer to figure 4-2.



Figure 4-2: Cable ties used to fix flexural and shear reinforcement together

After configuring the reinforcement cage, three strain gauges were attached to the flexural GFRP bars. As GFRP bars have a rough exterior sand coating, sandpaper was initially used to create a smooth surface. Each strain gauge was then attached using super glue as seen in figure 4-3. Once in position, electrical tape was wrapped around each gauge to protect it from moisture and aggregates within the cement mixture.



Figure 4-3: Attaching strain gauges to the GFRP bars using super glue

The reinforcement cage was then positioned in the precast sleeper mould ready for the concrete pour. Small spacers were attached to the cage to provide the specified 10mm of cover. Figure 4-4 shows the configuration of the reinforcement cage inside the precast mould.



Figure 4-4: The assembled reinforcement cage in the precast sleeper mould

The reinforcement cage for polymer sleeper was constructed in the same manner. The only difference being the concrete core in the middle of the reinforcement cage. The 60 x 180 mm concrete core was cast 28 days before being positioned inside the additional GFRP reinforcement cage; refer to figure 4-5.



Figure 4-5: The concrete core inside the GFRP reinforcement cage before the polymer concrete was poured

4.5 Concrete Pour

Portland and polymer cement with target strength of 32MPa was ordered from a local concrete manufacturer and delivered onsite. A high slump Portland cement mixture (200mm) was specially ordered to ensure uniform concrete compaction, even under the bars with very small cover. The polymer concrete had a 100:17.3 resin to hardener ratio by weight. The ratio and type of fillers used remains unknown as a premixed resin containing filler composites was supplied by ATL composites.

Many factors can affect the strength and workability of cement meaning it is unlikely that the concrete strength would exactly be 32MPa at the time of testing. Therefore, some cylinder concrete specimens were collected from both batches after the concrete pour. These specimens could be tested later if destructive or non-destructive test results seem unusual.

When pouring the concrete, the weather was not usual hence standard pouring procedures were followed. The cement was thoroughly vibrated to expel any trapped air and to optimise the density of the concrete. Figure 4-6 shows how the Portland concrete sleeper was poured.



Figure 4-6: Standard pouring methods were used to cast the sleepers

The cement was then hand screeded to achieve a level and smooth surface. Figure 4-7 shows the finished cast sleeper.



Figure 4-7: Screeded sleeper in its precast mould

After 28 days, the sleepers were taken out of their precast moulds. It was quite noticeable that the sleeper made from polymer concrete was significantly lighter than Portland concrete sleeper. This may be an advantage from a manufacturing point of view as more sleepers can be transported or lifted at the same time.

4.6 Non Destructive Testing Method

A standard three-point bend test as shown in figure 4-8 will be performed on both sleepers using a SANS machine. The purpose of this test was to load the sleeper with a force approximately equal to 40% of its total load capacity and develop a load vs displacement diagram while collecting strain data. The load vs displacement diagram will then be used to determine the sleeper's modulus of elasticity while strain data will be analysed to estimate the sleeper's. This theoretical value will then be compared against the sleepers true ultimate capacity obtained from destructive testing.

A support width of 1130 mm was chosen to replicate the track's gauge width while pieces of rubber were used to dampen the magnitude shear force at the supports. Two pieces of rubber were also positioned under the hydraulic jack. These rubbers were spaced 45mm either side of the sleepers centre, enabling enough room to attach a strain gauge to the top of the concrete sleeper. These rubbers were used to protect the strain gauge from the hydraulic cylinder and reduced the chance of concrete crushing. Once the sleeper was in position under the hydraulic cylinder, four strain gauges were connected to a nearby data logging computer. A constant load was then applied to the sleeper up to 20kN.

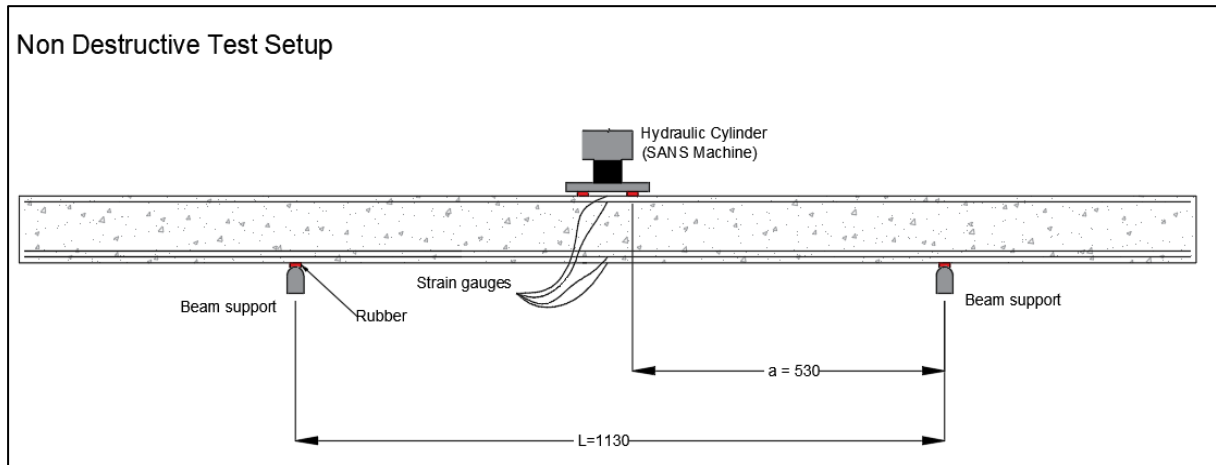


Figure 4-8: SANS machine setup for non-destructive testing

4.7 Destructive Testing Method

A five point bend test as shown in figure 4-9 will be used to determine the ultimate load capacity and failure method of both sleepers in comparison to theoretical predictions. As seen in figure 4-9, two point loads will act on the sleeper; as previously modelled in Strand 7. Results shall be able to validate whether polymer concrete has any noticeable advantages over traditional Portland concrete and whether GFRP bars are suitable. To reduce the magnitude of moment at the sleepers mid span, the centre support will be neoprene rubber as its modulus of elasticity is less than the steel supports at the sleepers ends. The steel supports will only be covered by a thin piece of rubber.

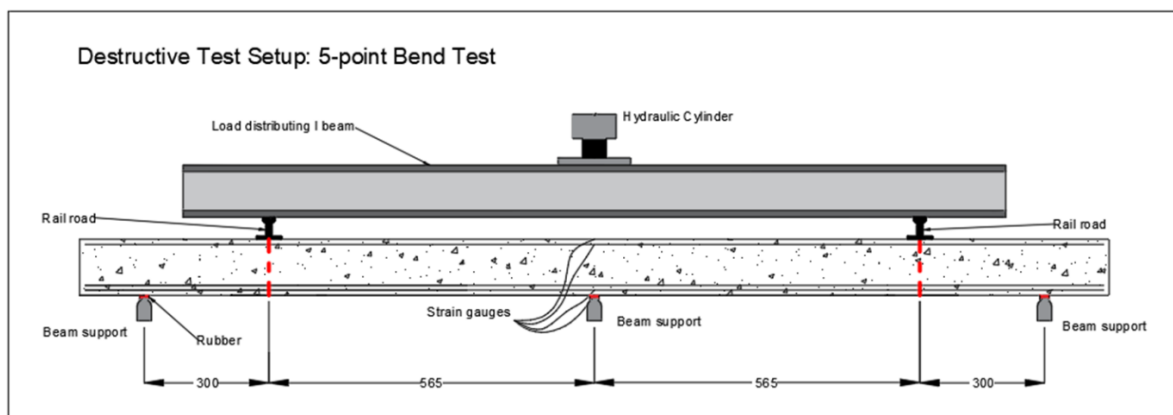


Figure 4-9: Destructive test setup

A five point bend test was chosen as this configuration best mimics how the sleeper would be loaded if the sleeper was to be positioned in-track. This decision is based on the fact that the bending moment diagram in this scenario should be very similar to the bending moment diagram derived from Model 2 in Strand 7 (refer to figure 3-11). Both bending moment diagrams will have the same general shape but the moment diagram will now be linear as the sleeper is not supported by ballast (elastic foundation theory) as modelled in Strand 7. Using neoprene rubber at the middle support has been proposed to dampen the magnitude of moment as the models developed in Strand 7 have calculated a moment ratio of 2.37 between the moment at the rail seat and the sleeper's mid-section. Therefore, this destructive test will try and replicate this moment ratio. This particular test setup is statically indeterminate meaning more complex methods may be required to determine the moment at failure once this load is known.

Chapter 5 Non-destructive Testing Observations, Results and Discussion

5.1 Chapter Overview

This chapter will analytically analyse the data collected during non-destructive testing. All data such as strain, load and deflection will be analysed using simple mathematical and stress analysis principles. Any key findings will then be discussed.

5.2 Non Destructive Testing Assessment

Initial non-destructive tests were unsuccessful as some strain gauges did not record any data. Therefore, a second three-point bend test was required where more creditable results were eventually obtained. The second attempt more successful as both sleepers behaved as expected and all necessary data was captured.

5.3 Non Destructive Testing Observations

Under loading, the traditional concrete sleeper seemed significantly stiffer compared to the polymer sleeper as little to no deflection was observed with the naked eye whereas deflection was quite obvious when testing the polymer sleeper. This observation is captured in figure 5-1. This result was expected as traditional concrete is significantly stiffer than polymer concrete based on literature.



Figure 5-1: Portland concrete sleeper under loading (left) and polymer concrete sleeper under loading (right)

Based on research analysed in Chapter 2, sleeper deflection was identified as a major design concern as GFRP reinforced sections may be governed by serviceability requirements. This belief was based on the fact that GFRP bars have a modulus of elasticity 25% less than mild steel while some finite element modelling done by T.Baker (2016) and A.Baker (2018) suggested that a GFRP reinforced sleeper will experience considerable deflection. However, after observing the degree of deflection during non-destructive testing, it initially seems plausible to use GFRP reinforcement. This is based on the observation that the Portland concrete sleeper did not deflect drastically. However, further data analysis and destructive testing will be required to provide a definite conclusion.

Research done by Gribniak, Rimkus, Torres and Hui (2018) suggests that GFRP reinforced sections are also more susceptible to cracking as a decrease in bar stiffness leads to increased beam deformation. Although GFRP bars are considerably more durable than steel bars, Yan et al. (2017) found that GFRP bars are still sensitive to alkaline environments, moisture, extreme temperatures and freeze thaw cycles. Therefore, excessive cracking still has the potential to significantly reduce the sleepers design life even if GFRP bars are used in lieu to steel.

During non-destructive testing, the Portland concrete sleeper started to develop flexural cracks; refer to figure 5-2. This observation concurs with previous research and suggests that the degree of cracking may become a point of concern during destructive testing.



Figure 5-2: Portland concrete sleeper developed flexural cracks during non-destructive testing

In comparison, the polymer concrete sleeper did not develop any flexural cracks during non-destructive testing; refer to figure 5-3. This is an excellent result as cracking is one of the leading causes of sleeper deterioration (Andersson et al., 2013). Although initial observations appear promising, the sleeper's overall mechanical performance needs to be verified.



Figure 5-3: No cracks were developed in the polymer concrete sleeper during non-destructive testing

5.4 Non-destructive Test Results and Discussion

5.4.1 Cracking

According to Table 2.3 in AS1085.14, no structural cracking should be present at a load equal to P_2 when conducting a rail seat positive bend test; as described in the Appendix E of AS1085.14. The non-destructive test setup shown in figure 4-8 essentially simulates a rail seat positive bend test. Therefore, P_2 shall be calculated to determine whether the manufactured sleepers surpassed this requirement. P_2 equals:

$$P_2 = \frac{2M^{CR}}{0.33 - 0.045} \quad (5.1)$$

Where:

$$M^{CR} = Z * \left(f' t + \frac{P}{A_t} \right) + eP$$

Therefore, calculating P_2 using equation 5.1:

$$M^{CR} = \frac{230 * 115^2}{6} * (0.75 * 32^{0.5} + 0) + 0$$

$$M^{CR} = 2.15 \text{ kNm}$$

$$P_2 = \frac{2 * 2.15}{0.33 - 0.045}$$

$$P_2 = 15.09 \text{ kN}$$

Footage of the non-destructive tests revealed that structural cracks only appeared in the Portland concrete once the applied load reached 16 kN which surpasses P_2 . However, as this sleeper only just passed this criterion, more tests are recommended to prove whether cracks structural cracks only develop once the load surpasses P_2 . In comparison, the polymer concrete sleeper showed no signs of structural cracks up to the applied load of 20kN. This means the polymer concrete sleeper easily surpasses this criterion and further justifies the use of polymer concrete as an exterior coating around a traditional concrete core.

5.4.2 Effective Modulus of Elasticity

Data from the SANS machine was outputted and analysed in excel to create a load versus deflection diagram as seen in figure 5-4. This graph indicates that both sleepers behaved almost linear elastic up to an applied load of 20 kN. This signifies that both sleepers will return to their unloaded state irrespective of their deformation. Figure 5-4 also validates the observation made about the sleeper's deflection. At 20kN, the polymer sleeper's deflection at its mid span is approximately 24.2% greater than the Portland concrete sleeper. This increase can only be accredited to the addition of polymer concrete as both sleepers have an identical reinforcement design.

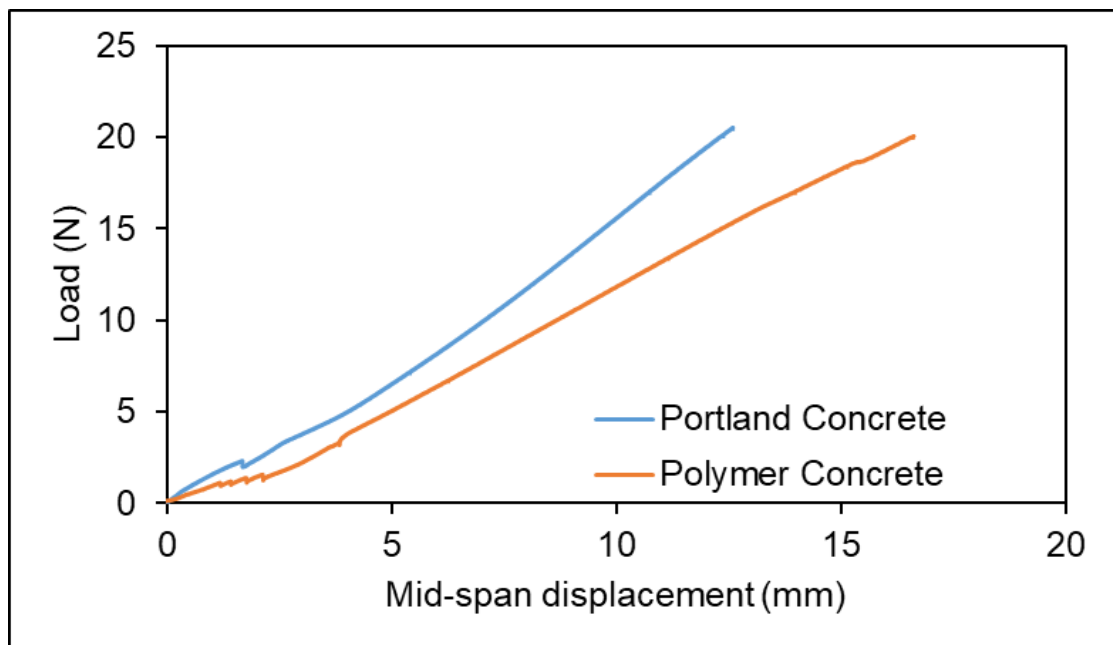


Figure 5-4: Non-destructive load versus deflection diagram

In conjunction with figure 5-4, the sleeper's effective bending stiffness (EI_{eff}) can be calculated using this this generic formula:

$$EI_{eff} = \frac{a}{48}(3l^2 - 4a^2) \left(\frac{\Delta P}{\Delta \delta}\right) \quad (5.2)$$

Where,

$a = \text{shear span} = 520 \text{ mm}$; refer to figure 4-8

$l = \text{Span length} = 1130 \text{ mm}$; refer to figure 4-8

$\left(\frac{\Delta P}{\Delta \delta}\right) = \text{slope of the load displacement curve}$; refer to figure 5-4

Portland Concrete Sleeper

$$\left(\frac{\Delta P}{\Delta \delta}\right) = 1.9287 \text{ kN/mm}$$

Using equation (5.2):

$$EI_{eff} = \frac{520}{48}(1130^2 - 4 * 520^2)(1.9287 * 1000)$$

$$EI_{eff} = 5.744 * 10^{10} \text{ N.mm}^2$$

Polymer concrete sleeper

$$\left(\frac{\Delta P}{\Delta \delta}\right) = 1.3693 \text{ kN/mm}$$

Using equation (5.2):

$$EI_{eff} = \frac{520}{48}(1130^2 - 4 * 520^2)(1.3693 * 1000)$$

$$EI_{eff} = 4.078 * 10^{10} \text{ N.mm}^2$$

Now that the sleeper's effective bending stiffness has been calculated, its effective bending modulus (E_{eff}) can be calculated:

$$E_{eff} = \frac{EI_{eff}}{I_{eff}} \quad (5.3)$$

First, determine I_{eff} :

$$I_{eff} = \frac{bh^3}{12} + (\text{neutral axis depth} - d/2)^2 \quad (5.4)$$

Portland Concrete Sleeper

Using equation (5.4):

$$I_{eff} = \frac{230 * 115^3}{12} + \left(17.99 - \frac{96.825}{2}\right)^2$$
$$I_{eff} = 29151029\text{mm}^4$$

Polymer Concrete Sleeper

Using equation (5.4):

$$I_{eff} = \frac{230 * 115^3}{12} + \left(68.96 - \frac{96.825}{2}\right)^2$$
$$I_{eff} = 29150526.37\text{mm}^4$$

Portland Concrete

Now, using equation (5.3):

$$E_{eff} = \frac{5.744 * 10^{10}}{29151029}$$
$$E_{eff} = 1.97 \text{ GPa}$$

Polymer Concrete

Now, using equation (5.3):

$$E_{eff} = \frac{4.078 * 10^{10}}{29150526.37}$$
$$E_{eff} = 1.39 \text{ GPa}$$

Both sleepers have achieved an acceptable effective modulus of elasticity in accordance with AMERA design standards; refer to table 5-1. This is significant as initial research highlighted that polymer concrete has a relatively low stiffness, hence it may not suit railway sleeper applications. Although its modulus is 29.44% less than its counterpart, it appears as though the traditional concrete core fulfilled its purpose and ensured that the polymer sleeper retained an acceptable effective modulus. If the sleeper's effective modulus was less than the AMERA minimum, train ride quality and top speed would be affected as the sleeper would deflect considerably under loading.

Table 5-1: Comparative sleeper modulus

	Minimum effective modulus (AMERA) (GPa)	Effective modulus (GPa)
Portland concrete sleeper	1.17	1.97
Polymer concrete sleeper		1.39

In comparison to timber sleepers, these two sleepers have a relatively low modulus of elasticity as timber sleepers generally have a modulus in the range of 7 – 12 GPa (Ferdous and Manalo, 2014). Consequently, these sleepers may not be compatible with timber sleepers in-track as they will deflect considerably more. This result was slightly unexpected as it was thought that the modulus of the composite sleepers would be similar to timber.

5.4.3 Recorded Strain Data

Experimental strain data was recorded using strain gauges which were attached to a data logger while the sleeper was loaded. This data was then exported into excel for analysis. The recorded strain data shows how the stress distribution over the sleeper section changes. Stress analysis principles have been used to evaluate the performance of the GFRP bars and predict how the sleeper will fail.

Portland Concrete Sleeper

It appears as though valid strain data was collected by all four strain gauges as the data is approximately linear; refer to figure 5-5. This is expected as the sleeper was loaded at a constant rate. Figure 5-5 also suggests that the sleeper’s neutral axis depth isn’t close at the sleeper’s midsection as the magnitude of negative strain is significantly less than positive strain.

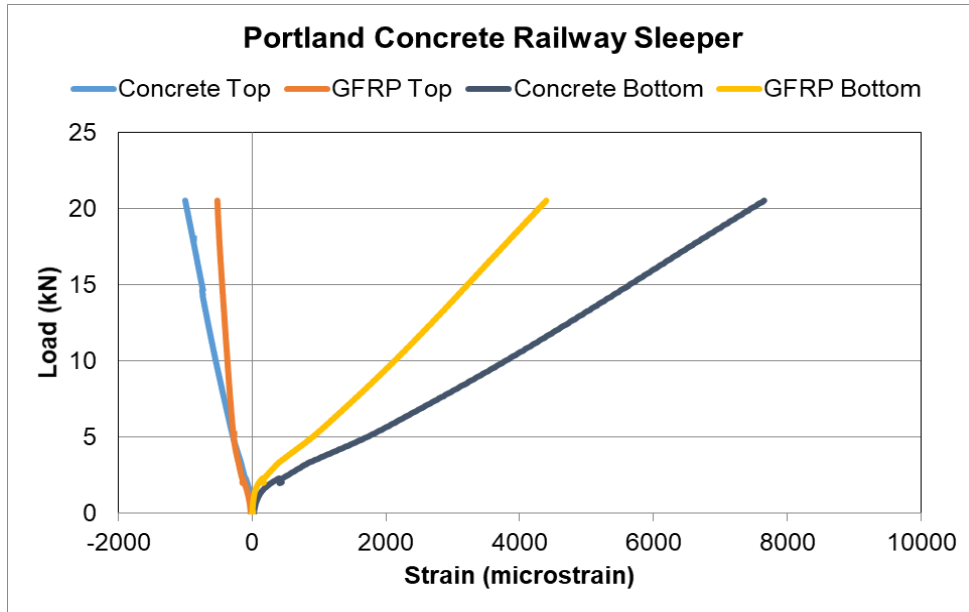


Figure 5-5: Recorded strain data vs load; Portland concrete sleeper

Based on the strain data shown in figure 5-5, figure 5-6 was produced. Figure 5-6 shows how strain varies over the sleeper's cross section at 20kN. For simplicity, it was then assumed that the strain distribution was linear and the sleeper's neutral axis depth was found. Based on the position of the neutral axis, it was determined that the GFRP bars in the top portion of the sleeper were actually contributing to the overall tensile force, meaning the compressive strength of the concrete was the only negative force keeping equilibrium around the neutral axis.

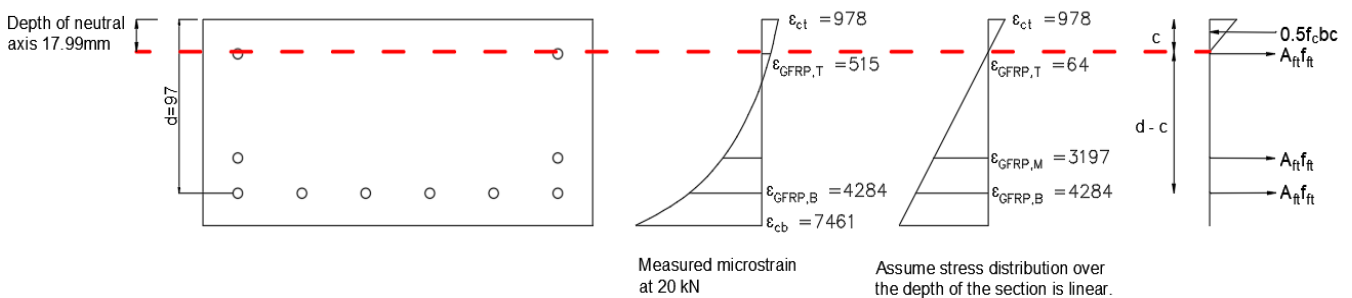


Figure 5-6: Strain distribution over the Portland concrete sleeper

Polymer Concrete Sleeper

All of the recorded strain data from this test seems reliable as it's approximately linear; refer to figure 5-7. Unlike the Portland concrete sleeper, the magnitude of negative and positive strain is quite similar; hence the neutral axis depth is more towards the midsection of the sleeper.

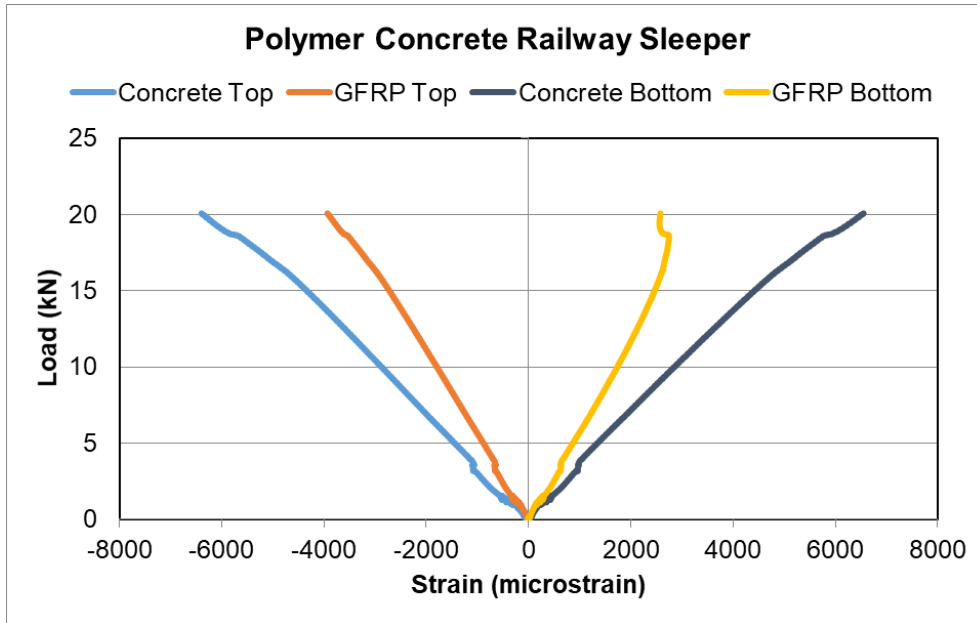


Figure 5-7: Recorded strain data vs load; Polymer concrete sleeper

Based on the strain data shown in figure 5-7, figure 5-8 was created. Figure 5-8 demonstrates that the proportion of positive and negative strain is approximately equal; hence the calculated neutral axis depth is much closer to the sleeper's midsection in comparison to the Portland concrete sleeper. This means the GFRP bars in the top portion of the sleeper will be contributing to the compressive force with the compressive strength of the concrete. As shown in figure 5-8, it's unlikely that the strain distribution for this sleeper is linear as this assumption suggests that the Portland concrete core has already crushed. Strain readings taken at the top and bottom of this sleeper must be greater than the Portland concrete sleeper as polymer concrete has a much low modulus. The magnitude of strain under the same loading is therefore greater according to Hooke's law.

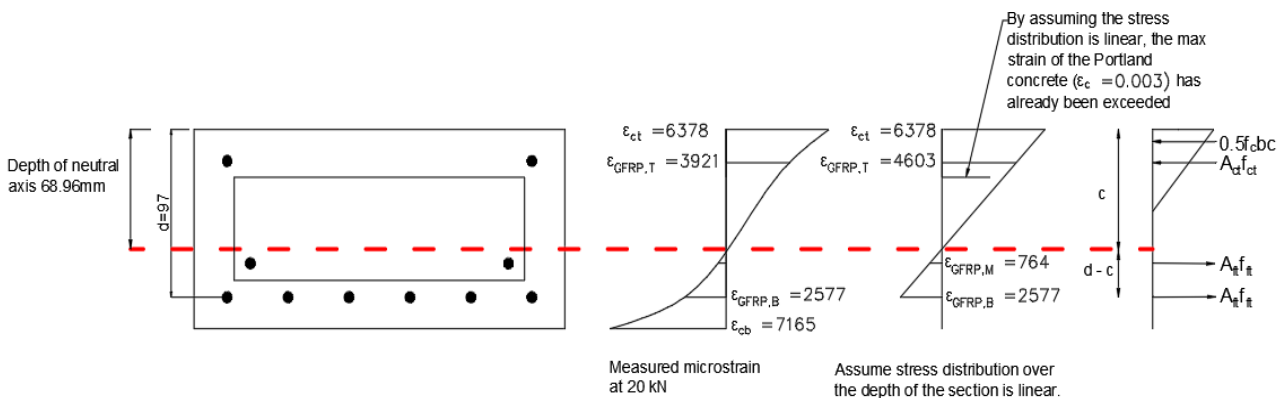


Figure 5-8: Strain distribution over the polymer concrete sleeper

5.4.4 Analysing Experimental Strain Data to Predict Mode of Sleeper Failure

Based on maximum theoretical strain values, the optimal position of the neutral axis can be determined. If the sleeper's neutral axis position was equal to the optimal neutral axis position, the sleeper would fail due to bar rupture and concrete crushing simultaneously. To predict the mode of failure, the location of the experimental neutral axis will be compared against the optimal neutral axis depth. Similar triangles can be used to determine the experimental neutral axis depth.

Portland Concrete Sleeper

The maximum theoretical strain value of Portland concrete is approximately equal to 0.003 while the maximum strain value of GFRP bars is 0.021; refer to Appendix E. Therefore, the optimal strain distribution is shown in figure 5-9.

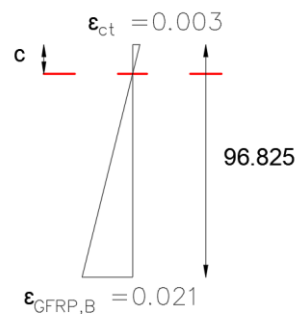


Figure 5-9: Optimal strain distribution for Portland concrete sleeper

Hence,

$$\frac{0.003}{c} = \frac{0.0211}{96.825 - c}$$

$$c = 12.05 \text{ mm}$$

In conclusion, the sleeper will likely fail due to concrete crushing if the experimental neutral axis is > 12.05 mm or bar rupture if the sleeper's neutral axis < 12.05 mm. Based on the strain values shown in figure 5-5, the experimental neutral axis depth has been calculated as:

$$\frac{978}{c} = \frac{4284}{96.825 - c}$$

$$c = 17.99 > 12.05 \text{ mm}$$

By using experimental data to determine the position of the neutral axis, it can be predicted that the sleeper will fail due to concrete crushing before bar rupture.

Polymer Concrete Sleeper

According to Lokuge & Aravinthan (2013), the ultimate strain capacity of epoxy based polymer concrete is approximately 0.02 and the maximum strain in GFRP bars is 0.021; refer to Appendix E. Therefore, the optimal strain distribution is shown in figure 5-10.

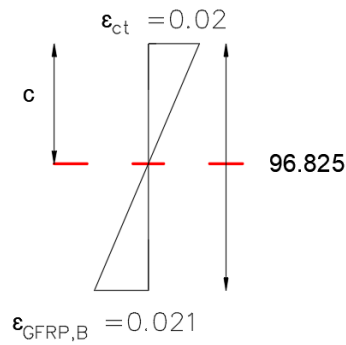


Figure 5-10: Optimal strain distribution for polymer concrete sleeper

Hence,

$$\frac{0.02}{c} = \frac{0.0211}{96.825 - c}$$

$$c = 47.23\text{mm}$$

As a result, if the sleeper's neutral axis is > 47.23 mm, the sleeper will likely fail due to concrete crushing. Alternatively, the sleeper will likely fail due to bar rupture if the sleeper's neutral axis is < 47.23 mm. Finding the sleepers neutral axis depth using similar triangles based on recorded strain data:

$$\frac{6378}{c} = \frac{2577}{96.825 - c}$$

$$c = 68.96 > 47.23 \text{ mm}$$

By using experimental data to determine the position of the neutral axis, it can be predicted that the sleeper will fail due to concrete crushing before bar rupture.

5.4.5 Determining the Sleepers Compressive Strength (f'_c)

For equilibrium around the neutral axis, the following generic formula can be applied:

$$(A_{ft}f_{ft})_B + (A_{ft}f_{ft})_M + (A_{ft}f_{ft})_T - 0.5f'_c bc = 0$$

By rearranging this equation and using the recorded strain data, the sleeper's actual f'_c can be determined:

$$f'_c = \frac{(A_{ft}f_{ft})_B + (A_{ft}f_{ft})_M + (A_{ft}f_{ft})_T}{0.5 * b * c} \quad (5.5)$$

Portland Concrete Sleeper

Strain in the middle and top GRFP bars can be predicted using similar triangles, refer to figure 5-6 for strain values:

$$\frac{4284}{96.825 - 17.99} = \frac{\varepsilon_{GFRP,M}}{96.825 - 17.99 - 20} = \frac{\varepsilon_{GFRP,T}}{19.175 - 17.99}$$

$$\varepsilon_{GFRP,M} = \frac{4284}{96.825 - 17.99} * (96.825 - 17.99 - 20)$$

$$\varepsilon_{GFRP,M} = 3197$$

$$\varepsilon_{GFRP,T} = \frac{4284}{96.825 - 17.99} * (19.175 - 17.99)$$

$$\varepsilon_{GFRP,T} = 64$$

Now the tensile and compressive forces can be calculated. The modulus of the GFRP bars can be taken as $65.1 * 10^3 \text{ MPa}$; refer to Appendix E.

$$(A_{ft}f_{ft})_i \text{ (kN)} = \varepsilon * E_{GFRP} * \text{Area of bars} \quad (5.6)$$

Using equation (5.6) to calculate contributing forces:

$$(A_{ft}f_{ft})_B = \frac{4258}{10^6} * 65.1 * 10^3 * 3.175^2 * \pi * 6$$

$$(A_{ft}f_{ft})_B = 52.993 \text{ kN}$$

$$(A_{ft}f_{ft})_M = \frac{3197}{10^6} * 65.1 * 10^3 * 3.175^2 * \pi * 2$$

$$(A_{ft}f_{ft})_M = 13.183 \text{ kN}$$

$$(A_{ft}f_{ft})_T = \frac{64}{10^6} * 65.1 * 10^3 * 3.175^2 * \pi * 2$$

$$(A_{ft}f_{ft})_T = 0.264 \text{ kN}$$

Therefore, the compressive strength of the concrete can be calculated using (5.5):

$$f'_c = \frac{52.993 + 13.183 + 0.264}{0.5 * 230 * 17.99}$$

$$f'_c = 32.104 \text{ MPa}$$

As the target strength of the concrete was 32MPa, any anomalies in the data when conducting the destructive testing won't be related to the compressive strength of the concrete.

Polymer Concrete Sleeper

As it's unlikely that the strain distribution for this sleeper is linear (refer to figure 5-8), this equation would not be able to accurately calculate the compressive strength of the concrete. As the effective modulus calculated from the load vs displacement diagram is slightly lower than the Portland concrete, it can be assumed that f'_c for the polymer concrete is slightly less than 32.1MPa which was calculated for the Portland concrete sleeper. Therefore, assume that $f'_c = 30 \text{ MPa}$ for the polymer concrete sleeper.

5.4.6 Predicting Moment at Failure

The predicted moment at failure can be calculated using the following equation:

$$M = (A_{ft}f_{ft})_B (d - c) + (A_{ft}f_{ft})_M (d - c - 0.020) + (A_{ft}f_{ft})_T((d, top) - c) + 0.5f'_c bc \left(\frac{2}{3} * c\right) \quad (5.7)$$

Portland Concrete Sleeper

As determined earlier, assume the sleeper will fail due to concrete crushing. Figure 5-11 shows the predicted strain distribution at failure.

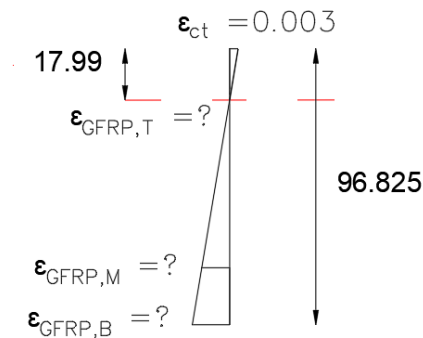


Figure 5-11: Predicted failure distribution for the Portland concrete sleeper

By using similar triangles, strain in the bottom, middle and top GRFP bars can be approximated:

$$\frac{0.003}{17.99} = \frac{\epsilon_{GFRP,T}}{19.175 - 17.99} = \frac{\epsilon_{GFRP,M}}{96.825 - 17.99 - 20} = \frac{\epsilon_{GFRP,B}}{96.825 - 17.99}$$

$$\epsilon_{GFRP,T} = \frac{0.003}{17.99} * (19.175 - 17.99)$$

$$\epsilon_{GFRP,T} = 0.000197$$

$$\epsilon_{GFRP,M} = \frac{0.003}{17.99} * (96.825 - 17.99 - 20)$$

$$\epsilon_{GFRP,M} = 0.009807$$

$$\epsilon_{GFRP,B} = \frac{0.003}{17.99} * (96.825 - 17.99)$$

$$\epsilon_{GFRP,B} = 0.013141$$

Using equation (5.6) to determine tensile and compressive forces:

$$(A_{ft}f_{ft})_T = 0.000197 * 65.1 * 10^3 * 3.175^2 * \pi * 2$$

$$(A_{ft}f_{ft})_T = 0.8104 \text{ kN}$$

$$(A_{ft}f_{ft})_M = 0.009807 * 65.1 * 10^3 * 3.175^2 * \pi * 2$$

$$(A_{ft}f_{ft})_M = 40.438 \text{ kN}$$

$$(A_{ft}f_{ft})_B = 0.013141 * 65.1 * 10^3 * 3.175^2 * \pi * 6$$

$$(A_{ft}f_{ft})_B = 162.560 \text{ kN}$$

Now the moment around the neutral axis can be calculated using equation (5.7):

$$M = 162.560 * (0.096825 - 0.01799) + 40.438 (0.096825 - 0.01799 - 0.02) \\ + 0.8104(0.19175 - 0.01799) + 0.5 * 32.104 * 230 * 0.1799 \left(\frac{2}{3} * 0.01799\right)$$

$$M = 15.991 \text{ kNm}$$

Polymer Concrete Sleeper

As determined earlier, assume the sleeper will fail due to concrete crushing. Figure 5-12 shows the predicted strain distribution at failure.

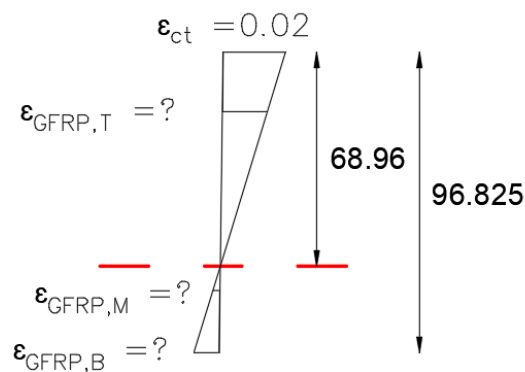


Figure 5-12: Predicted failure distribution for the polymer concrete sleeper

By using similar triangles, strain in the bottom, middle and top GRFP bars can be approximated:

$$\frac{0.02}{68.96} = \frac{\varepsilon_{GFRP,T}}{68.96 - 19.175} = \frac{\varepsilon_{GFRP,M}}{96.825 - 20 - 68.96} = \frac{\varepsilon_{GFRP,B}}{96.825 - 68.96}$$

$$\varepsilon_{GFRP,T} = \frac{0.02}{68.96} * (68.96 - 19.175)$$

$$\varepsilon_{GFRP,T} = 0.014438$$

$$\varepsilon_{GFRP,M} = \frac{0.02}{68.96} * (96.825 - 20 - 68.96)$$

$$\varepsilon_{GFRP,M} = 0.002281$$

$$\varepsilon_{GFRP,B} = \frac{0.02}{68.96} * (96.825 - 68.96)$$

$$\varepsilon_{GFRP,B} = 0.0080814$$

Using equation (5.6) to determine tensile and compressive forces:

$$(A_{ct}f_{ct})_T = 0.014438 * 65.1 * 10^3 * 3.175^2 * \pi * 2$$

$$(A_{ft}f_{ft})_T = 59.54 \text{ kN}$$

$$(A_{ft}f_{ft})_M = 0.002281 * 65.1 * 10^3 * 3.175^2 * \pi * 2$$

$$(A_{ft}f_{ft})_M = 9.41 \text{ kN}$$

$$(A_{ft}f_{ft})_B = 0.0080814 * 65.1 * 10^3 * 3.175^2 * \pi * 6$$

$$(A_{ft}f_{ft})_B = 99.96 \text{ kN}$$

Now the moment around the neutral axis can be calculated using equation (5.7):

$$M = 99.96 * (0.096825 - 0.06896) + 9.41 * (0.096825 - 0.06896 - 0.02) + 59.54 * (0.06896 - 0.019175) + 0.5 * 30 * 0.23 * 0.06896 * \left(\frac{2}{3} * 0.06896\right)$$

$$M = 16.76 \text{ kNm}$$

5.4.7 Theoretical Strain Developed in the GFRP Bars at Failure

If both sleepers fail due to concrete crushing as predicted, the full strength of the GFRP bars won't be utilised. Therefore, it is worth theoretically calculating how close the GFRP bars come to rupturing and comment on the suitability of GRFP reinforcement.

Portland Concrete Sleeper

Determine the maximum strain developed in either the top, middle or bottom row of GFRP reinforcement as calculated previously in section 5.4.6:

$$\text{Max strain calculated} = [\varepsilon_{GFRP,T}, \varepsilon_{GFRP,M}, \varepsilon_{GFRP,B}]$$

$$\text{Max strain} = [0.000197, 0.009807, 0.013141]$$

$$\text{Max strain} = \varepsilon_{GFRP,B} = 0.013141$$

The maximum strain value of GFRP bars is 0.021. Therefore:

$$\text{Ultimate strain capacity reached in the GFRP bars at failure (\%)} = \frac{0.013141}{0.021} * 100 = 62.6\%$$

Polymer Concrete Sleeper

Determine the maximum strain developed in either the top, middle or bottom row of GFRP reinforcement as calculated previously in section 5.4.6:

$$\text{Max strain calculated} = [\varepsilon_{GFRP,T}, \varepsilon_{GFRP,M}, \varepsilon_{GFRP,B}]$$

$$\text{Max strain} = [0.014438, 0.002281, 0.0080814]$$

$$\text{Max strain} = \varepsilon_{GFRP,T} = 0.014438$$

The maximum strain value of GFRP bars is 0.021. Therefore:

$$\text{Ultimate strain capacity reached in the GFRP bars at failure (\%)} = \frac{0.014438}{0.021} * 100 = 68.75\%$$

5.5 Key Findings from Non-destructive Testing

A summary of calculations based on strain data can be seen in table 5-2.

Table 5-2: Predicted behaviour and performance of the sleepers based on non-destructive test results

	Predicted Mode of Failure	Ultimate strain capacity reached in the GFRP bars at failure (%)	Predicted moment at failure (kN.m)
Portland Concrete Sleeper	Concrete Crushing	62.6	15.99
Polymer Concrete Sleeper	Concrete Crushing	68.75	16.76

Using strain data collected from non-destructive testing, the Portland concrete sleepers neutral axis depth (17.99mm) and the concrete's actual compressive strength ($f'_c = 32.1\text{Mpa}$) was calculated. Based on the position of the neutral axis, it was predicted that the sleeper will fail due to concrete crushing. Strain developed in the GFRP bars at failure was then approximated. At failure, strain in bottom GFRP bars will only reach 62.6% of its ultimate strain capacity. This suggests that GFRP reinforcement can be used in lieu to steel without great implications. The moment at beam failure has been predicted as 15.991 kNm or 0.935% less than M^* (16.24 kNm) which was used to design the beam. As the predicted theoretical and experimental moment at failure is approximately equal, the following conclusions can be made about the Portland concrete sleeper:

- Manufacturing was of a high quality
- The target strength of the concrete was achieved
- The GFRP bars have bonded well with the concrete; much the same as steel reinforcement
- The assumption made about the stress distribution over the depth of the section being approximately linear is fair and reasonable
- GFRP reinforcement design should be able to adequately resist the calculated rail seat loads

Using strain data collected from non-destructive testing, the polymer concrete sleepers neutral axis depth (68.96mm) was calculated. The position of the neutral axis is significantly different in comparison to the Portland concrete sleeper. The concrete's actual compressive strength couldn't be calculated as strain distribution over the depth of the section isn't linear due to the two different cementitious materials used.

Based on the position of the neutral axis, it was predicted that the sleeper will fail due to concrete crushing. Strain developed in the GFRP bars at failure was then approximated. At failure, strain in bottom GFRP bars only reached 38.48% of their ultimate strain capacity while the GFRP bars at the top of the sleeper reached 68.75% of their ultimate strain capacity. The moment at beam failure has been predicted as 16.76kNm or 3.7% greater than M^* (16.142 kNm) which was used to design the beam. As the true strain distribution over the depth of the sleeper and the true compressive strength of the concrete is unknown, the predicted moment at beam failure may not be accurate. Therefore, destructive testing is required before commenting further on the polymer sleeper's performance.

Based on the result gathered thus far, using GFRP reinforcement instead of steel doesn't appear to have significant characteristics that reduces the sleepers overall performance. However, the magnitude of deflection may be an area of concern. The use of polymer concrete seems to be justified as its use has reduced the degree of cracking which is one of the leading causes of premature concrete sleeper failure. In order to accurately justify the sleeper's strength and deflection, a timber sleeper should be included in the destructive testing for comparative purposes. It would be beneficial to see how these composite sleeper concepts compare to traditional timber sleepers as mimicking their behaviour is the ultimate goal.

Chapter 6 Destructive Testing Observations, Results and Discussion

6.1 Chapter Overview

This chapter will analytically analyse the data collected during destructive testing. All data such as strain, load and deflection will be analysed using simple mathematical and stress analysis principles. Any key findings will then be discussed.

6.2 Destructive Testing Assessment

Both tests were successful as the testing equipment used was able to load both sleepers until failure. Before conducting the tests, there were some concerns that the sleepers wouldn't fail as the chosen test equipment had a load limit of 300 kN or a rail seat load of 150 kN. However, this wasn't the case as both sleepers failed well before this load limit. After perusing some of the captured strain data, it appears as though some of the data was noisy but acceptable. For comparison purposes, a traditional timber sleeper was also tested using the same experimental setup.

6.3 Destructive Testing Observations

Destructive testing was performed at USQ and no changes were made to the proposed test setup as shown in figure 4-9. To help measure the sleeper's deflection under loading, a digital image correlation (DIC) measuring instrument was setup and connected to a computer; refer to figure 6-1. Images taken from the DIC were saved onto a lab computer and was analysed at a later time using a specialised software package.



Figure 6-1: The destructive test setup and the DIC device in front of load cell

The observed deflection at the maximum load was significantly higher for the polymer sleeper in comparison to the Portland concrete sleeper as seen in figure 6-2 and 6-3 respectively. This was expected as non-destructive testing determined that the Portland concrete sleeper has a higher stiffness. Deflection was greatest underneath the rail seat whereas maximum deflection occurred at the sleeper's midsection in Strand 7. The location of maximum deflection has changed as the sleeper is now supported in the middle, unlike the sleeper in Strand 7 which has been modelled based on beam on elastic foundation theory. It also appears that maximum deflection was much greater than 5.84 mm which was the maximum theoretical deflection calculated from the models Strand 7.



Figure 6-2: Observed deflection at maximum applied load for the polymer concrete sleeper



Figure 6-3: Observed deflection at maximum applied load for the Portland concrete sleeper

Portland Concrete Sleeper

The first signs of significant cracking occurred around 64.3 kN at the sleepers midsection. Based on the shape and direction of these cracks, it can be assumed that these were flexural cracks caused by tension stresses. Significant cracks can be defined as any cracks greater than 0.5mm as research suggests that cracks should be limited to this width to help protect GFRP bars from any aggressive environments (Newhook & Svecova, 2007). The first sight of flexural cracks above the middle support can be justified as the middle support would have the greatest support reaction as both loads points are contributing to its magnitude. A large crack noise was heard around 100 kN which might dictate when the sleeper initially failed. The sleeper was further loaded to 108.55 kN before significant cracking was observed underneath the rail seat. Cracks observed at the rail seat seemed to

be a combination of flexural and diagonal tension failure cracks. Diagonal tension failure can occur if the shear span is three times greater than the effective depth. This is the case in this scenario; $300 \text{ mm} > 3 * 96.825 \text{ mm}$. The degree of cracking or the number of cracks at the rail seat increased significantly once the applied load reached 125 kN, while flexural cracks at the middle support have since propagated over half the sleepers depth. By 150 kN, most cracks had surpassed 1mm in width and it appeared as though the sleeper was nearly at its ultimate limit. At 155 kN, some concrete directly underneath the applied load at the rail seat started to spall which indicated that some of the concrete had been crushed. The load acting on the beam could not physically surpass 160 kN. Figure 6-4 was taken when the beam was loaded at 160kN and shows the nature, type and size of the cracks developed in the sleeper.



Figure 6-4: Cracking observed in the Portland concrete sleeper at the middle support and the rail seat

Based on what was observed, some of the cracks developed in the sleeper might have been caused indirectly by the experimental setup rather than a lack of reinforcement or poor reinforcement design. For future reference, the shear span might need to be reduced if the results show that diagonal tension failure is a reason why the sleeper failed.

Polymer Concrete Sleeper

Significant flexural cracking was first observed again at the middle support for the polymer concrete sleeper. These flexural cracks were developed around an applied load of 90kN. This load is significantly greater than the load at which the Portland concrete sleeper started developing significant flexural cracks. This supports what was found during non-destructive testing and demonstrates that concrete cracking can be reduced if polymer concrete is used, even when the sleeper is loaded in a manner that mimics how the sleeper would be loaded in-track. Some cracking noises were heard around 95kN which might dictate when the sleeper initially failed. It wasn't until the load reached 110 kN before significant cracks appeared around the rail seat which was again, a higher load in

comparison to the Portland concrete sleeper. In this case, it appeared as though nearly all cracks were propagating from the tension side of the sleeper which differs from the other test which had some cracks related to shear.

At this stage, it was evident that both sleepers had quite unique cracking patterns. Firstly, the degree of cracking in the polymer sleeper is comparatively much lower while the rate at which the cracks widened was much higher. Unlike the Portland concrete, the polymer concrete sleeper didn't develop any hairline cracks which slowly increased in width over the duration of the test. Instead, cracks only appeared around 100 kN. This observation became even more prominent as the load increased beyond 110kN as crack widths continued to expand in the polymer concrete as shown in figure 6-5. Once the load reached 165kN, some cracks in the sleeper surpassed 5mm in size. Noticeably, this load was already greater than the maximum load applied to the Portland concrete sleeper. At 190kN, a noticeably large shear crack developed at the left rail seat as shown in figure 6-5. This indicates that polymer concrete might be more resistant to shear cracking as well as flexural. The beam could not physically be loaded beyond 195 kN. At maximum load, it was noted that the no concrete spalling was observed. Figure 6-5 shows the nature, type and size of the cracks developed in the sleeper.



Figure 6-5: Cracking observed in the polymer concrete sleeper at the middle support and the rail seats

6.4 Destructive Test Results and Discussion

6.4.1 Determining Possible Modes of Failure

After conducting the destructive tests, it was apparent that both sleepers failed well before they reached the calculated rail seat load of 117.12 kN which was used as the basis of all reinforcement design calculations. A rail seat load of this magnitude would be equivalent to an applied load of 234.24 kN as the two experimental rail seat loads were applied by a single hydraulic ram. The Portland and polymer concrete sleeper could not be loaded past 160 and 195 kN respectively. This result indicates that both sleepers have failed in an unusual circumstance or the proposed 5-point bend test doesn't accurately replicate how the sleeper would be loaded in track. Potential problems associated with manufacturing the sleeper, the strength of the concrete, the bond of the GFRP bars

with the concrete and the GFRP reinforcement design itself can be disregarded as non-destructive testing has proven that these potential problems are non-existent. Therefore, it is likely that the experimental setup itself is the reason why the load at failure was must lower than expected.

As highlighted in section 6.2, it appears as though some diagonal tension failure cracks were developed in the Portland concrete sleeper and could be a cause of failure. This indicates that high shear stresses were developed in the shear span; the region between the rail seat and the outside steel support. It was also noted that some concrete had begun to crush. After the Portland concrete was unloaded, some of the spalled concrete was manually flaked away to expose some of the internal GFRP reinforcement, as shown in figure 6-6. After closer inspection, it was observed that one of the longitudinal GFRP flexural bars was actually ruptured; refer to figure 6-6. It appears as though this bar has failed in shear as the fracture is approximately 45° and replicates the direction of the major diagonal tension crack. After reviewing the mechanical properties of GFRP bars themselves in Appendix E, the transverse shear capacity of the longitudinal bars is approximately 41 kN meaning it is quite possible that the sleeper has ultimately failed in shear.

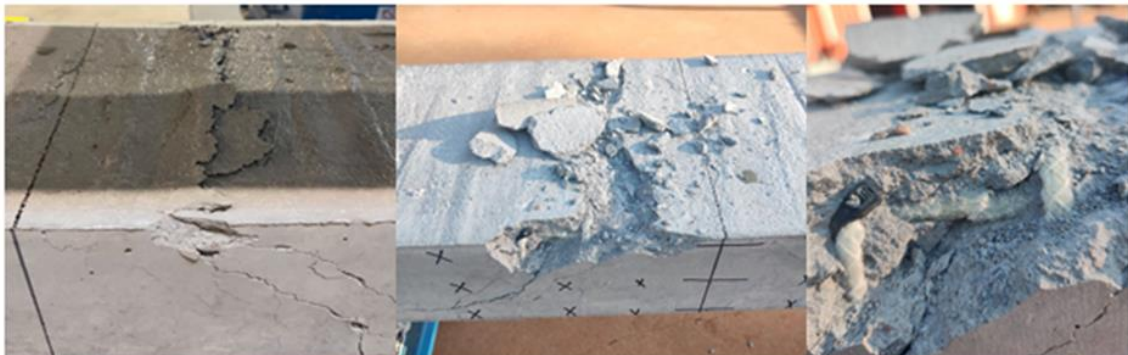


Figure 6-6: Spalled concrete was removed to reveal a ruptured longitudinal GFRP bar

Due to the size of the crack developed at the middle support, especially when testing the polymer concrete sleeper, there is a possibility that the sleeper has failed at this location in bending before failing in shear. The sleeper is vulnerable to flexural failure at the middle support as the sleeper only has 2 flexural bars in the tensile region, compared to 8 flexural bars in the tensile region at the exterior supports. Essentially, if the neoprene rubber didn't dampen the moment at the middle support as much as expected, the moment may have surpass the maximum negative moment used to design the amount of reinforcement required. If the sleeper did fail in this manner, the test setup should alter to ensure flexural failure occurs at the bottom of the sleeper where the 8 flexural bars have been

positioned. It is best to simulate flexural failure at the bottom of the sleeper as this is where the most critical moment acts when positioned in-track.

To help distinguish how both sleepers failed, the 5-point bend test shall be modelled in Strand 7 to determine the moment and shear forces acting on the sleeper at the point of failure. These values should then be compared against the values listed in table 3-4. To model the 5-point bend test, the exact load acting on the sleeper at failure must be determined. It is best to model the sleeper in Strand 7 as the test setup is statically indeterminate.

6.4.2 Load at Failure

Portland Concrete sleeper

Experimental strain data was recorded using strain gauges which were attached to a data logger while the sleeper was incrementally loaded. This data was then exported into excel for analysis. One strain gauge was attached directly underneath the rail seat while the other gauge was attached above the middle support. Consequently, both strain gauges should only record positive strain as they are both positioned in a tensile region. However, by looking at figure 6-7, it appears as though some negative strain was recorded when testing the Portland concrete sleeper. This indicates that the strain gauge positioned at the rail seat may have been damaged prior testing or it was damaged during the test. As a result, strain data recorded at the rail seat was ignored when trying to determine the load at failure for the Portland concrete sleeper as this data appears to be unreliable.

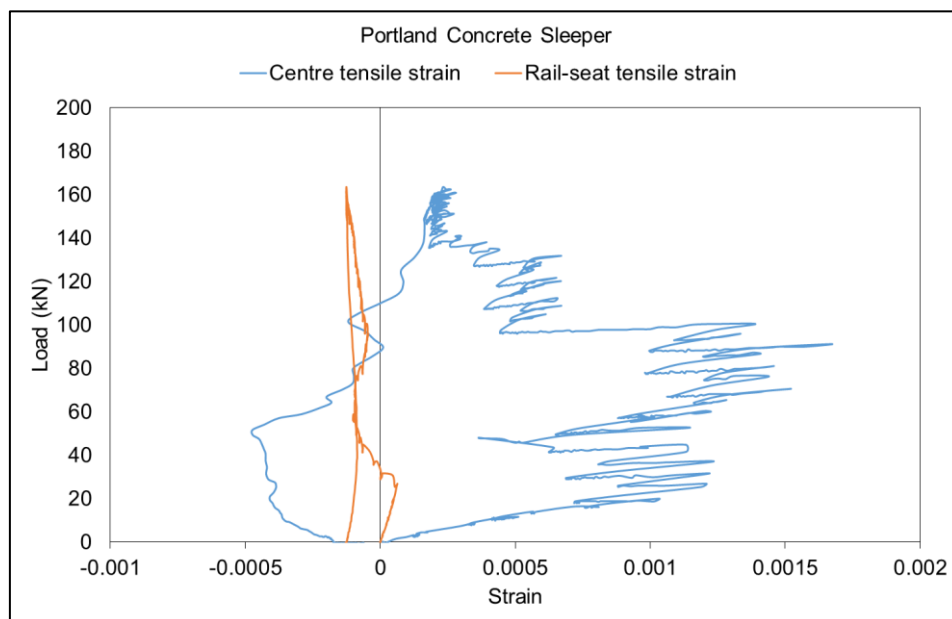


Figure 6-7: Load versus strain plot for the Portland concrete sleeper

Strain data recorded at the middle support seems more plausible as it's positive. However, the data seems to have a high level of variance as load increases. In conjunction with the observations made during the test, a large cracking noise was heard around 100 kN. This observation imitates with an anomaly in the strain data as it reduces from 0.00139 to 0.00044 quite quickly around the same load. The load acting on the sleeper instantaneously changes from 100.47 kN to 95.99kN. This anomaly suggests that failure has occurred. After observing this significant reduction in strain, strain at the middle support never returned to the same magnitude. Therefore, it can be concluded that the Portland concrete sleeper has failure at a load of 100.47 kN.

Polymer Concrete Sleeper

Strain data recorded at the middle support and the rail seat appear to be more accurate for the polymer concrete sleeper. This can be said as both strain gauges recorded positive strain while strain at the middle support doesn't vary rapidly with load, as observed with the Portland concrete sleeper. As shown in figure 6-8, recorded strain at the rail seat is almost linear with load. This indicates that the bottom portion of the sleeper, designed with 8 flexural bars, was not close to failing due to the moment generated by the applied load. Alternatively, the strain gauge at the middle support, which is also fixed to the top of the sleeper, indicates that failure has occurred as figure 6-8 clearly shows a major anomaly in strain once the applied load reached 95.49 kN. At this load, strain instantaneously changed from 0.00781 to 0.001886. This confirms that the sleeper has either failed in the top portion of the sleeper instead of bending at bottom where failure is most desired.

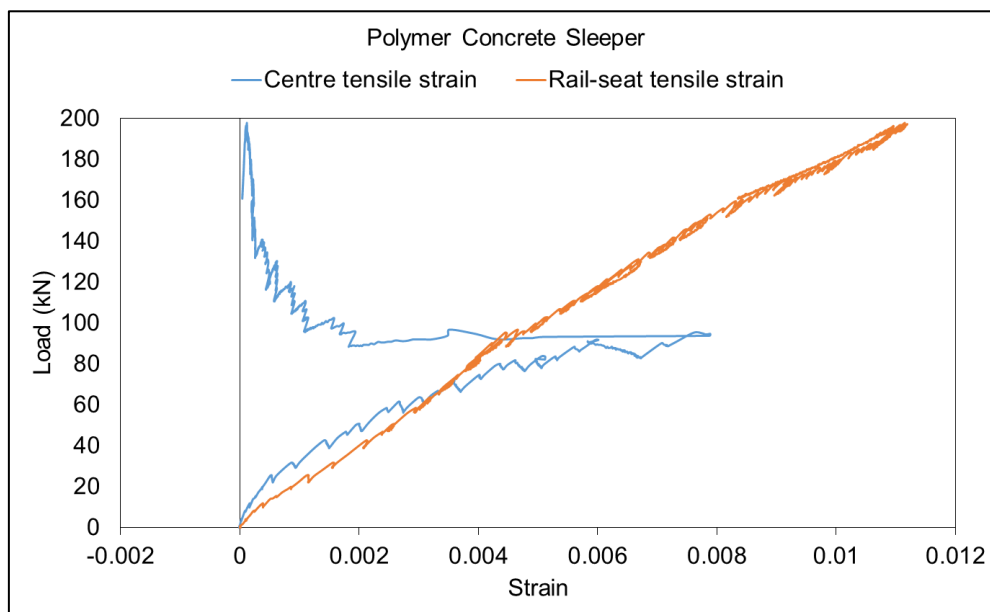


Figure 6-8: Load versus strain plot for the Polymer concrete sleeper

In comparison to both composite sleepers, a timber sleeper was also tested. As seen in figure 6-9, the timber sleeper significantly out-performed both composite sleepers as it did not fail even though it was subjected to a load of 300kN, the maximum safe load of the test equipment. Based on the strain data collected, it appears as though the timber sleeper was yet to even exceed its elastic limit as both strain gauges behaved almost linear elastic and essentially returned to zero strain once unloaded.

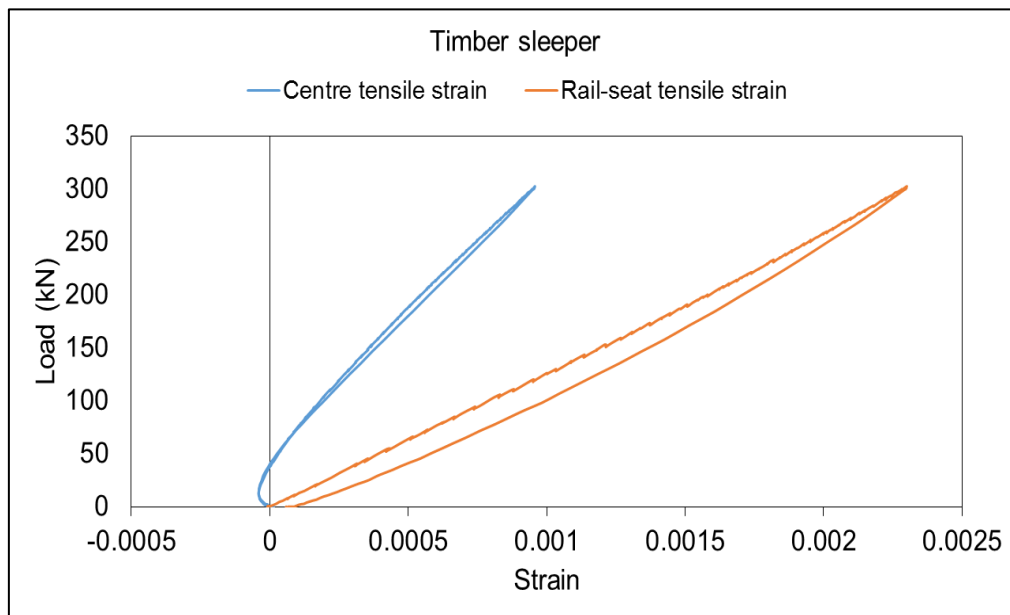


Figure 6-9: Load versus strain plot for the timber sleeper

This result is quite significant as it suggests that the two composite sleepers cannot withstand loads similar to its timber counterpart. However, the influence of the test setup has not been determined yet as the reinforcement within these composite sleepers may not suit the loading configuration of the 5-point bend test. Results from Strand 7 must now be obtained before further commenting on the performance of the composite sleepers.

6.4.3 Modelling the 5-point Bend Test

A model was created in Strand 7 to calculate the moment and shear forces acting on the sleeper at failure. As this model is simulating the 5-point bend test, nodes were positioned as illustrated in figure 6-10. Nodes at the exterior steel supports were restrained in such a way to allow rotation but restrict movement in the x or y plane. The middle support was restrained differently to account for the use of rubber as its modulus is significantly different to the steel supports. The modulus of

elasticity for polymer rubbers such as neoprene can vary between 0.001 and 4.8 GPa (Data Materials Book, 2003). Due to a lack of time, determining the exact modulus of the neoprene rubber used at the middle support was abandoned. For modelling purposes, it was assumed that the rubbers modulus was in the higher range of this bracket as it only compressed around 2mm underneath the sleeper at maximum load; hence it can be assumed that its stiffness is reasonably high. The middle support was modelled as a spring support with a stiffness equivalent to that of the neoprene rubber. This was done using a function in Strand 7 known as ‘translational node stiffness’. The basic model and node constraints applied can be seen in figure 6-10.

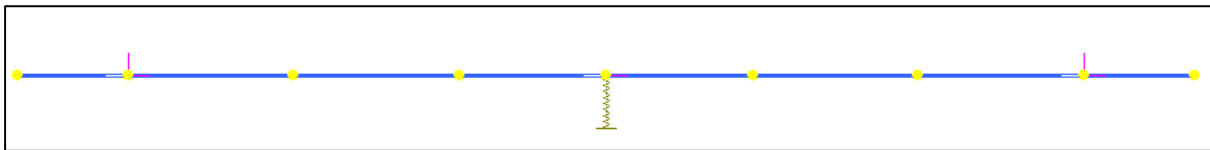


Figure 6-10: The node and element configuration of the 5-point bend test in Strand 7

As determined earlier, the load at failure for the Portland and polymer concrete sleepers was 100.47 kN and 95.49 kN respectively. These loads were applied in Strand 7 and the following results were obtained. Results are shown below.

Portland Concrete Sleeper

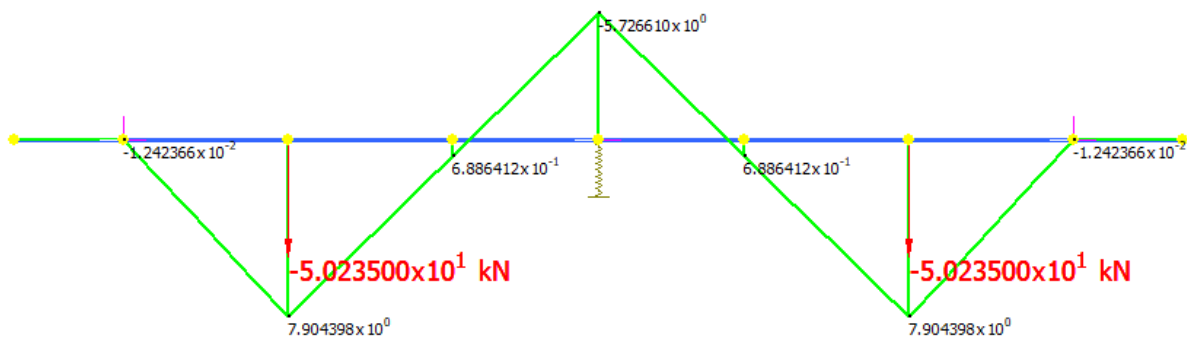


Figure 6-11: Bending moment diagram at failure for the Portland concrete 5-point bend test

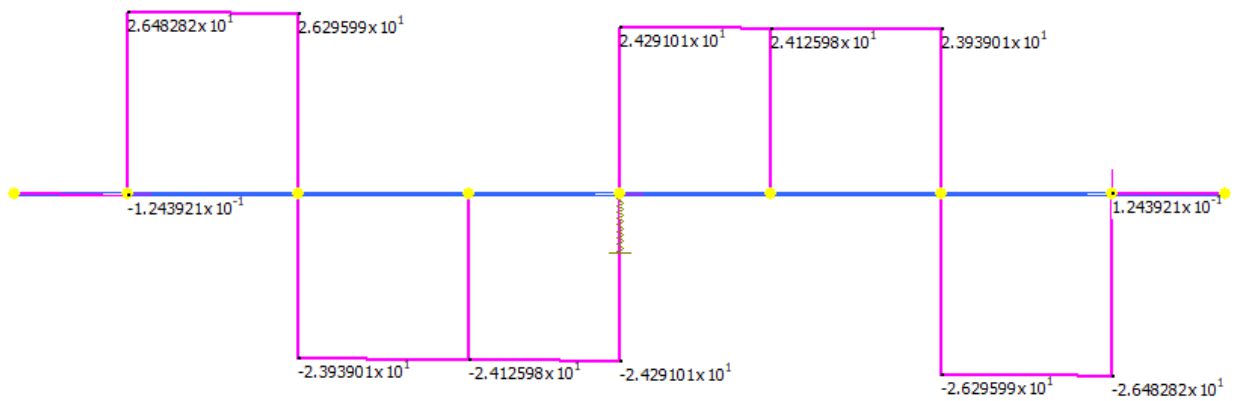


Figure 6-12: Shear force diagram at failure for the Portland concrete 5-point bend test

Polymer Concrete Sleeper

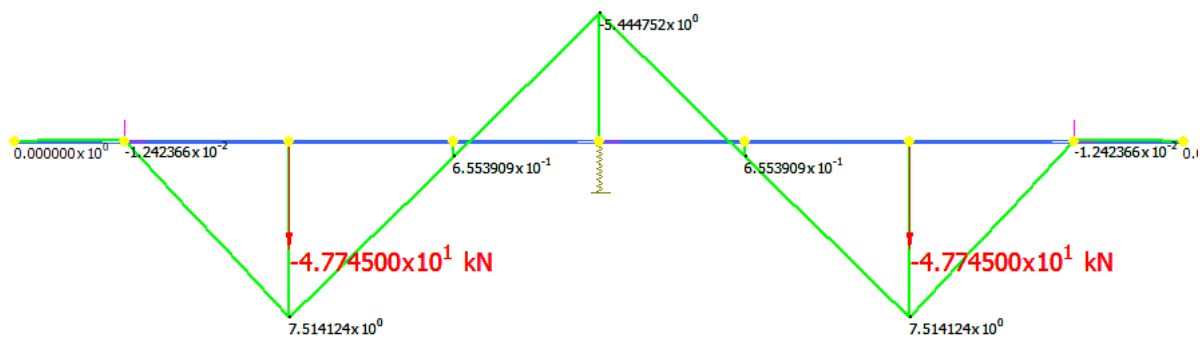


Figure 6-13: Bending moment diagram at failure for the polymer concrete 5-point bend test

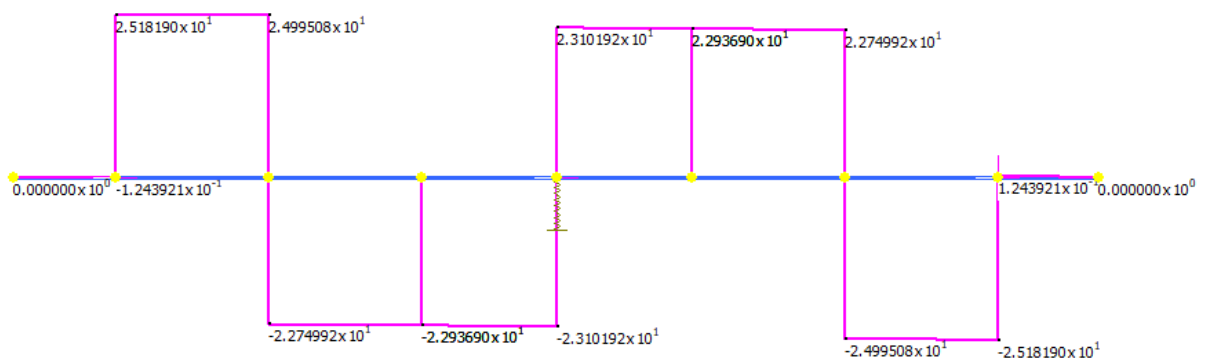


Figure 6-14: Shear force diagram at failure for the polymer concrete 5-point bend test

6.4.4 Evaluating 5-point Bending Test Results

The purpose of using neoprene rubber at the middle support was to achieve a moment ratio of 2.37 between the moment at the rail seat and the sleeper's mid-section. The actual ratio, based on the results obtained from Strand 7, was approximately 1.38. This result suggests that the neoprene rubber didn't dampen the moment at the middle support enough to accurately mimic how the sleeper would be loaded in-track. For comparison, another model was created with three steel supports to determine how the spring support changed the bending moment diagram. By using a spring support with a stiffness equivalent to that of the neoprene rubber, the moment at the middle support has only been reduce by approximately 1 kNm.

The use of neoprene at the middle support slightly increases the shear force at the rail seat. Noticeably, the shear force diagram is significantly different to the theoretical shear force diagram which was based on beam on elastic foundation theory. This change means that more than minimum shear reinforcement would actually be required through the midsection of the sleeper because shear is now greater than ϕV_{uc} which differs from previous calculations.

Table 6-1 summarises the results of the 5-point bend test and compares them to the theoretical design values (table 3-4) to help determine the mode of failure.

Table 6-1: Comparison between theoretical and experimental results

	Theoretical	Experimental	
		Portland Concrete	Polymer Concrete
Maximum positive moment (kNm)	16.142	7.904	7.514
Maximum negative moment (kNm)	5.229	5.726	5.444
Shear (kN)	68.188	26.296	24.995

Based on these results, it appears as though flexural failure has occurred first at the middle support as the maximum negative moment exceeds the moment used to calculate the number of flexural bars in the top of each sleeper. This result does not align with the predicted failure mode, concrete crushing, which was based on the non-destructive test results. It is more likely that flexural failure has occurred before shear as the magnitude of shear in both sleepers is comparatively much lower than the theoretical shear value.

Results from Strand 7 helps justify why loud cracking noises were physically heard when the load reached 95 to 100 kN and why strain recorded at the middle support suddenly changed. As the sleeper failed in this unforeseen manner, the rail seat load at failure only reached 42.7% and 40.6% of what was expected for the Portland and polymer concrete sleeper respectively. The compressive strength (f_c) or small variances in the manufacturing process could have caused the small variance in load at failure between the two sleepers.

To overcome this issue, the amount of flexural reinforcement in the top of the sleeper could be increased or the neoprene rubber could be replaced with a material that has a lower modulus to further reduce the magnitude of the maximum negative moment at the middle support as the goal is to achieve a moment ratio of 2.37 with the maximum positive moment. It would be more practical to replace the neoprene as adding more GFRP bars would unnecessarily increase the cost of the sleeper which is undesirable.

Results obtained from 5-point bend test still don't fully justify how the GFRP bar at the rail seat shown in figure 6-6 failed in shear. Based on the observation made during testing that the severity of shear cracks at the rail seat increased considerably around an applied load of 150 kN, this load was applied to an additional Strand 7 model to determine shear at this particular load; refer to figure 6-15.

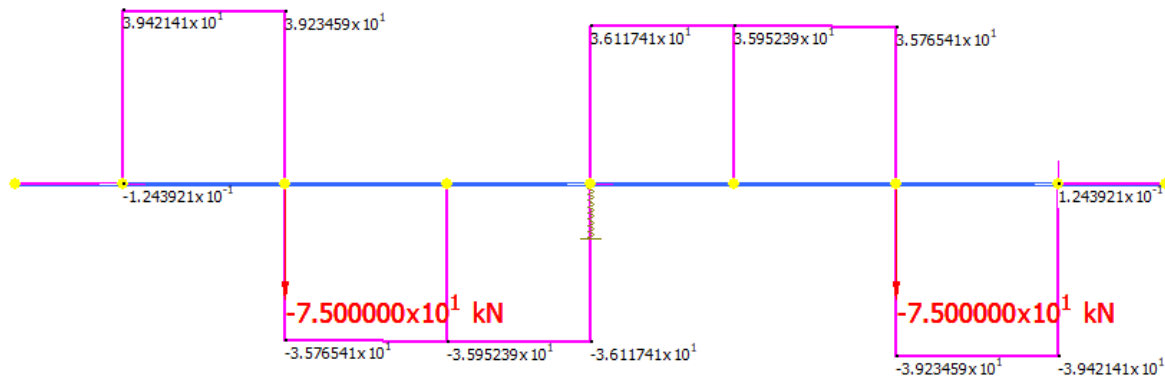


Figure 6-15: Experimental Shear force at 150 kN

Results indicate that the shear force at the rail seat is around 39.23 kN. This indicates that shear is approaching 41 kN, the transverse shear capacity for 6mm diameter GFRP bars (refer to appendix E). Based on what was observed, it can be assumed that the GFRP bar ruptured because it reached its transverse shear capacity. This result highlights a design flaw as this parameter was not identified as

a potential cause of failure when designing the sleeper. Evidently, both composite sleepers would have failed well before their predicted failure load of 234.24 kN even if the sleepers didn't fail in bending at the middle support first.

It can be approximated that shear failure would have occurred around 155 kN, the same load at which concrete directly underneath the rail seat started to spall. To improve the sleepers design, the diameter of the flexural bars used in the top portion of the sleeper should be increased. A bar diameter of 12.7mm has a transverse shear capacity of 67 kN which is much closer to the maximum theoretical shear; refer to Appendix E. The test-setup itself could also be improved as diagonal tension cracks were able to form in the sleepers shear span was three times greater than the sleepers effective depth; $300\text{mm} > 3 \times 96.825$. Therefore, additional modelling or testing could be performed to optimise the position of the supports and help reduce the degree of cracking in the shear span.

Even though the polymer concrete sleeper initially failed before the Portland concrete sleeper, this sleeper was able to withstand a higher load before ultimate failure. This can be accredited to the fact that polymer concrete can withstand higher strain values than Portland concrete; as mentioned in Chapter 5. Importantly, polymer concrete is used around the exterior of the concrete core, which is also where maximum strain is measured because strain increases with distance from the neutral axis. This has two benefits; the polymer concrete can resist higher strain at the sleeper's surface while it reduces the distance from the neutral axis to the verge of Portland concrete core. This means the sleeper can resist higher loads before the Portland concrete core reaches its strain capacity.

6.4.5 Serviceability Considerations

Images taken from the DIC device were analysed and the following graphs were produced. All of the deflection curves seem very incremental as the sleepers weren't loaded at a constant rate. Deflection at the rail seats was a lot higher than anticipated. However, considering that both composite sleepers failed at a much lower load than anticipated, higher deflection values are somewhat justified.

The DIC software has determined that deflection at the right rail seat is higher than the left for the Portland concrete sleeper; refer to figure 6-16. This result is unusual as deflection at both rail seats should be approximately equal. Interestingly, during the test it was observed that the degree of cracking around the right rail seat was much higher than the left meaning this result is plausible. When the beam initially failed in bending around 100 kN, no real anomalies exists. In comparison, when the load exceeded 150 kN, the predicted load for shear failure, the rate of deflection at the right rail seat increased greatly. This justifies why the sleeper couldn't be loaded past 160 kN as the sleeper didn't have the capacity to resist the load anymore.

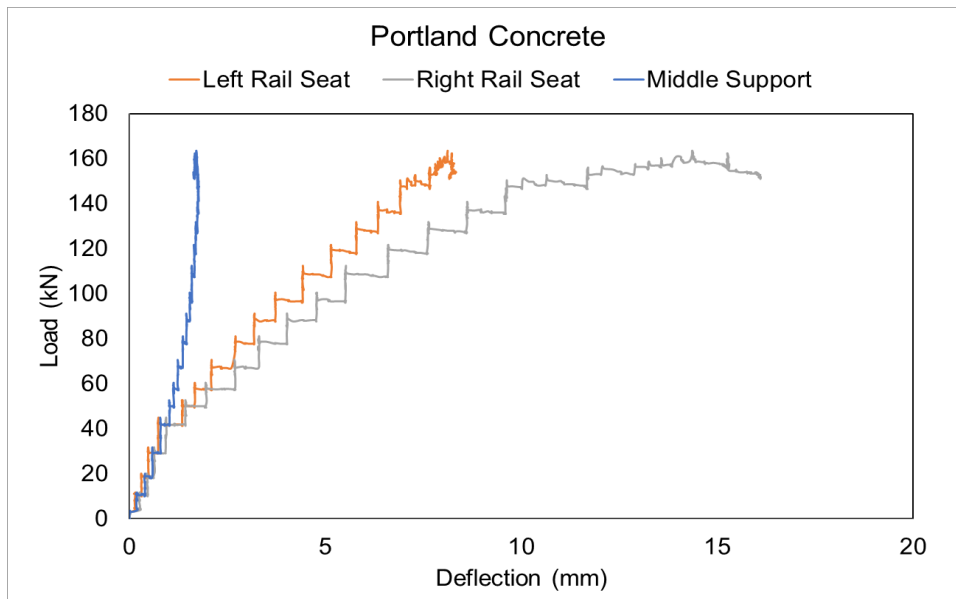


Figure 6-16: Destructive Load vs deflection diagram for the Portland concrete sleeper

The DIC software has again found that deflection at the right rail seat is higher than the left; refer to figure 6-17. As both sleepers have behaved in this unusual manner, the experimental setup or the testing equipment itself might be causing bias deflection at the right rail seat. It should be noted that deflection at the middle support or the compression of the neoprene rubber is maximum around 95 kN. This is the same load at which the sleeper has failed in bending at the middle support. This further validates the assumption made that the sleeper failed in bending before shear. The rate of deflection increased once the applied load reached 190 kN which suggests that the sleeper didn't have the capacity to resist any more load.

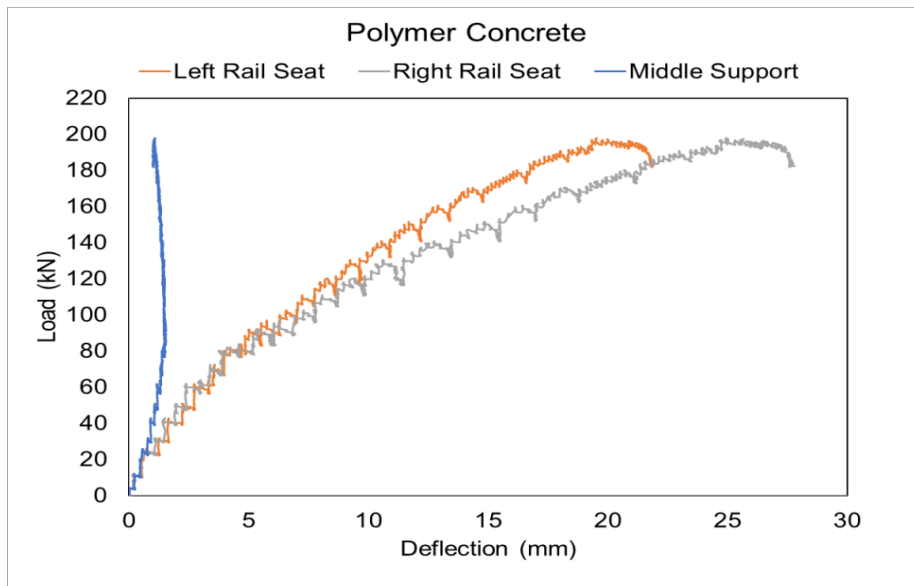


Figure 6-17: Destructive Load vs deflection diagram for the polymer concrete sleeper

As discussed in Chapter 5, the two composite sleepers have a much lower effective modulus compared to regular timber sleepers. Therefore, it's not surprising that the timber sleeper deflected very little in comparison to the two composite sleepers; refer to figure 6-18. The DIC software has determined that deflection at the left and right rail seat are quite similar but deflection at the right rail seat was again slightly higher.

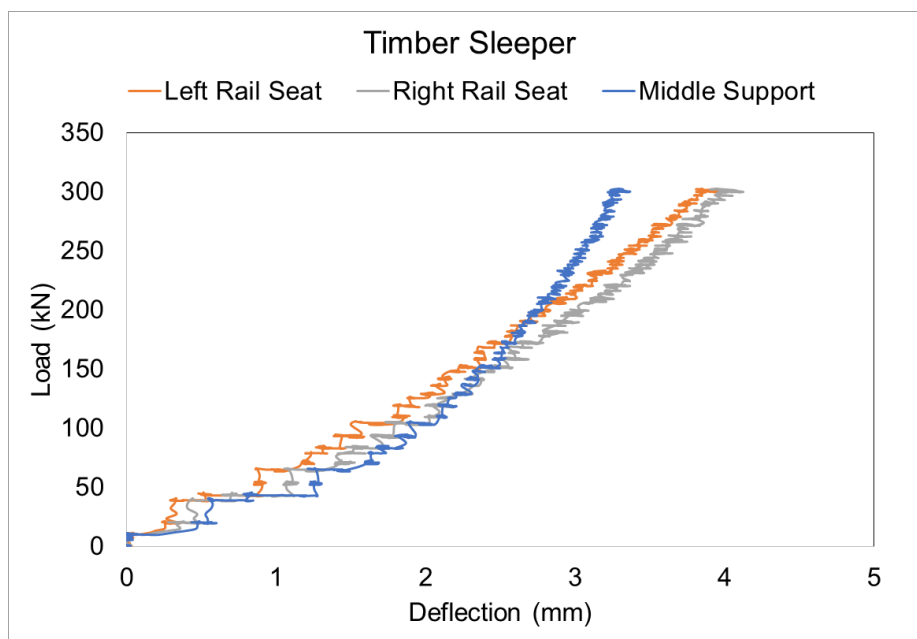


Figure 6-18: Destructive Load vs deflection diagram for the timber sleeper

It isn't logical to compare experimental and theoretical deflection values as the sleeper is now supported in the middle thus changing the location of maximum deflection from the middle to the rail seat. Deflection at significant loads have been summarised in table 6-2 for comparison. Even though the timber sleeper didn't fail, deflections at similar loads have been provided.

Table 6-2: Deflection at failure

	Initial failure in Bending			Failure in Shear		
	Load (kN)	Middle support Deflection (mm)	Average rail seat deflection (mm)	Load (kN)	Middle support Deflection (mm)	Average rail seat deflection (mm)
Portland Concrete	100.47	1.542	4.968	150	1.782	8.387
Polymer Concrete	95.49	1.443	6.568	150	1.32431	13.883
Timber Sleeper	100	1.889	1.646	150	2.459	2.352

At initial failure, the average rail seat deflection for the Portland and polymer sleeper was 302% and 399% greater than timber respectively. This is a major increase and highlights that deflection may be a limiting factor in design. These results validates claims made by T.Baker (2016) and A.Baker (2018) as their theoretical models suggested that excessive deflection was a potential problem with GFRP reinforced railway sleepers. As deflection is much higher than timber, it wouldn't be easy to integrate the two together in-track. This means that the entirety of a track segment would have to be replaced at a single time. Although the magnitude of deflection is significantly higher, it is important to remember that both sleepers were still able to meet the minimum effective modulus set by AREMA.

The use of polymer concrete in comparison to Portland concrete has increased deflection by 24.4% which is a similar result to the non-destructive tests. Although deflection has slightly increased, the use of polymer concrete is still favourable as it reduces the degree of cracking. Therefore, to minimise deflection while still utilising the non-crack characteristics of the polymer concrete, the compressive strength of the traditional concrete core could possibly be increased from 32 MPa to improve the sleeper's modulus.

Chapter 7 Conclusion

7.1 Project Outcomes

The aim of this research was to design, manufacture and evaluate the performance of two new composite sleepers using Portland concrete and epoxy based polymer concrete reinforced with GFRP bars. The scope of this work was to determine the sleeper's maximum flexural capacity, the mode of failure, measure deflection and observe cracking behaviour. Destructive and non-destructive test methods were used to evaluate these parameters and determine whether GFRP bars and polymer concrete have any significant advantages which could improve the design of narrow gauge track railway sleepers.

By completing this research project, the following outcomes with respect to the research objectives were achieved:

1. Research the properties of polymer concrete and the behaviour of GFRP reinforcement

Although the popularity of GFRP bars continues to rise around the world, no codes or standards currently exist in Australia which is severely affecting their acceptance in the broader construction industry. After completing the literature review, a list of key design factors relating to GFRP reinforced sections was compiled:

- Reducing the bar diameter increases peak bond strength
- The shear strength of GFRP bars is generally 20% of its tensile strength
- GFRP reinforced specimens achieve about 60% of the bond strength compared to steel
- At the same reinforcement ratio and geometric size, GFRP and steel reinforced beams roughly have the same bearing capacities
- GFRP reinforced have poorer crack control.

Some research claimed that polymer concrete products can surpasses some of the structural benefits of Portland concrete and can reduce carbon emissions related to cement production. Most importantly some research already supports the idea of using polymer concrete to manufacture railway sleepers. Polymer concrete is more durable in harsh climates, more resistant to cracking and chemical attack. Research also highlighted that its modulus is quite low in comparison to traditional concrete. Therefore, it was hypothesised that the polymer sleeper would be designed with a traditional concrete core to help improve sleeper stiffness and reduce manufacturing costs.

2. *Review existing standards relating to railway sleepers and GFRP materials*

The most widely accepted and recognised GFRP standard, CSA S806-12, was used to design the flexural reinforcement while the shear reinforcement was designed in accordance with AS3600 for simplicity. Although CSA S806-12 suggests applying a significantly large reduction factor (0.25) to the total f_u value of GFRP bars, this was ignored to minimise the amount of reinforcement required. The factor of safety or the ϕ value was also slightly increased to reduce the amount of reinforcement required.

The rail seat load was calculated in accordance with Australian Standard AS1085.14; Railway track material – Prestressed Concrete Sleepers. Accurately calculating the rail seat load was an essential component of this research project as all design parameters are dependent on its magnitude. The rail seat load was calculated as 117.12 kN.

3. *Theoretically determine maximum bending moments and shear forces acting on the sleeper and predict the sleeper's general behaviour under loading in Strand 7*

Two finite element simulation models based on elastic foundation theory were created to determine maximum bending moment and shear force acting on sleepers. The accuracy of both models was validated against the analytical and empirical method outlined in AS1085.14. It was determined that the sleeper needed to be designed for a maximum positive bending moment of 16.142 kNm and a maximum shear force of 68.188 kN. The GFRP reinforcement cage was then designed.

4. *Manufacture two railway sleepers and conduct experimental testing*

The reinforcement cage was constructed first at USQ in accordance with the illustrated detail drawings in Chapter 3. Three strain gauges were attached to the flexural GFRP bars and the concrete was poured. After 28 days, the sleepers were taken out of their precast moulds. It was quite noticeable that the sleeper made from polymer concrete was significantly lighter than Portland concrete sleeper.

5. *Critically analyse the test data and compare results with the theoretical models and previous research*

Non-destructive tests proved that both sleepers achieved an acceptable effective modulus of elasticity in accordance with AREMA standards. By using polymer concrete, the sleeper's modulus was reduced by 29.44% compared to Portland concrete. This result further justified the use of a traditional concrete core to retain an acceptable effective modulus. Stress analysis principles were then used to predict that both sleepers will fail due to concrete crushing while the GFRP bars at failure will only utilised up to 70% of their tensile strength. This helped to justify that GFRP bars are a suitable replacement for steel reinforcement. Importantly, non-destructive results were relied upon when the destructive tests didn't go as planned as both sleepers failed at a much lower load than expected. Potential problems related to the manufacturing process, the strength of the concrete, the bond of the GFRP bars and the reinforcement design itself were disregarded as non-destructive testing proved otherwise.

The 5-point bend test didn't accurately replicate how the sleeper would be loaded in-track. This theory was proven when the test setup was simulated in Strand 7. The model in Strand 7 indicated that flexural failure first occurred at the middle support which isn't ideal and doesn't align with the predicted failure mode. Although both sleepers failed prematurely, some creditable results were found:

- Flexural failure first occurred around an applied load of 100 kN as moment at the middle support surpassed the maximum negative design moment
- Once the load approached 155 kN, the 6 mm diameter GFRP bars reached their transverse shear capacity causing ultimate failure
- At initial failure, the average rail seat deflection for the Portland and polymer sleeper was 302% and 399% greater than timber respectively

Based on these results, it appears as though shear and deflection are the two limiting design factors. This coincides with some previous research which identified that excessive deflection might be a concern. However, both sleepers were still able to meet the minimum effective modulus set by AREMA. Therefore, it would be worth measuring and comparing deflection when the sleepers are actually supported by ballast.

6. *Conclude whether polymer concrete has any noticeable advantages over traditional Portland concrete*

The use of polymer concrete is recommended as it definitely helped to reduce the degree of cracking; one of the major causes of concrete sleeper deterioration. Significant flexural cracking was first observed around an applied load of 90kN which is considerably higher than 64 kN, the load at which flexural cracks first appeared in the Portland concrete sleeper. The use of polymer concrete also seemed to reduce the number of shear cracks and no concrete crushing was observed. Testing also demonstrated that the polymer concrete sleeper could withstand a greater load than its Portland concrete counterpart because it can be subjected to higher strains.

7. *Provide comments on the sleeper's performance and give recommendations if necessary*

The destructive 5-point bend test configuration should be altered so the moment ratio between the rail seat and the sleeper's mid-section is closer to 2.37. This ratio is most desirable as it best mimics how the sleeper would be loaded in-track. The actual ratio achieved during testing was much lower than 2.37 meaning the sleeper failed in bending at the middle support which was undesirable. Although neoprene rubber was used to reduce the magnitude of moment at the middle support, it was not able to sufficiently dampen the moment at the middle support as its stiffness was too high. Due to this unforeseen problem, both sleepers failed well before their predicted failure load meaning their true performance is still somewhat unknown. Therefore, more destructive tests are required to determine which type of rubber can achieve the best moment ratio. The location of the supports could also be slightly altered to reduce the chance of cracking in the shear span. With these modifications, the load at failure would be more representative of the sleeper's ultimate flexural and shear capacity.

Based on the results obtained, the sleepers design could be further improved. The diameter of the flexural GFRP bars must be increased to improve their transverse shear capacity while the compressive strength of the concrete core could be increased to nullify greater deflection due to the addition of polymer concrete.

7.2 Future Work

Further research could be done to determine whether using a rectangular GFRP hollow section could outperform GFRP bars; refer to figure 7-1. If it was possible to use a rectangular GFRP hollow section, manufacturing would become considerably more efficient as it would eliminate the need to assemble a GFRP reinforcement cage, which was quite a tedious task. Another benefit of this design would be that the Portland concrete core and the exterior polymer concrete coating could be poured at the same time, in the same precast mould as the two cementitious materials would be separated by the premade GFRP section.

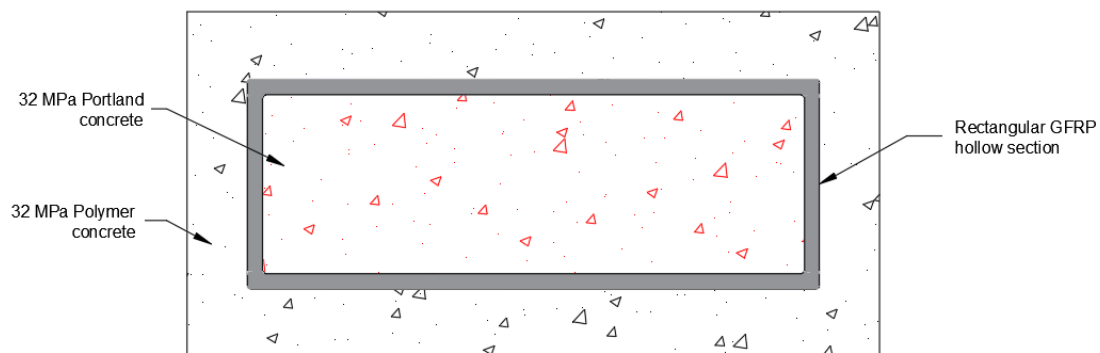


Figure 7-1: Future research could be done on a sleeper reinforced with a rectangular GFRP hollow section

To help reduce high maintenance costs associated with timber, the rail industry is continuously looking for sleepers that are more durable. Consequently, these sleepers have purposely been designed with GFRP bars and polymer concrete in an attempt to improve durability as research indicated that these products are very robust in harsh climates. As destructive and non-destructive tests have now proven that it is mechanically plausible to use these materials, some deterioration testing could now be conducted to determine the expected design life of these sleepers. It is expected that the average design life of these sleepers should surpass what is currently available on the market.

Reference List

Abbasi, R & Ali Zakeri, J 2013, 'Field investigation of variation of loading pattern of concrete sleeper due to ballast sandy contamination in sandy desert areas', no. 2, pp. 216-27.

Alachek, I, Reboul, N & Jurkiewicz, B 2018, 'Bond strength's degradation of GFRP-concrete elements under aggressive exposure conditions', *Construction and Building Materials*, vol. 179, pp. 512-25

Aldred, J., 2013, "Engineering Properties of a Proprietary Premixed Geopolymer Concrete", *Proceedings Concrete Institute of Australia Biennial Conference, Concrete 2013 – Understanding Concrete*, Gold Coast, Australia

Ali Zakeri, J & Abbasi, R 2013, 'Field investigation of variation of loading pattern of concrete sleeper due to ballast sandy contamination in sandy desert areas', no. 2, pp. 216-27.

Andersson, A, Berglund, H, Blomberg, J & Yman, O, 2013, *The Influence of Stiffness Variation in Railway Track*, Chalmers University Of Technology, Sweden

Arias, J, Vazquez, A, Escobar, M, 2012, 'Use of sand coating to improve bonding between GFRP bars and concrete', *Journal of Composite Materials*, Volume: 46 issue: 18, page(s): 2271-2278

Baker, A, 2018, 'Behaviour of GFRP Reinforced Concrete Railway Sleepers: Finite Element and Fibre Model Analyses', The University of Southern Queensland, Toowoomba

Baker, T 2016, 'Analysis on the Behaviour of FRP Reinforced Concrete Railway Sleepers', Faculty of Health, Engineering and Sciences, University of Southern Queensland

Bărbuță, M., Harja, M., & Baran, I. (2009). Comparison of Mechanical Properties for Polymer Concrete with Different Types of Filler. *Journal of Materials in Civil Engineering - J MATER CIVIL ENG*, vol.22., pp27-32.

Bennett-Huntley, E. (2014). *Epoxy Resin vs Vinylester vs Polyester Use and Application Overview*, Composite Resin Developments, Kent, UK

Bezgin, NÖ 2017, 'High performance concrete requirements for prefabricated high speed railway sleepers', *Construction and Building Materials*, vol. 138, pp. 340-51

Canadian Standards Association 2012, Design and Construction of Building Structures with Fibre Reinforced Polymers, S806-12, Canadian Standards Association, Ontario, Canadian

Carey, A, 2012, Wooden sleepers plan 'off the rails', viewed 1st of April 2019 <<https://www.theage.com.au/national/victoria/wooden-sleepers-plan-off-the-rails-20120924-26he9.html>>

Cement Hazards and Controls, 2019, The Electronic Library of Construction Occupational Safety and Health, viewed on the 30th of April 2019 <<http://elcosh.org/document/1563/d000513/cement-hazards-and-controls-health-risks-and-precautions-in-using-portland-cement.html>>

Concrete Technology, 2014, CIV2605 Construction Engineering Studybook, University of Southern Queensland, Toowoomba

Corrosion of Embedded Metals, 2018, viewed 1st of April 2019 <<https://www.cement.org/learn/concrete-technology/durability/corrosion-of-embedded-materials>>

Material Supply Specification TRACK-CT.172, 2015, 'Alternative Sleepers', Queensland Rail, volume 1, pp.2-11

Data Materials Book, 2003, Cambridge University Engineering Department, viewed on the 1st of October <<http://www-mdp.eng.cam.ac.uk/web/library/enginfo/cueddatabooks/materials.pdf>>

Designing with composite Rebar, (n.d), VRod Australia, viewed 5th of April 2019 <<https://www.vrodaustralia.com.au/designing-with-composite-rebar/>>

Doroudiani, S., 2012, 'Toxicity of FRP building materials' viewed on the 30th of April 2019 <<https://www.materialstoday.com/composite-industry/comment/guest-blog-toxicity-of-frp-building-materials/>>

Eco-friendly Construction, 2016, Nationwide Construction, viewed on the 26th of June 2019 <<https://nationwideconstruction.us/eco-friendly-construction-8-advantages-of-green-building/>>

El-Hawary, M., Al-Khaiat, H., & Fereig, S. (2000). Performance of epoxy-repaired concrete in a marine environment. Cement and Concrete Research, 30(2), 259-266.

El-Nemr, A, Ahmed, EA, El-Safty, A & Benmokrane, B 2018, 'Evaluation of the flexural strength and serviceability of concrete beams reinforced with different types of GFRP bars', *Engineering Structures*, vol. 173, pp. 606-19.

Ferdous, W & Manalo, A 2014, 'Failures of mainline railway sleepers and suggested remedies – Review of current practice', *Engineering Failure Analysis*, vol. 44, pp. 17-35.

Ferdous, W, Manalo, A, Van Erp, G, Aravinthan, T, Kaewunruen, S & Remennikov, A 2015, 'Composite railway sleepers – Recent developments, challenges and future prospects', *Composite Structures*, vol. 134, pp. 158-68

Ferdous, W., Manalo, A., Aravinthan, T., & Van Erp, G. (2016). Properties of epoxy polymer concrete matrix: Effect of resin-to-filler ratio and determination of optimal mix for composite railway sleepers. *Construction and Building Materials*, vol. 124, pp. 287-300.

Fergani, H, Di Benedetti, M, Miàs Oller, C, Lynsdale, C & Guadagnini, M 2018, 'Durability and degradation mechanisms of GFRP reinforcement subjected to severe environments and sustained stress', *Construction and Building Materials*, vol. 170, pp. 637-48.

GFRP Characteristics and Behaviours, 2018, Prince Engineering, viewed 12th of May 2019 <<https://www.build-on-prince.com/fiber-reinforced-polymers.html#sthash.IDlaMN11.dpbs%3E>>

GFRP Components for Facades, (n.d), Permasteelisa Group, viewed 12th of May 2019 <https://www.permasteelisagroup.com/media/3250/rd-flyer_gfrp-components-for-fa-cades.pdf>

Gribniak, V, Rimkus, A, Torres, L & Hui, D 2018, 'An experimental study on cracking and deformations of tensile concrete elements reinforced with multiple GFRP bars', *Composite Structures*, vol. 201, pp. 477-85.

Gribniak, V, Rimkus, A, Torres, L & Hui, D 2018, 'An experimental study on cracking and deformations of tensile concrete elements reinforced with multiple GFRP bars', *Composite Structures*, vol. 201, pp. 477-85.

Gu, X, Yu, B & Wu, M 2016, 'Experimental study of the bond performance and mechanical response of GFRP reinforced concrete', *Construction and Building Materials*, vol. 114, pp. 407-15.

Hillston, J., 2003, 'Model Validation and Verification', Chapter 14, viewed on the 30th of June <<http://www.inf.ed.ac.uk/teaching/courses/ms/notes/note14.pdf>>

History and development of the wooden sleeper, CH-2855, Glovelier: Ets Rothlisberger SA

Hollingworth, K, Brown, E, 2017, War on Waste: Railway sleepers made from recycled plastic could replace timber on heritage tracks, viewed 5th of February 2019 <<http://www.abc.net.au/news/2017-05-15/plastic-railway-sleepers/8526114>>

Hossain, A, 2016, A dozen facts about transport in Australia, Australian Government; Department of infrastructure and regional development, viewed 5th of February 2019 <https://bitre.gov.au/publications/2016/files/is_075.pdf>

Hu, H & Liu, Y 2010, '11 - High modulus, high tenacity yarns', in R Alagirusamy & A Das (eds), Technical Textile Yarns, Woodhead Publishing, pp. 329-86.

Jabbar, SA & Farid, SBH 2018, 'Replacement of steel rebars by GFRP rebars in the concrete structures', Karbala International Journal of Modern Science, vol. 4, no. 2, pp. 216-27.

Kaewunruen, S & Remennikov, A 2008, 'Dynamic properties of railway track and its components : a state-of-the-art review', Faculty of Engineering and Information Sciences, vol. 113, pp. 103-11

Kaewunruen, S, Martin, M & Remennikov, A 2008, 'Dynamic design guidelines for prestressed concrete sleepers', Faculty of Engineering and Information Sciences, vol. 116, pp. 134 -47

Khorramian, K & Sadeghian, P 2017, 'Experimental and analytical behavior of short concrete columns reinforced with GFRP bars under eccentric loading', Engineering Structures, vol. 151, pp. 761-73.

Kirlikovali, E., (1981). Polymer/Concrete Composite – A review. Polymer Engineering and Science, Vol. 21, pp507-509

Low CO₂ Concrete, 2016, EF Technology, viewed 7th of February 2019 <<https://www.us-concrete.com/sustainability/ef-technology/>>

Manalo, A, Aravinthan, T, Karunasena, W & Stevens, N 2012, 'Analysis of a Typical Railway Turnout Sleeper System Using Grillage Beam Analogy', Finite Elements in Analysis and Design, vol. 48, pp.1376-1391.

Manalo, A., 2018, CIV3505 Concrete Structures, Shear Design Lecture Slides, University of Southern Queensland, Toowoomba

McMillan, K, 2018, The rise of composite materials, viewed 6th of April 2019 <<https://www.qimtek.co.uk/blog/rise-composite-materials>>

Merkert, R., & Hensher, D. A. 2014, 'Open access for railways and transaction cost economics – Management perspectives of Australia's rail companies', *Research in Transportation Economics*, 48, 227-236.

Momtazi, A., Khoshkbijari, R., Mogharab. (2015). Polymers in Concrete: Applications and Specifications. *European Online Journal of Natural and Social Sciences* Vol.3, No.3 pp4-11

Newhook, J & Svecova, D 2007, 'ISIS Canada Research Network - Reinforcing Concrete Structures with Fibre Reinforced Polymers', Design Manual No. 3

Note, A, 2018, Typical track structure - ballasted track, viewed 6th of February 2019 <<https://www.anatomynote.com/transportation-anatomy/train-anatomy/typical-track-structure-ballasted-track/>>

PreTechnologies, 2014, 'Advantages of finite element analysis (FEA)', viewed on the 16th of June 2019 <<http://www.pretechnologies.com/services/finite-element-analysis/advantages>>

Prince Engineering, (n.d), 'Fibre Reinforced Polymers Characteristics and Behaviours', viewed on the 18th of May 2019 <<https://www.build-on-prince.com/fiber-reinforced-polymers.html>>

Queensland Rail; QRP-15-150A Tender Information Report, 2016, 'Invitation for Expression of interest for Alternative Composite Sleeper Product', vol.1, pp3-9

Railway Sleepers, 2018, viewed 5th of February 2019 <<https://www.abis.com.au/railway-sleepers>>

Sadeghi J., & Youldashkhan M., 2005, 'Investigation on the Accuracy of the Current Practices In Analysis of Railway Track Concrete Sleepers', *International Journal of Civil Engineering*, vol. 3(1), pp. 31-45.

Sheikh, SA & Kharal, Z 2018, 'Replacement of steel with GFRP for sustainable reinforced concrete', *Construction and Building Materials*, vol. 160, pp. 767-74

Standards Australia 2012, *Railway track material*, Part 14: Prestressed concrete sleepers, AS1085.14, Standards Australia, Sydney, viewed 4th of February 2019, < <https://www.saiglobal.com.ezproxy.usq.edu.au/PDFTemp/osu-2019-07-23/0417838263/1085.14-2012.pdf>>

Standards Australia, 2009, *Concrete Structures: AS3600*, Standards Australia, Sydney, viewed 20th of May 2019, <[https://www-saiglobal-com.ezproxy.usq.edu.au/PDFTemp/osu-2019-07-23/0417838263/3600-2009\(+A2\).pdf](https://www-saiglobal-com.ezproxy.usq.edu.au/PDFTemp/osu-2019-07-23/0417838263/3600-2009(+A2).pdf)>

The Concrete Conundrum, 2008, Chemistry World, viewed 5th of February 2019, <http://www.rsc.org/images/Construction_tcm18-114530.pdf>

Thermal Decomposition of Calcium Carbonate, (n.d), EdPlace, viewed 7th of February 2019 <https://www.edplace.com/worksheet_info/science/keystage4/year10/topic/711/3075/thermal-decomposition-of-calcium-carbonate>

Trejo, D., Gardoni, P., Kim, J. J., & Zidek, J. (2009). 'Long-term performance of GFRP reinforcement: technical report', Texas Transportation Institute, vol. 151, pp. 761-73

Understanding Cement, 2005, 'Portland cement clinker – overview', viewed 7th of February 2019 <<https://www.understanding-cement.com/clinker.html>>

Van Dyk, B. J., Scheppe, A. J., Edwards, J. R., Dersch, M. S., & Barkan, C. P. L. (2016). Methods for quantifying rail seat loads and a review of previous experimentation. *Proceedings of the Institution of Mechanical Engineers, Part F: Journal of Rail and Rapid Transit*, 230(3), 935-945.

V-ROD Fiberglass Rebar Canada, 2012, Pultrall Incorporated, viewed on the 14th of July 2019 <<http://www.vrodcanada.com/about-us/pultrall-inc>>

W. Lokuge, T. Aravinthan, Effect of fly ash on the behaviour of polymer concrete with different types of resin, *Mater. Des.* 51 (2013) 175–181.

Yan, F, Lin, Z, Zhang, D, Gao, Z & Li, M 2017, 'Experimental study on bond durability of glass fiber reinforced polymer bars in concrete exposed to harsh environmental agents: Freeze-thaw cycles and alkaline-saline solution', *Composites Part B: Engineering*, vol. 116, pp. 406-21.

Appendix A ENG4111/4112 Research Project

For: Jacob Verrall

Title: Comparative Evaluation of the flexural Performance of GFRP Reinforced Railway Sleepers

Major: Civil

Supervisors: Allan Manalo

Enrolment: ENG4111 – ONC S1, 2019
ENG4112 – ONC S2, 2019

Project Aim: To successfully develop and evaluated the flexural performance of a GFRP reinforced railway sleeper in accordance with Material Supply Specifications (TRACK-CT.172) released by Queensland Rail.

In conjunction, two different railway sleepers will be manufactured for comparison purposes; one from Polymer cement and the other from ordinary Portland concrete. The aim is to evaluate the flexural performance of GFRP reinforced railway sleepers in order to determine their suitability for narrow gauge track applications across Queensland.

Programme: Version 2, last updated on the 27th of March 2019

1. Refine project objectives and provide a background of the research project. This research should particularly focus on current demands, trends, products and standards associated with the rail industry in Australia. This information should be used to justify how this research project will benefit the civil and rail industry.
2. Conduct a critical review of the literature including railway sleepers and how they are designed, the physical properties of GFRP bars and the advantages/disadvantages of polymer cement. During this phase, it will be critical to start examining relevant standards to help identify what materials and testing equipment will be required.

3. Finite element analysis using BOEFM to evaluate the bending moment and shear forces acting on the sleeper based on the loading conditions specified by Queensland Rail. This bending moment and shear forces will be used to design the amount of GFRP reinforcement for the polymer concrete and normal concrete following appropriate design standards.
4. Experimental testing and evaluation to assess the overall performance of a railway sleeper. The testing will focus on the following parameters as specified in TRACK-CT.172:
 - The flexure of the sleeper in service
 - Failure under ultimate loading
 - Material strain failure based on characteristic or appropriately tested values
 - Deflection under serviceability loading
 - Local failure if any

All of these variables can be measured in a single test. TRACK-CT.172 specifies that a sleeper's performance can be measured by applying two point loads to replicate a passing train. The distance between the point loads should equal the track gauge.

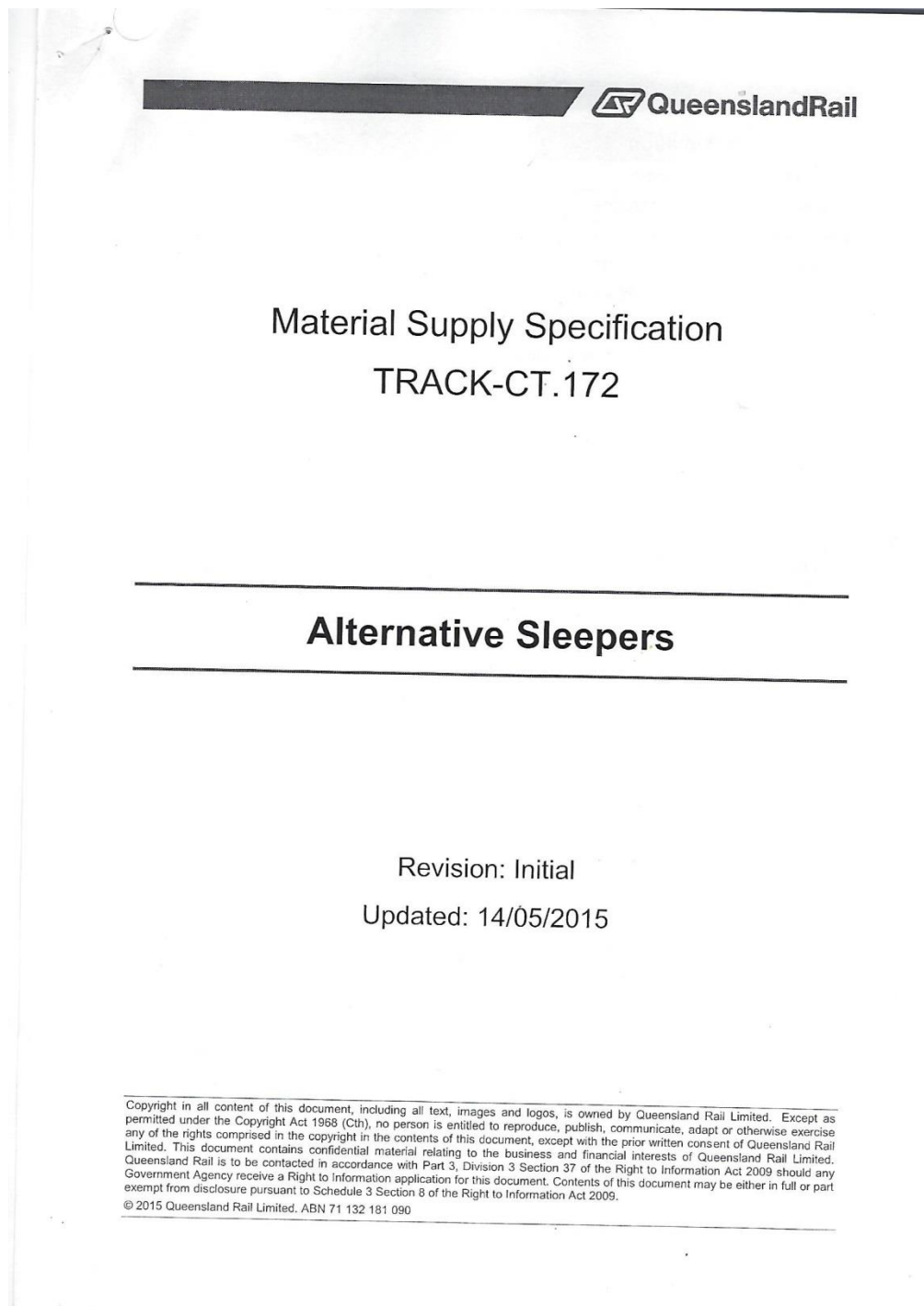
5. Critically analyse and interpret test results. Comparisons should be made between theoretical predictions
6. Submit final dissertation on research, theoretical analysis, testing, results and conclusion

If time and resources permit:

- Evaluate the overall cost of sleeper and determine whether the GFRP reinforced polymer cement sleeper is practically feasible.

Appendix B TRACK-CT.172 Design Specifications

Key snippets have been taken from TRACK-CT.172 Design Specifications.



CLAUSE	QUALITY POINT	TYPE
5.8	Rejection of out of specification sleepers	Quality
7.1	Storage of sleepers	Quality
7.2	Loading of sleepers	Quality

2 PRODUCT PERFORMANCE REQUIREMENTS

2.1 Performance Principles

Alternative sleepers and associated components designed, manufactured and supplied in accordance with this specification shall:

- Conform to all requirements of this specification.
- Provide acceptable performance for the duration of the designated design life when installed and maintained in accordance with Queensland Rail's normal practice.
- Performance includes the ability of the sleeper to restrain the rail in order to maintain track gauge, and restraint against and transfer of repeated lateral, vertical and longitudinal forces to the supporting ballast and formation. Loads include rail vehicle live loading, thermal loading and loads generated during maintenance and handling.
- Minimise vibration and noise from passing trains.
- Have a lateral, longitudinal and vertical stability greater or equivalent to timber sleepers. This may be achieved through surface slip resistance and sleeper shape.
- Shall not warp, sag, permanently deform, split or crack under loading for the duration of its design life.
- Shall not degrade due to in track conditions, including but not limited to wear from ballast abrasion, exposure to sunlight or extreme temperatures.
- Be electrically insulating in order to avoid rail to rail shorts (additional care to be taken where steel is incorporated into the design).
- Do not require the use of specialised or non-standard Personal Protective Equipment (PPE) during handling, installation or maintenance.
- Defined failure mechanisms to allow identification that the sleeper has reached the end of its operational life and requires repair or replacement.

2.2 Product Application

Alternative sleeper types listed in clause 1.1 are intended for use in the following applications:

- As a timber-replacement sleeper in mixed-traffic lines with traffic to a maximum of 16 tonne axle load at 120km/hr or 20 tonne axle load at 100 km/h.
- As turnout and special long-length sleepers in all applications throughout Queensland Rail's network with traffic to a maximum of 25 tonne axle load at 100km/h and/or 20 tonne axle load at 160 km/h.
- Installed on a face or as interspersed sleepers with existing in track timber or steel sleepers.
- Installed under mechanical joints.

2.3 Environmental considerations

The environmental performance and benefits associated with the design, manufacture and utilisation of alternative sleepers shall consider whole of life impacts and serviceability. Environmental claims should be demonstrated as applicable – this may be via the provision of Environmental Product Declarations, life cycle analysis, or similar, if available.

Whilst ensuring technical performance and other requirement as per this specification, preference will be given to products that:

- Have intrinsically lower embodied carbon characteristics. Carbon balance credentials (or similar) should be provided
- Do not leach toxic or hazardous chemicals over the design life specified in clause 4.1
- Do not generate hazardous waste during manufacture, use, fire events and disposal
- Use renewable materials and/or with a high recycled content
- Are reusable and/or repairable, including with replacement components as applicable
- Are recyclable, or partially recyclable at end of life
- Do not require the use of toxic or hazardous chemical applications as part of maintenance or repair processes.

3 GENERAL REQUIREMENTS FOR DESIGN

3.1 Sleeper design requirements

Alternative sleepers and associated components shall be designed, manufactured and supplied in accordance with this specification.

Sleepers shall be designed for both structural and fatigue failure modes associated with normal operation loading conditions. Sleepers shall also be designed for a range of environmental factors, durability, exposure, chemical resistance, biological resistance (e.g. infestations), UV stability and temperature extremes relevant to a railway environment in Queensland.

DESIGN REQUIREMENT	QUEENSLAND RAIL'S REQUIREMENTS
	Queensland Rail upon request.
(iii) Centre of gravity of vehicle types above top of running rail	Narrow gauge rollingstock operating on Queensland Rail lines typically has a loaded centre of gravity in the range 1800mm ± 200mm above rail level. Information for specific rollingstock is available from Queensland Rail upon request.
(iv) Train consist configuration including axle loads and associated axle spacing, bogie spacing and inter car spacing	Information for specific train configurations is available from Queensland Rail upon request.
Track information:	
(i) Nominal track gauge	Refer to Clause 4.3 of this Specification
(ii) Rail size	Mainline sleepers – Ranges from 21kg/m rail sections through to 60kg/m as used within the Queensland Rail network. Turnout, diamond and catch point sleepers – as shown on the drawings, available from Queensland Rail. Guard rail sleepers shall be designed to accommodate guard rails the same or one size smaller than the nominated running rail size. Alternative derailment guiding systems may be proposed by the supplier for approval by Queensland Rail. Splay rail sleepers shall be designed to accommodate splay rails of AS41, AS47, AS50 or AS60kg/m
(iii) Nominal cant of rails	Queensland Rail may specify variations to the nominal rail cant requirements for sleepers for specific applications, however generally rail cants are: Turnout sleepers – zero rail cant Rail cant transition sleepers – 1 in 30, 1 in 40 and 1 in 80. All other sleepers – Zero rail cant or 1 in 20
(iv) Depth of ballast	Nominal depth of 150 - 250mm (consideration to be given to special cases where ballast depth may be as low as 100mm).
(v) Type and quality of ballast	Ballast is crushed, screened rock to Queensland Rail's specification. In-service condition of ballast varies from good to moderately fouled. Specific technical information on ballast may be available from Queensland Rail upon request.
(vi) Design bearing pressure	The design bearing pressure exerted by a sleeper on the supporting ballast shall not exceed 750 kPa or the maximum pressure nominated by the supplier and accepted by Queensland Rail.
(vii) Quality of formation	Formation quality varies from engineered subgrades to in-situ materials, ranging in capacity typically from CBR3 to CBR80. Information on formation quality for specific lines or locations may be available from Queensland Rail upon request.

DESIGN REQUIREMENT	QUEENSLAND RAIL'S REQUIREMENTS
(viii) Track modulus	<p>Shall be determined by the Supplier:</p> <ul style="list-style-type: none"> - From field measurements relevant for the application of the sleepers, or - Calculated using industry-recognised methods from information on track structure configuration and condition provided by Queensland Rail.
(ix) Any special installation requirements	<p>Sleepers will be installed using both mechanical equipment and manual handling.</p> <p>The Supplier shall provide information on handling and installation methods required to assure the performance of the product in accordance with this Specification.</p>
Sleeper assembly design information:	
(i) Sleeper spacing	<p>Turnout, diamond and catch point sleepers – between 550mm and 660mm in accordance with bearer layout drawings</p> <p>All other sleepers – 610 or 685mm as per CETS - Module 3.</p>
(ii) Minimum length of sleeper and any additional limits on cross-sectional dimensions	Refer to Clause 4.6 of this Specification
(iii) Details of the fastening type	Refer to Clause 3.2 of this Specification
(iv) Acceptable types of pads and attenuation requirements.	Refer to Clause 3.2 of this Specification
Testing facilities:	
(i) Qualification and level of independence of the facility carrying out type testing.	<p>Facilities for type testing must be NATA-certified and independent of:</p> <ul style="list-style-type: none"> - The Supplier, and - Providers to the Supplier of any products or services associated with the design or manufacture of the sleepers and associated components.
(ii) Qualification and level of independence of the facility carrying out proof testing.	<p>Facilities for proof testing must be NATA-certified.</p> <p>If not independent of the Supplier, testing must be conducted in accordance with a process agreed with Queensland Rail and embedded in the Supplier's Quality System.</p>
Packaging information:	
(i) Rail wagon loading details	Shall be agreed with Queensland Rail
(ii) Associated fastening packaging requirements	Refer to Clause 7.3 of this Specification

- Maintenance inspection period requirements and frequency, noting the variance from the requirements in accordance with CETS.
- Repair methodologies, e.g. plugging holes

The design report shall be RPEQ certified.

Queensland Rail review and acceptance shall not relieve the contractor of responsibility in respect to the requirements of this specification.

3.4 Sleeper design drawings

Along with the sleeper design report (clause 3.3) RPEQ certified drawings shall be submitted to Queensland Rail and include dimensions, design loading, manufacture requirements, tolerances, reference relevant standards, cut and drill limits, fastening details and reinforcing fibre details/sleeper cross section.

Any subsequent drawing revisions shall also be submitted.

4 SPECIFIC REQUIREMENTS FOR DESIGN

4.1 Design life

Products shall have a minimum design life when installed and maintained in accordance with Queensland Rail's normal practice, of:

- Sleepers – 50 years
- Incorporated (cast in) fastening components – 50 years
- All other loose fastening components – 25 years

4.2 Design for serviceability

The designer shall demonstrate to Queensland Rail:

- The contribution of the sleeper to stability of the track structure both laterally and longitudinally, including use on tight radius curves. ✓
- That the sleeper base and rail seat have appropriate resistance to potential abrasion and/or deterioration in service. ✓
- That flexure of the sleeper in service (under load including temperature effects) will not result in exceeding allowable track geometry limits in accordance with CETS.

4.3 Track gauge

Sleepers shall be designed to provide the range of track gauges shown in table 4.3-1. Tolerances on track gauge are as specified in Table 5.4-1.

The track gauge shall be determined as the distance in millimetres between the inner faces of

the two running rails of a track measured 16 mm below the top of each rail.

Table 4.3-1: Sleeper design track gauge

SLEEPER TYPE	DESIGN TRACK GAUGE
Narrow gauge sleepers	1067mm
3GW gauge-widened narrow gauge sleepers	1070mm
6GW gauge-widened narrow gauge sleepers	1073mm
9GW gauge-widened narrow gauge sleepers	1076mm
12GW gauge-widened narrow gauge sleepers	1079mm
Standard gauge sleepers	1435mm
Dual gauge sleepers	1067mm and 1435mm
Turnout, diamond crossing and catch point sleepers	As shown on the drawings.

4.4 Design load factors

For the purpose of calculating the vertical design rail seat load, the combined vertical design load factor (ks) for calculation of the design wheel load (P_{dv}), shall be greater than or equal to 2.5. (Refer to AS1085.14 for guidance on calculation of the Vertical design Rail seat load).

Material reduction factors shall be determined by use of appropriate industry standard methods, such as use of the Eurocomp design code for the structural design of polymer composites.

The designer shall include any other applicable load factors required to complete the design.

All load factoring may be determined:

- From in-field measurements for a representative sample of the traffic under which the sleepers will operate, or
- Through calculation or vehicle / track modelling using industry-recognised methods allowing for the quasi-static and dynamic effects of vehicle / track interaction.

4.5 Axle load distribution factor

The axle load distribution factor, DF, for calculation of the proportion of the vertical axle load taken by an individual sleeper may be determined:

- From the information provided in AS1085.14, or
- Through calculation using industry-recognised methods, considering the physical properties of the rail sections with which the sleepers will be used.

The axle load distribution factor shall be not less than 48%.

4.6 Sleeper dimensions

Sleepers shall have dimensions within the envelopes given in table 4.6-1. Table 4.6-1 shall be read in conjunction with the Notes provided.

Sleeper design shall consider the dimensional tolerances given in 5.4, in particular the effect of cumulative sleeper, fastening and rail tolerances on track gauge.

The sleeper shall have a rail seat area which allows for all rail foot sizes, gauge variances and fastening systems.

4.7 Moments at rail seat and track centre-line

Moments at rail seat and track centre-line shall be determined:

- From in-field measurements for a representative sample of the traffic under which the sleepers will operate, or
- Through calculation or vehicle / track modelling using industry-recognised methods.

4.8 Design for sleeper failure

Given the variability of potential alternative sleeper design proposals, material type and performances, the designer shall address the expected failure modes relevant to the proposal. The parameters that shall be addressed as a minimum include, but are not limited to:

- Permanent deformation
- Failure under ultimate loading
- Material strain failure based on characteristic or appropriately tested values.
- Material fatigue, under specified load cycles
- Excessive deflection under serviceability loading or residual deflection which results in track geometry that is out of tolerance in accordance with CETS (e.g. track gauge).
- Buckling or surface wrinkling
- Local failure (e.g. ply adhesions failures)
- Excessive rail seat abrasion or rail seat cut

Non ductile failure (such as resin or adhesive dominated failure modes) shall not be permitted.

The sleeper shall be designed to give reasonable warning of failure before reaching an ultimate limit state.

4.9 Track stability

The sleepers shall be designed to provide lateral and longitudinal track stability. This may be achieved through sleeper shape and surface

patterns/textures which create a mechanical interlock between the sleeper and the ballast.

The track stability of the sleeper shall be greater than that of timber in fully consolidated track, taking into account the ballast "digging in" to the timber sleeper over time.

4.10 Thermal Properties

The sleeper shall be stable in a range of rail temperatures expected in track, typically between -10°C and 70 °C, site dependant. Thermal expansion or contraction due to temperature changes shall not result in out of tolerance track gauge over seasonal changes. Thermal coefficients of the sleeper material shall be provided to Queensland Rail as part of the sleeper design report.

Consideration shall also be addressed for effect on the sleeper from track hot work, such as rail welding, where extreme temperatures may be encountered.

4.11 Fire resistance

Sleepers shall be designed with consideration given to the following factors:

- High fire resistance
- Low ease of ignition
- Low surface spread of flame
- Low fire propagation
- Low fire penetration
- Non-combustible
- Very low emission of smoke or low smoke density
- No emission of toxic and noxious fumes
- Low loss of structural integrity

The design engineer shall use good engineering judgement and apply good fire safety principles to select suitable materials applicable to the fire conditions which a sleeper may be subjected to.

4.12 Ultraviolet radiation exposure

Sleeper material degradation due to ultraviolet (UV) radiation exposure shall not exceed 0.08mm per year. Use of UV stabiliser in the resin mix is acceptable.

4.13 Materials

Choice of materials shall be made to meet the requirements of this specification, whilst balancing cost efficiencies or cost minimisation.

Table 4.6-1: Dimensional envelope for sleepers

SLEEPER TYPE	DIMENSION	DESIGN DIMENSIONAL ENVELOPE	
		MINIMUM (mm)	MAXIMUM (mm)
Main line sleepers – Standard Size (115mm)	Length	2125	2175
	Width at base	225	255
	Depth at rail seat	110	125
Main line sleepers – Special Size (150mm)	Length	2125	2175
	Width at base	225	255
	Depth at rail seat	145	160
Sleepers for mounting wayside equipment	Length	3000	3100
	Width and Depth	As per Main line Sleepers	
Splay rail sleepers	Length	(as per Drawings)	
	Width and Depth	As per Main line Sleepers	
Sleepers for turnouts, diamond crossings and catch points	Length	(as per Drawings)	
	Width and Depth	As per Main line Sleepers	

Notes to Table 4.6-1:

- 'Mainline' sleepers include plain, guard rail, wide gauge, gauge transition, level rail cant, cant transition and dual gauge (except dual gauge splay rail) types.
- Depth shall be constant for full length of turnout bearers.
- Dimensional envelopes for standard or dual gauge sleepers are available from Queensland Rail upon request.

Appendix C Table 4.1 from Australian Standard; AS1085.14

TABLE 4.1
DESIGN PRESSURES AND MOMENTS—EMPIRICAL METHOD

Distance between rail centres (g) m	Length of ballast support beneath each rail seat (a) m	Design values (see Note 1) kPa or kNm		
g > 1.5 m (standard and broad gauge)	a = L - g	1 Design ballast pressure (p _{ab})	$p_{ab} = \frac{R}{(w(L-g))}$	
		2 Design positive bending moment at rail seat (M _{R+})	$M_{R+} = \frac{R(L-g)}{8}$	
		3 Design negative bending moment at rail seat (M _{R-})	$M_{R-} = 0.67 M_{R+}$	
	a = 0.9 (L - g)	4 Design positive bending moment at the centre (M _{C+})	$M_{C+} = 0.05R (L - g)$	
		5 Design negative bending moment at the centre (M _{C-})	For Standard gauge: (see Note 2)	$M_{C-} = \frac{R(2g-L)}{4}$
		For Broad gauge: (1600 mm or greater, see Note 3)	$M_{C-} = 0.5 \left[Rg - (kg(L-g)) - \frac{k(2g-L)^2}{8} \right]$ where $k = \frac{4R}{(3L-2g)}$	
1.5 m ≥ g > 1.0 m (narrow gauge)	a = 0.8 (L - g)	6 Design ballast pressure (p _{ab})	$p_{ab} = \frac{R}{(0.8w(L-g))}$	
		7 Design positive bending moment at rail seat (M _{R+})	$M_{R+} = \frac{R(L-g)}{6.4}$	
		8 Design negative bending moment at rail seat (M _{R-})	$M_{R-} = 0.67 M_{R+}$	
		9 Design positive bending moment at the centre (M _{C+})	$M_{C+} = 0.10R (L - g)$	
		10 Design negative bending moment at the centre (M _{C-})	$M_{C-} = \text{as spec by purchaser} \geq 0.67 M_{C+}$ (see Note 4)	

NOTES:

- 1 Calculation of the maximum rail seat positive bending moment may be varied by allowing uniform distribution of the applied load over the foot of the rail and taking moments at the outside edge of the rail foot.
- 2 Ballast support is assumed to be uniform.
- 3 Ballast support is assumed to be as shown in Figure 4.1(b).
- 4 The purchaser may need to consider the support conditions in determining the value of M_{C-}. An increased value may provide some measure of confidence in situations where centre binding might occur.

Appendix D Materials list

Product	Quantity	Source/supplier	Cost
GFRP bars	16 x 2.13m, 6mm diameter	Inconmat Australia/ University	Nil
GFRP Shear reinforcement coil	2	Inconmat Australia/ University	Nil
Hacksaw	1	University	Nil
Cable ties	100	University	\$5
Strain gauges and cables	6	University	\$15 each
Sand paper	1	University	Nil
Glue	1 tube	University	\$3
Electrical tape	1 roll	Student	\$2
Individual concrete test moulds	3	University	Nil
Precast sleeper mould	2	University	Nil
Portland concrete	0.5m ³	University	\$100
Polymer concrete	0.5m ³	University	\$100
Reinforcement spacers	5	University	Nil
Tamping rod	1	University	Nil
Slump cone	1	University	Nil
Compression tester	1	University	Nil
Concrete compacting tools (vibrator and trowels)	1	University	Nil
Crayon	1	University	Nil
Hydraulic test machine (SANS machine; 3 point bend test)	1	University	Nil
Hydraulic test machine (300 kN)	1	University	Nil
Lab Computer	1	University	Nil
DIC Camera	1	University	Nil

Appendix E Mechanical Characteristics of GFRP bars

PULTRALL

V-ROD HM

Revision: Oct 2012

V-Rod HM straight bars only, there are no HM bent bars

		#3 GFRP	#4 GFRP	#5 GFRP	#6 GFRP	#7 GFRP	#8 GFRP	#10 GFRP
		V-ROD HM						
Minimum guaranteed tensile strength * (ASTM D7205)	MPa	1372	1312	1184	1105	1059	1000	1093
	ksi	199	190	172	160	153	145	158
Nominal tensile modulus (ASTM D7205)	GPa	65,1 ±2,5	65,6 ±2,5	62,6 ±2,5	63,7 ±2,5	62,6 ±2,5	66,4 ±2,5	65,1 ±2,5
	ksi	9435 ±363	9507 ±363	9072 ±363	9232 ±363	9072 ±363	9623 ±363	9435 ±363
Tensile strain	%	2,11	2,00	1,89	1,73	1,69	1,51	1,68
Poisson's ratio	(-)	0,25	0,26	0,25	0,25	0,26	0,28	0,28
Nominal Flexural strength (ASTM D790)	MPa	1734	1377	1239	1196	1005	1064	1105
	ksi	251	200	180	173	146	154	160
Nominal Flexural modulus (ASTM D790)	GPa	65,5	64,9	63,5	60,2	60,0	65,4	65,8
	ksi	9493	9406	9203	8725	8696	9478	9536
Flexural strain	%	2,65	2,12	1,95	1,99	1,68	1,63	1,68
Transverse shear capacity (ACI 440.3R B4 two cross sections)	kN	41	67	94	127	156	187	232
	lbs	9217	15062	21131	28550	35069	42038	52154
Nominal Bond strength (ACI 440.3R B3)	MPa	14						
	psi	2029						
Bond dependent coefficient	(-)	0,8						
Longitudinal coefficient of thermal expansion (ASTM E831)	xE-6/C	6,2						
	xE-6/F	3,5						
Transverse coefficient of thermal expansion (ASTM E831)	xE-6/C	23,8						
	xE-6/F	13,2						
Moisture absorption (ASTM D570)	%	0,25	0,38	0,44	0,38	0,21	0,29	0,29
Glass content (ASTM D3171)	% vol	65						
	% weight	83						
Weight	g/m	243	380	558	811	1156	1524	2488
	lb/ft	0,163	0,255	0,375	0,545	0,777	1,024	1,672
Effective cross-sectional area (including sand coating) ** (CSA S806 Annex A)	mm ²	170,0	197,0	291,0	394,0	550,0	674,0	1028,0
	inch ²	0,2635	0,3054	0,4511	0,6107	0,8525	1,0447	1,5934
Nominal cross-sectional area	mm ²	71,3	126,7	197,9	285,0	388,0	506,7	791,7
	inch ²	0,1105	0,1963	0,3068	0,4418	0,6013	0,7854	1,2272

* the minimum guaranteed tensile strength must not be used to calculate the strength of the bent portion of a bent bar. Instead use the minimum guaranteed tensile strength found in the technical data sheet of bent V-Rod bars.

** Please contact the manufacturer for dowelling applications.

Development and splice lengths are available upon request but should be properly calculated by a design engineer.

Please refer to the bent bar data sheet for designs using bent V-Rod bars.

It is the responsibility of the design engineers to contact the bar manufacturer to get the latest updates of this technical data sheet (also available at www.pultrall.com).